

**MICROBIAL NITRIFICATION IN THE MARINE
EUPHOTIC ZONE: RATES AND RELATIONSHIPS WITH
NITRITE DISTRIBUTIONS, RECYCLED PRODUCTION
AND NITROUS OXIDE GENERATION**

A DISSERTATION SUBMITTED TO THE GRADUATE DIVISION OF THE
UNIVERSITY OF HAWAII IN PARTIAL FULFILLMENT OF THE
REQUIREMENTS FOR THE DEGREE OF

DOCTOR OF PHILOSOPHY

IN

OCEANOGRAPHY

MAY 1995

By

John Eric Dore

Dissertation Committee:

David M. Karl, Chairperson
Robert R. Bidigare
David W. Muenow
Brian N. Popp
Francis J. Sansone

UMI Number: 9532586

**Copyright 1995 by
Dore, John Eric
All rights reserved.**

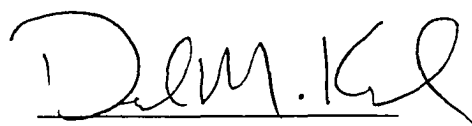
**UMI Microform 9532586
Copyright 1995, by UMI Company. All rights reserved.**

**This microform edition is protected against unauthorized
copying under Title 17, United States Code.**

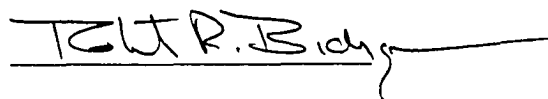
UMI
**300 North Zeeb Road
Ann Arbor, MI 48103**

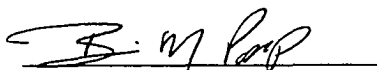
We certify that we have read this dissertation and that, in our opinion, it is satisfactory in scope and quality as a dissertation for the degree of Doctor of Philosophy in Oceanography.

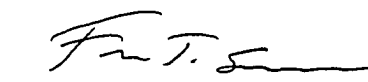
DISSERTATION COMMITTEE



Chairperson









© Copyright 1995

by

John Eric Dore

iii

DEDICATION

This work is dedicated to my brother Michael, who taught me to view the universe through the questioning eyes of a scientist, and who also taught me that the pursuit of the answers could be great fun.

ACKNOWLEDGEMENTS

This work would not have been possible without the contributions of many individuals and institutions, and I would like to express my sincere thanks to each and every person, listed here or not, who contributed to this dissertation.

The members of my dissertation committee were quite helpful in shaping this document and in directing the course of my research. Particular thanks go to my committee chairperson, research advisor and mentor, David M. Karl, who never failed to offer advice and support when I needed them.

Thanks are due to all persons involved in the Hawaii Ocean Time-Series project. Roger Lukas and his team provided invaluable shipboard support and hydrographic data. Ricardo Letelier and Dale Hebel were always willing to help me with experiments, regardless of the weather, and moreover never tired of discussing my (sometimes wild) ideas. Similarly, I frequently relied on the assistance of Chris Carrillo, Jim Christian, Lance Fujieki, Terry Houlihan, Ursula Magaard, Dan Sadler, Georgia Tien, Luis Tupas and Chris Winn. Financial support for this research was provided principally by National Science Foundation grants OCE87-17195 (R. Lukas, P.I.), OCE88-00329 (D. Karl, P.I.) and OCE93-01368 (D. Karl, P.I.), and by a graduate fellowship from the Research Corporation of the University of Hawaii.

I received essential technical advice on gas chromatographic nitrous oxide determinations from Chris Measures, John Priscu and Frank Sansone. Colleen Allen taught me the ins and outs of chemiluminescent nitrite and nitrate analyses. Ted Walsh performed numerous high-quality automated nutrient analyses. Dale Kiefer and Bob Bidigare gave helpful comments on early versions of my PNM model. Special thanks are due to the hard-working and talented captains and crews of the research vessels Alpha

Helix, Kaimalino, Kila, Moana Wave, Nathaniel B. Palmer, New Horizon, Thomas G. Thompson, Townsend Cromwell and Wecoma. I would also like to express my gratitude to Rob Olson and Bess Ward for their pioneering studies on marine nitrification, which set up the framework that I have built upon.

Finally, I thank Mary Elizabeth Stanley for putting up with my long absences and for staying with me through thick and thin.

ABSTRACT

Concerns are mounting that rising levels of carbon dioxide and other greenhouse gases in the atmosphere will lead to global warming and global environmental change. At the same time, there is growing evidence that chlorofluorocarbons and other trace gases are depleting Earth's protective stratospheric ozone layer. Microbial nitrification, the biologically mediated oxidation of ammonium to nitrite to nitrate, plays a key role in both of these issues: (1) nitrification may complicate measurements of new production, resulting in inaccurate estimates of the amount of carbon dioxide that can be removed from the atmosphere by the ocean's natural biological pump, and (2) nitrification may produce nitrous oxide as a by-product, a trace greenhouse gas that also depletes ozone.

In this study I have utilized sensitive chemical and radioisotopic techniques to measure relevant nitrogen compounds and to estimate in situ nitrification rates. This work has been carried out during the regular cruises of the Hawaii Ocean Time-series (HOT) project to the oligotrophic Station ALOHA in the subequatorial North Pacific Ocean. The study has focused on the lower euphotic zone, which is characterized by an accumulation of nitrite (the primary nitrite maximum or PNM). The goals of the study were to assess the role of nitrification in the recycling of nitrogen within the euphotic zone of a well-characterized oligotrophic site, to investigate the influence of nitrification on the structure and variability of nitrite distributions and to examine the relationship between nitrification and the production of nitrous oxide.

Nitrification rates in the euphotic zone were found to be highly variable, ranging from <2 to $123 \mu\text{mol m}^{-3} \text{d}^{-1}$. Nitrate production via nitrification within the euphotic zone was several times greater than the estimated eddy-diffusive flux of nitrate into the

euphotic zone from below, indicating that nitrate-based production cannot be equated with new production at Station ALOHA.

Chemiluminescent nitrite measurements revealed that the PNM exhibits a double-peaked structure, with a large upper maximum at a depth of 126 ± 18 m and a lower maximum of lesser magnitude at 149 ± 15 m. The vertical distributions of nitrogenous compounds and nitrification rates suggest that the upper peak of the PNM is produced through the incomplete assimilatory reduction of nitrate by phytoplankton, while the lower peak is maintained through the differential photoinhibition of nitrifying bacteria. This vertical separation of nitrite-producing processes and the observed vertical nitrite profiles were successfully recreated using a light-dependent model.

Water column profiles of nitrous oxide showed significant supersaturation, even within the surface mixed layer. A mass balance of nitrous oxide within the euphotic zone, based on measured concentrations and nitrification rates, suggests that in situ production of nitrous oxide, rather than a flux from below the euphotic zone, is the dominant term in supporting the sea-air flux of this trace gas at Station ALOHA. However, much of this in situ nitrous oxide generation appears to be fueled by a process other than nitrification which remains uncharacterized.

TABLE OF CONTENTS

ACKNOWLEDGEMENTS	v
ABSTRACT	vii
LIST OF TABLES	xii
LIST OF FIGURES	xiii
CHAPTER 1: INTRODUCTION AND RATIONALE FOR THE PRESENT RESEARCH..... 1	
<u>BACKGROUND</u>	1
<u>SYNOPSIS</u>	13
<u>REFERENCES</u>	17
CHAPTER 2: FREEZING AS A METHOD OF SAMPLE PRESERVATION FOR THE ANALYSIS OF DISSOLVED INORGANIC NUTRIENTS IN SEAWATER 23	
<u>ABSTRACT</u>	23
<u>INTRODUCTION</u>	23
<u>BACKGROUND</u>	25
<u>MATERIALS AND METHODS</u>	33
<i>Sample collection</i>	33
<i>Analytical methods</i>	35
<i>Experiments on the effects of freezing samples</i>	37
<i>Experiments on the filtration of samples</i>	38
<i>Experiments on the long-term frozen storage of samples</i>	39
<u>RESULTS</u>	40
<i>Experiments on the effects of freezing samples</i>	40
<i>Experiments on the filtration of samples</i>	40
<i>Experiments on the long-term frozen storage of samples</i>	46
<u>DISCUSSION</u>	46
<u>CONCLUSIONS</u>	53
<u>REFERENCES</u>	54
CHAPTER 3: NITRITE DISTRIBUTIONS AND DYNAMICS AT STATION ALOHA 59	
<u>ABSTRACT</u>	59
<u>INTRODUCTION</u>	59
<u>MATERIALS AND METHODS</u>	62
<i>Station location</i>	62
<i>Sampling</i>	62

<i>Chemiluminescent analyses</i>	63
<i>Detection limits, precision and accuracy</i>	64
<i>Precautions</i>	65
<u>RESULTS AND DISCUSSION</u>	66
<i>Storage experiments</i>	66
<i>Nitrite in the upper water column</i>	69
<i>PNM structure and the nitracline</i>	76
<i>The PNM and particle flux</i>	80
<i>Midwater and deep nitrite profiles</i>	82
<u>CONCLUSIONS</u>	85
<u>REFERENCES</u>	87

CHAPTER 4: NITRIFICATION IN THE EUPHOTIC ZONE AS A SOURCE FOR NITRITE, NITRATE AND NITROUS OXIDE AT STATION ALOHA..... 90

<u>ABSTRACT</u>	90
<u>INTRODUCTION</u>	91
<u>MATERIALS AND METHODS</u>	93
<i>Station location</i>	93
<i>Sampling</i>	93
<i>Nutrients and dissolved oxygen</i>	94
<i>Nitrous oxide</i>	94
<i>Nitrification rates</i>	97
<u>RESULTS AND DISCUSSION</u>	100
<i>Nitrification rates</i>	100
<i>Nitrification and the primary nitrite maximum</i>	105
<i>Nitrification and N₂O</i>	113
<i>Nitrification and new production</i>	120
<u>CONCLUSIONS</u>	129
<u>REFERENCES</u>	130

CHAPTER 5: COMBINED OXIDATION/REDUCTION MODEL OF THE PRIMARY NITRITE MAXIMUM AT STATION ALOHA..... 139

<u>ABSTRACT</u>	139
<u>INTRODUCTION</u>	139
<u>MATERIALS AND METHODS</u>	141
<i>Station location and sampling</i>	141
<i>Optical measurements</i>	142
<i>Nutrient analyses</i>	143
<i>HOT-50 in situ incubations</i>	143
<i>Model code</i>	144
<i>Model equations</i>	145
<i>Model assumptions</i>	148
<u>RESULTS AND DISCUSSION</u>	151

<i>Measurements of model input parameters</i>	151
<i>Determination of model constants</i>	154
<i>Model PNM simulations</i>	158
<i>Sensitivity analysis</i>	165
<i>Strengths and weaknesses of the model</i>	166
<u>CONCLUSIONS</u>	168
<u>REFERENCES</u>	170
CHAPTER 6: CONCLUSIONS AND DIRECTIONS FOR FUTURE RESEARCH...	173
<u>SUMMARY</u>	173
<u>FUTURE RESEARCH DIRECTIONS</u>	175
<u>REFERENCES</u>	178
APPENDIX A: MATLAB™ ROUTINES	179
APPENDIX B: MODEL CONSTANTS AND VARIABLES	188
APPENDIX C: INPUT DATA FOR FIVE MODELED CRUISES	190

LIST OF TABLES

<u>Table</u>		<u>Page</u>
2.1	Chronology of research into the effects of sample freezing on dissolved nutrient assays of natural waters	26
2.2	Model II reduced major axis linear regression statistics for seawater sample storage experiments.....	44
2.3	Student's t-test statistics for long-term frozen storage experiments	48
3.1	Results of an experiment to determine the effects of several sample storage methods on the concentration of nitrite	67
4.1	Nitrification rates at Station ALOHA.....	101
5.1	Surface PAR fluxes used in PNM model	152

LIST OF FIGURES

<u>Figure</u>	<u>Page</u>
1.1	The five principle inorganic compounds of nitrogen in seawater, with nitrogen redox states and major pathways 3
1.2	Schematic diagram of the distribution of nitrite in relation to nitrate, chlorophyll-a and light flux in the upper 200 m of the water column in oligotrophic oceanic waters 6
1.3	Location of Station ALOHA north of the island of Oahu, Hawaii..... 14
2.1	Plots of frozen vs. fresh concentration determinations on unfiltered samples: (a) nitrate+nitrite, (b) nitrite, (c) soluble reactive phosphate, (d) ammonium 41
2.2	Plot of frozen vs. refrigerated concentration determinations on unfiltered samples: (a) soluble reactive silicate, full range of data shown, (b) soluble reactive silicate, only values >120 μ M shown 42
2.3	Plots of filtered vs. unfiltered concentration determinations (all samples frozen): (a) nitrate+nitrite, (b) soluble reactive phosphate, (c) soluble reactive silicate..... 43
2.4	Results of long-term frozen storage experiments: (a) time-course of nitrate+nitrite concentration during frozen storage, (b) as in (a) except for soluble reactive phosphate, (c) as in (a) except for soluble reactive silicate 47
2.5	Plots of frozen vs. fresh determinations; data taken from Venrick and Hayward (1985): (a) nitrate+nitrite, (b) soluble reactive phosphate, (c) soluble reactive silicate 51
3.1	Results of an experiment to determine the effects of frozen storage of nitrite samples with respect to samples analyzed at sea..... 68
3.2	Upper water column profiles of [nitrite], [nitrite+nitrate] and [chlorophyll-a] taken during HOT-41 (Oct. 1992)..... 70

<u>Figure</u>	<u>Page</u>	
3.3	Upper water column profiles of nitrite sampled twelve hours apart during HOT-19 (July 1990): (a) Vertical axis shows in situ depth in m, (b) Vertical axis shows depth in m after employing density-averaging.....	73
3.4	Time-series contour plot of nitrite concentration in the upper 200 m at Station ALOHA during the first five years of the HOT program.....	74
3.5	Relationship between the positions of the upper primary nitrite maximum (UPNM) and the nitracline at Station ALOHA.....	78
3.6	Time-series of the positions of the nitracline, upper primary nitrite maximum (UPNM) and lower primary nitrite maximum (LPNM) at Station ALOHA	79
3.7	Time-series of (a) 0-200 m depth-integrated nitrite and (b) mean particulate nitrogen flux at 150 m as collected by sediment traps at Station ALOHA	81
3.8	Midwater profiles of nitrite from Station ALOHA.....	83
3.9	Deep water profiles of nitrite from Station ALOHA.....	84
4.1	Depth distribution (0-200 m) of nitrification rates from five cruises at Station ALOHA.....	104
4.2	Depth profiles (0-200 m) of selected parameters at Station ALOHA during HOT-31 (Oct. 1991)	106
4.3	Depth profiles (0-200 m) of selected parameters at Station ALOHA during HOT-36 (Apr. 1992).....	107
4.4	Depth profiles (0-200 m) of selected parameters at Station ALOHA during HOT-40 (Sept. 1992)	108
4.5	Depth profiles (0-200 m) of selected parameters at Station ALOHA during HOT-41 (Oct. 1992)	109
4.6	Depth profiles (0-200 m) of selected parameters at Station ALOHA during HOT-45 (Feb. 1993)	110

<u>Figure</u>	<u>Page</u>
4.7	Depth profiles (0-200 m) of selected parameters at Station ALOHA during HOT-50 (Oct. 1993) 111
4.8	Depth profiles (0-200 m) of selected parameters at Station ALOHA during HOT-57 (Sept. 1994) 112
4.9	Depth profiles (0-1000 m) of [N ₂ O] and [O ₂] at Station ALOHA 114
4.10	Schematic diagrams of the nitrogen cycle in the oligotrophic oceanic euphotic zone: (a) "Traditional" model. (b) proposed model including "nitrifier loop" 123
5.1	Distributions of PAR used in model simulations for HOT-36 and HOT-50 153
5.2	Distributions of nitrate used in model simulations for HOT-31 and HOT-50 155
5.3	Distributions of biomass carbon estimated from ATP and chlorophyll-a used in model simulations for HOT-50 156
5.4	Results of HOT-50 in situ incubation: left panel: initial concentrations of nitrite and nitrate, right panel: net changes in nitrite and nitrate during 3-day incubation 157
5.5	Model output for HOT-50 (Oct. 1993): left panel: ATP used to estimate phytoplankton biomass, right panel: chlorophyll-a used to estimate phytoplankton biomass 159
5.6	Model output as in Fig. 5.5 except for HOT-40 (Sept. 1992) 160
5.7	Model output as in Fig. 5.5 except for HOT-41 (Oct. 1992) 161
5.8	Model output as in Fig. 5.5 except for HOT-36 (Apr. 1992) 162
5.9	Model output as in Fig. 5.5 except for HOT-31 (Oct. 1991) 163
5.10	Demonstration of model sensitivity to changes in [NH ₄ ⁺] profile 167

CHAPTER 1

INTRODUCTION AND RATIONALE FOR THE PRESENT RESEARCH

BACKGROUND

In most oceanic regions, primary photosynthetic production is believed to be limited by the supply of fixed nitrogen (Ryther, 1959; Caperon and Meyer, 1972; Eppley et al., 1977). The large reservoir of dissolved nitrogen gas (N_2) in the sea is generally unavailable as a nutrient, except to specialized nitrogen-fixing organisms whose importance in oceanic nitrogen cycling is still under debate (Carpenter, 1983; Karl et al., 1992). Nitrate (NO_3^-) is the next most abundant nitrogenous nutrient in the oceans (Sharp, 1983). Other less abundant inorganic forms occur, including nitrite (NO_2^-), ammonium (NH_4^+ , and ammonia, NH_3), and nitrous oxide (N_2O). Dissolved organic nitrogen (DON), which is present in far greater abundance in oligotrophic surface waters than all inorganic nitrogen forms combined (excluding N_2), is usually not considered a significant nitrogen source for phytoplankton growth. This is because it is generally believed that DON compounds must be mineralized to ammonium by bacteria (Paul, 1983) or by the extracellular enzymes of phytoplankton (Palenik and Morel, 1991) before assimilation by phytoplankton. However, the direct assimilation by marine microalgae of small DON compounds such as adenine (Karl and Winn, 1984) and hypoxanthine (Antia et al., 1980) has been demonstrated, but its magnitude is uncertain.

Dugdale and Goering (1967) suggested that primary production in the euphotic zone of the sea be partitioned into "new" and "regenerated" categories; new production is that which is supported by inputs of exogenous nitrogenous nutrients, while regenerated

production is that which is supported by nitrogen that has been recycled within the euphotic zone. In the oligotrophic open ocean, the vertical flux of nitrate from high concentration in deep waters to the impoverished surface layer is commonly believed to be the largest contributor to new production, while ammonium is considered the dominant form of recycled inorganic nitrogen (Eppley et al., 1973; Eppley and Peterson, 1979; Platt et al., 1989).

The nitrification process is a fundamental component of the marine nitrogen cycle (Ward, 1986). Nitrification refers to the two-step oxidation of ammonium to nitrate via the intermediate nitrite (Fig. 1.1). Each step of the reaction is mediated by a separate group of chemolithoautotrophic bacteria: ammonium oxidizers such as *Nitrosomonas* gain energy by converting ammonium to nitrite, and nitrite oxidizers such as *Nitrobacter* capitalize on the conversion of nitrite to nitrate (Kaplan, 1983). Nitrification is believed to be responsible for the production and accumulation of nitrate in the deep ocean, and as such is a crucial link in the overall process of returning new nitrogen to the euphotic zone. Some studies implicate nitrification as a process in direct competition for reduced nitrogenous substrates with combined phytoplankton and bacterial assimilation within the euphotic layer (e.g. Olson, 1980; Ward, 1982a; Ward et al., 1989).

Growing concerns about rising carbon dioxide (CO₂) levels in the atmosphere, which may influence global climate change through the greenhouse effect, have prompted research into the oceans' potential ability to act as a sink for anthropogenic CO₂. This removal is mainly accomplished through the partitioning of CO₂ into surface waters and the subsequent physical transport of these waters to the deep ocean, where the CO₂ remains out of contact with the atmosphere for 100-1000 years or more. The photosynthetic fixation of CO₂ by phytoplankton and its subsequent sinking from the euphotic zone as particulate organic matter (POM) or diffusing downward as dissolved

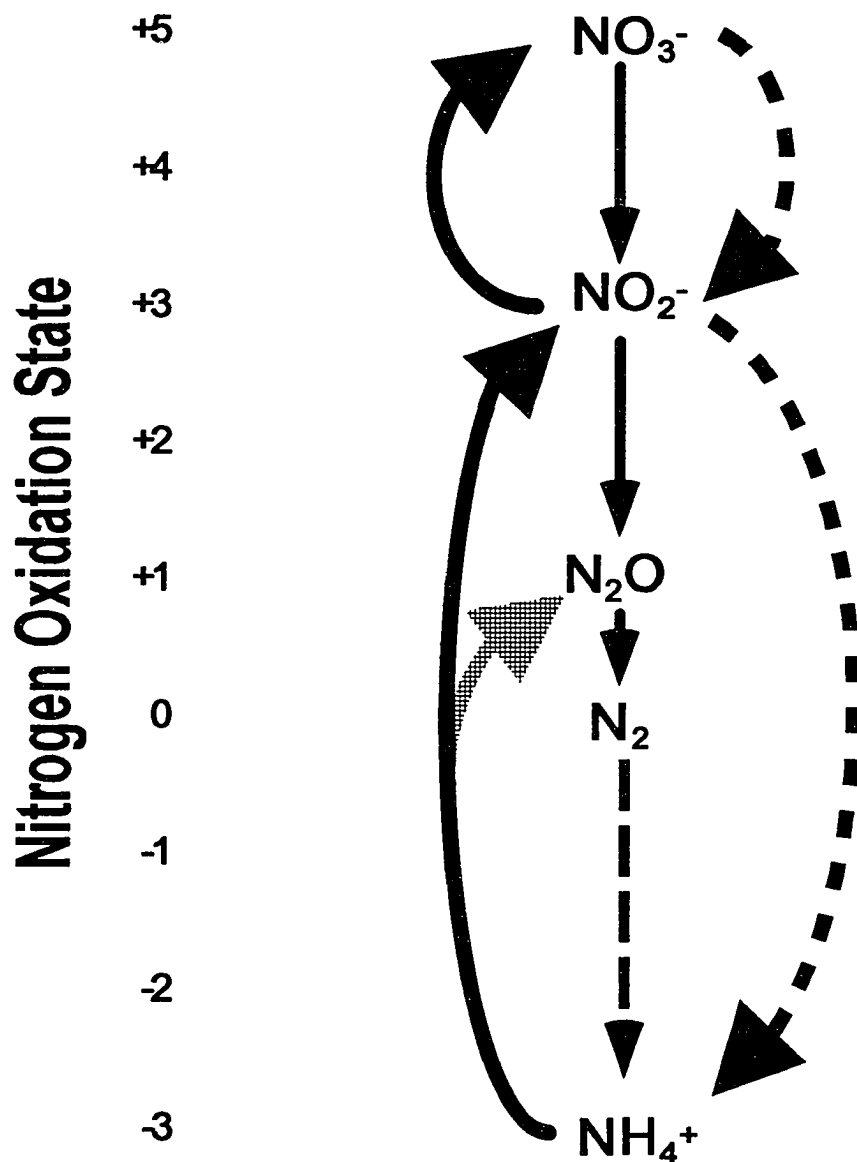


Fig. 1.1. The five principle inorganic compounds of nitrogen in seawater, with nitrogen redox states and major pathways. Wide solid arrows represent nitrification; wide shaded arrow shows release of nitrous oxide (N_2O) as a by-product of nitrification. Wide dotted arrows represent assimilatory reduction of nitrate (NO_3^-) to nitrite (NO_2^-) and ammonium (NH_4^+). The three narrow solid arrows represent denitrification from nitrate to nitrite to nitrous oxide to dinitrogen (N_2). The narrow dashed arrow represents dinitrogen fixation to ammonium.

organic matter (DOM) constitutes another removal pathway. In this way, the oceans' "biological pump" (Longhurst and Harrison, 1989) removes a fraction of the carbon fixed from the surface waters, hence out of contact with the atmosphere. At steady state, the fraction of total primary production lost from the euphotic zone in this manner must balance that fraction which is supported by exogenous nitrogen, i.e. "export" production must balance "new" production (Eppley and Peterson, 1979). The measurement of new production and the ratio of new to total production (f-ratio) at sites representative of the major oceanographic provinces is thus of great importance. It is recognized that the "extra" anthropogenic CO₂ from emissions cannot be removed from the atmosphere by the biological pump without an increase in the rate of supply of fixed nitrogen to oceanic biota (Shaffer, 1993); while such an increase is thought to have occurred since pre-industrial times due to the growing use of chemical fertilizers in agriculture, the effect is believed to be minor (Houghton et al., 1990). Despite this fact, the biological pump remains important in the *natural* cycle of carbon, and we must understand the natural nitrogen and carbon cycles if we are to make predictions about the consequences of anthropogenic perturbations.

Frequently estimates of new production are made by measuring phytoplankton nitrate uptake rates in bottle incubations of water samples using a ¹⁵NO₃⁻ tracer (Harrison, 1983; Harrison et al., 1989). Similarly, a ¹⁵NH₄⁺ tracer can be used to estimate regenerated production. The use of this technique assumes that all NH₄⁺ is regenerated and all NO₃⁻ is new, and that NO₂⁻, DON and N₂ are negligible N sources. If some of the assimilated NO₃⁻ is being formed in situ rather than diffusing upward from the deep water reservoir, then this fraction is in fact regenerated, and new production estimates based on the ¹⁵N tracer method will overestimate the true contribution of nitrate to new production. Several recent studies have presented evidence for substantial nitrification within the

euphotic zone, providing an internal source of nitrate significant when compared to phytoplankton uptake rates (Olson, 1981a; Priscu and Downes, 1985; Ward, 1987; Ward et al., 1989). If this source of "regenerated" NO_3^- is significant over much of the world's oceans, we should scrutinize our current models of marine nitrogen cycling and re-examine current measurement protocols for new production.

Nitrite-nitrogen has a redox position between that of ammonium and nitrate, thus the nitrite accumulations seen in certain layers within the ocean indicate zones in which transformations of combined nitrogen occur (Rakestraw, 1936; Vaccaro and Ryther, 1960). One such layer is the primary nitrite maximum (PNM), found near the base of the euphotic zone over much of the world's coastal and oceanic regions (Fig. 1.2); the PNM has in fact been suggested as a chemical indicator of the base of the euphotic zone (Kiefer et al., 1976; Herbland and Voituriez, 1979). Concentrations of nitrite within the PNM are seasonally and regionally variable but are usually less than about $1 \mu\text{M}$ (Wada and Hattori, 1991).

Various investigators have suggested a number of possible mechanisms for the formation and maintenance of the PNM. These involve production of nitrite via: (1) chemoautotrophic oxidation of ammonium by nitrifying bacteria (Brandhorst, 1959; Olson, 1981b), (2) incomplete assimilatory reduction of nitrate by phytoplankton (Vaccaro and Ryther, 1960; Kiefer et al., 1976), and (3) dissimilatory reduction of nitrate by heterotrophic bacteria (Wada and Hattori, 1972). The production of nitrite from nitrate by denitrifying bacteria, while potentially significant in areas of severe oxygen depletion (Brandhorst, 1959; Fiadeiro and Strickland, 1968; Codispoti and Richards, 1976), is not thought to play a role in the well-oxygenated PNM (Wada and Hattori, 1972; Ward, 1986). Possible anoxic microsites suitable for denitrifiers might be found within large particles and the guts of macrozooplankton (Karl et al., 1984; Alldredge and

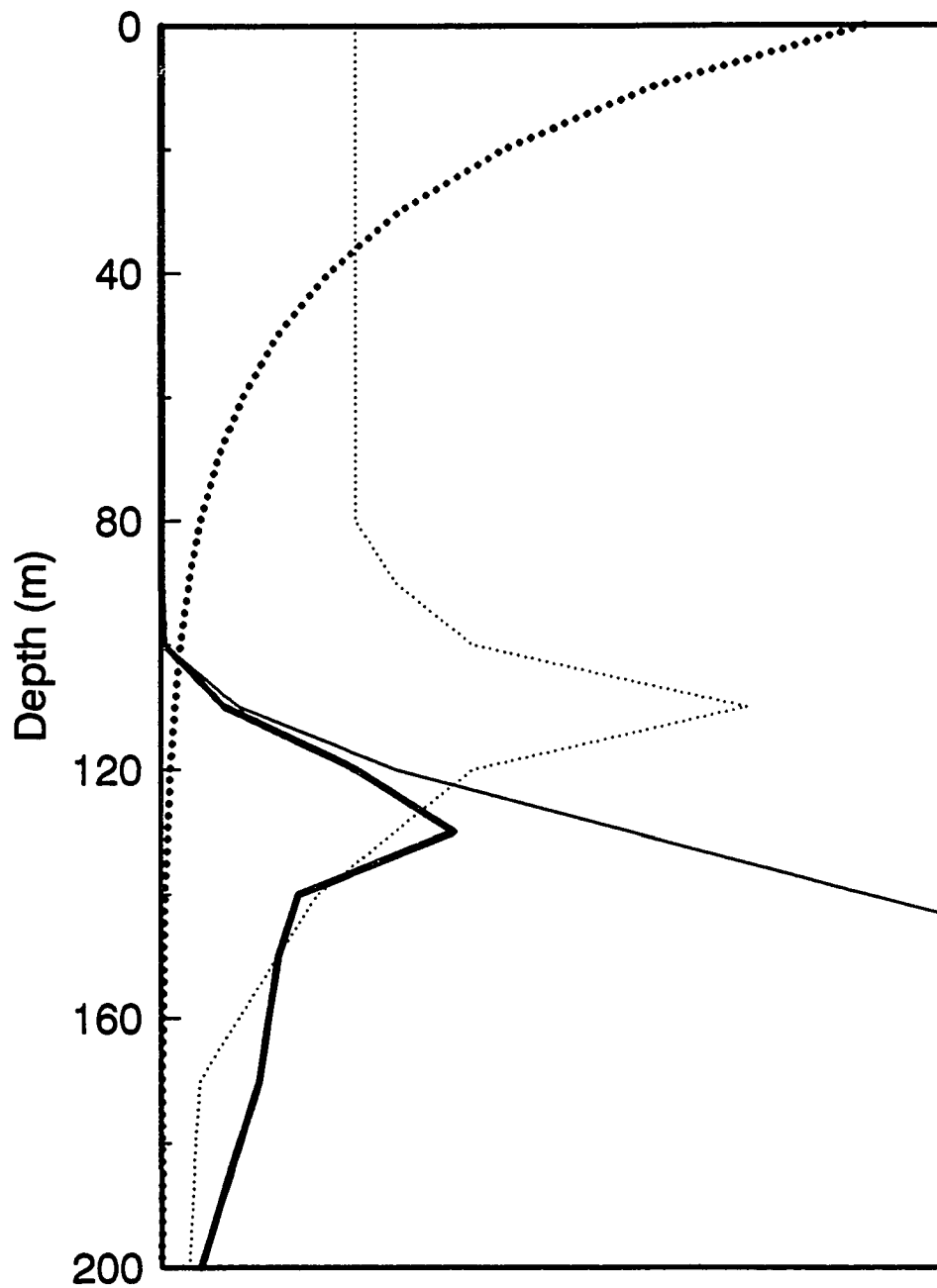


Fig. 1.2. Schematic diagram of the distribution of nitrite (wide solid curve) in relation to nitrate (narrow solid curve), chlorophyll-a (narrow dotted curve) and light flux (wide dotted curve) in the upper 200 m of the water column in oligotrophic oceanic waters.

Cohen, 1987). Particles large enough to maintain anoxic interiors in the euphotic zone would presumably be rare and rapidly sinking, but the potential contribution of such microsites to nitrite production should not be ignored. Similarly, macrozooplankton are relatively scarce in oligotrophic waters, yet still may make some contribution and should not be entirely overlooked.

It is of interest to compare previous investigators' data regarding the source of the nitrite in the PNM, and to examine consistencies among them. The production of significant amounts of extracellular nitrite by marine phytoplankton cultures during nitrate assimilation was demonstrated by Vaccaro and Ryther (1960). These researchers also found that the highest nitrite concentrations were produced by cultures recovering from nitrogen deficiency and grown under reduced light conditions. They made the suggestion that in the open ocean near the base of the photic zone, where nitrate becomes plentiful and phytoplankton are light-limited, this reductive pathway leads to the formation of the observed maximum in nitrite concentration. Further laboratory studies by Carlucci et al. (1970) supported their results, and their ideas were again reexamined in a field study by Kiefer et al. (1976). The latter study employed a simple box model using measured profiles of nitrite, nitrate and phytoplankton carbon, along with an eddy diffusivity constant from the literature, to show that rates of nitrite production are consistent with the hypothesis of Vaccaro and Ryther. Kiefer et al. (1976) suggested that the PNM "exists at a given depth because the cells above the maximum are depleted of nitrate while the cells below the maximum receive insufficient radiant energy to maintain intracellular rates of nitrate reduction." When light levels are low, nitrate reduction to nitrite exceeds nitrite reduction to ammonium which can be incorporated into cellular materials. A large intracellular pool of nitrite develops, and some of this diffuses out of the cells as nitrous acid (HNO_2). Nitrous acid subsequently dissociates in seawater to produce free nitrite.

Indirect evidence supporting the phytoplankton reduction model was presented by Herbland and Voituriez (1979). They performed a statistical analysis of 123 measurements of the depths of the PNM and the top of the nitracline, and found a strong correlation. They also found a significant offset of about 11 m between these two features, the PNM falling below the top of the nitracline. Moreover, in an earlier study (Herbland and Voituriez, 1977), these authors showed that, in tropical areas, nitrite is never detectable when nitrate is not present. Thus, they concluded that the PNM "stands where the chlorophyll concentrations decrease in a light limited regime and where nitrate is abundant" (Herbland and Voituriez, 1979).

The condition of low light level for phytoplankton nitrite production suggested by Vaccaro and Ryther (1960) is apparently not necessary. Culture studies by Olson et al. (1980) and field work by Wada and Hattori (1971) both show that nitrite production by phytoplankton is positively correlated with both nitrate concentration and light intensity. Furthermore, in boreal areas rich in surface nitrate, an annual accumulation of nitrite closely matches the annual depletion of nitrate as light levels increase during the spring (e.g. see Verjbinskaya, 1932; Dore and Karl, 1993). It is therefore probable that the phytoplankton contribution to the PNM is not due to low light, but to *sufficient* light and *ample* nitrate, enabling phytoplankton cells to maintain a high rate of nitrate reduction. This view is consistent with the correlation of the depth of the PNM and the nitracline seen by Herbland and Voituriez (1979); indeed, the depth of maximal nitrate uptake measured by Eppley and Koeve (1990) for stations with nitrate-depleted surface layers and steep nitraclines was always a few meters below the top of the nitracline.

The dissimilatory reduction of nitrate to nitrite by heterotrophic bacteria cannot be discounted as a contributor to the PNM (Wada and Hattori, 1991), however, it is generally not considered to be as significant as the other two processes examined here.

Hattori and Wada (1971) suggested the importance of nitrate-reducing bacteria in the production of the PNM in the equatorial South Pacific Ocean. They surveyed euphotic zone nitrate-reducing, nitrifying and denitrifying bacteria along the 155°W meridian, finding no denitrifiers in nitrite-rich waters, few if any nitrifiers, but ubiquitous nitrate-reducers up to several tens of cells ml⁻¹. Moreover, the nitrate-reducing bacteria which they were able to isolate in a medium containing glucose as an energy source, produced nitrite under both aerobic and anaerobic conditions, with nitrate as the sole nitrogen source. The correlation between nitrate-reducers and nitrite was upheld in profiles taken by Gundersen et al. (1976) off the Hawaiian Islands. However, these investigators found that water samples enriched with spikes of nitrate and organic matter would not produce nitrite under aerobic conditions. Furthermore, both of these studies utilized plate counts in estimating bacterial populations; these methods have numerous shortcomings and their results may not be trustworthy (Karl, 1986).

Nitrifying bacteria were first isolated from the marine environment by Watson (1965). However, the most probable number (MPN) methods he used to estimate in situ concentrations yielded population estimates from zero to at most a few cells l⁻¹; not only was the method used questionable (Karl, 1986), but also the result left doubt on the ability of these organisms to nitrify at sufficient rates to satisfy the requirements of the mass balance of oceanic nitrogen (Ward, 1986). Despite the observed low abundance of marine nitrifiers, several investigators were able to demonstrate nitrite production from ammonium within the PNM. Wada and Hattori (1971), using a sensitive chemical assay to measure changes in nitrite in incubated samples, concluded that ammonium was the major source of PNM nitrite in the central North Pacific Ocean. Miyazaki et al. (1973, 1975), using a ¹⁵N tracer method, found that in Sagami Bay and in the western North Pacific, ammonium and nitrate are both sources of PNM nitrite.

In a landmark study, Olson (1981a) used improved ^{15}N tracer methods to measure the production of nitrite from nitrate and ammonium, and the uptake of nitrate and ammonium, in coastal, subtropical, and Antarctic waters. He found that in subtropical waters and in the Ross Sea in summer, ammonium was the major source of nitrite in the PNM, while in the Scotia Sea in early spring, nitrate and ammonium were equally important. In addition, he found that a large fraction of the ammonium-oxidizing activity passed through a $0.6\ \mu\text{m}$ filter but was retained on a $0.2\ \mu\text{m}$ filter, suggesting that bacteria were responsible. The rate of nitrite production from ammonium in the central North Pacific gyre was found to be from 2.24 to $7.30\ \mu\text{mol m}^{-3}\ \text{d}^{-1}$, yielding a turnover time of 25 ± 10 days for PNM nitrite.

In a related paper, Olson (1981b) proposed a mechanism by which nitrifying bacteria might form and maintain the PNM, involving the differential photoinhibition of ammonium oxidizers and nitrite oxidizers. Light inhibition of the soil nitrifiers *Nitrobacter winogradsky* and *Nitrosomonas europaea* were reported by Müller-Neuglück and Engel (1961) and Schön and Engel (1962); these studies also collectively showed that the nitrite oxidizer was more sensitive to light than the ammonium oxidizer. These results were confirmed by Bock (1965), who suggested that the inhibition was caused by the photo-oxidation of cytochrome c, which is found in lower concentration in *Nitrobacter* than it is in *Nitrosomonas*. Olson, having found evidence for ammonium oxidation occurring within and below the PNM but nitrite oxidation occurring only below (Olson, 1981a), suspected that nitrite was accumulating because at the light levels associated with the PNM nitrite oxidation was being inhibited, while ammonium oxidation was not. In studies of coastal seawater samples, he found that nitrite oxidation was indeed inhibited by light of an intensity less than that required to inhibit ammonium oxidation, and that the critical intensity was about 1% of surface irradiance, about the light level found at the PNM.

Subsequently, he used a model calculation to generate a computer simulation of the formation of the PNM; though the shape of the simulated peak differed from that of the actual PNM, the magnitude and the depth at which it formed were approximately consistent with field observations.

Support for Olson's hypothesis was presented by Ward (1982a, 1982b), who, using an immunofluorescent assay for marine ammonium oxidizers, found that the in situ concentration of these organisms was much higher than had been previously estimated from MPN techniques. Concentrations in the oligotrophic Pacific were found to be from 10^3 to 10^4 cells l^{-1} and showed no consistent trend with depth. Though these and other studies using immunofluorescent assays of nitrifiers (Ward et al., 1982; Ward and Carlucci, 1985) provided for the first time evidence of nitrifying bacterial populations of sufficient size to account for the observed ammonium oxidation rates, it still remains unclear how the pattern of ammonium oxidizing activity with depth, with its maximum value near the PNM, can be reconciled with nearly uniform cell distributions. Furthermore, the differential photoinhibition model and the ^{15}N -measured nitrification rates are not consistent with the rapid turnover of PNM nitrite observed by French et al. (1986). These authors observed diel changes in nitrite in the Gulf of Mexico that indicated nitrite production rates 1-3 orders of magnitude higher than those measured by previous investigators. To resolve such discrepancies, it is necessary to combine concurrent data on nitrification rates and in situ substrate/product concentration changes within the PNM.

Nitrous oxide is a key intermediate in both nitrification and denitrification in the aquatic environment (Vincent et al., 1981; Yoshida et al., 1989). Recently, a great deal of interest in this trace gas has arisen, primarily due to its role in global climate change. N_2O has the potential to destroy stratospheric ozone, and at the same time is a greenhouse gas 200 times more potent, molecule for molecule, than CO_2 (Yoshida et al., 1989; Kim and

Craig, 1990). N_2O is responsible for 6% of the rise in radiative forcing of the atmosphere from 1980-1990 that can be attributed to gas emissions (Houghton et al., 1990). Moreover, its steady rate of increase in the atmosphere of 0.25% per year and its long residence time there of almost 100 years make it a factor of great concern. Unfortunately, assessments of the magnitudes of its sources are diverging rather than converging (Cicerone, 1989). In particular, the nature and magnitude of what is believed to be an oceanic source are not well understood (Houghton et al., 1990).

The oceanic N_2O source is believed to be mediated primarily through its production as a by-product of microbial nitrification, in all but the most oxygen-deficient waters (Yoshida, 1988; Yoshida et al., 1989). However, the main peak in N_2O concentrations in the western North Pacific Ocean is associated with low O_2 and high NO_3^- at a depth of about 1 km, indicating a possible denitrification-related source (Yoshida et al., 1989). At this time, the relative importance of the two processes in N_2O production is under debate (Naqvi and Noronha, 1991). Still, a second smaller maximum of N_2O is often located within the lower part of the euphotic zone in the vicinity of the PNM (Hahn, 1975; Hahn, 1981), and has been correlated with high nitrification rates (Yoshida et al., 1989). These data collectively indicate a possibly important source for N_2O within the PNM through the action of nitrifying bacteria. Though much smaller than the deep N_2O maximum, this shallow peak has a greater potential for exchange with the atmosphere, and hence a better understanding of its generation and maintenance is of considerable interest.

SYNOPSIS

The Global Geosciences Program was established by the National Science Foundation in 1987 with two stated goals: (1) to understand the earth-ocean-atmosphere system and how it functions, and (2) to describe and eventually predict major cause-and-effect relationships. Under this program are supported multidisciplinary studies of the "global system": the combination of interrelated physical, chemical and biological processes that regulates the planetary environment and ultimately determines the habitability of Earth.

The Hawaii Ocean Time-series (HOT) project, since October 1988, has made repeated observations of physical, chemical and biological parameters of the North Pacific Ocean at a site 100 km north of the island of Oahu, Hawaii. The site, dubbed Station ALOHA (A Long-term Oligotrophic Habitat Assessment), was chosen to be representative of the North Pacific subtropical gyre, and is visited approximately monthly (Fig. 1.3). The HOT project is funded under the United States-World Ocean Circulation Experiment (U.S.-WOCE) and the United States-Joint Global Ocean Flux Study (U.S.-JGOFS), two components of the Global Geosciences Program focusing on physical oceanographic and biogeochemical processes, respectively (Karl and Lukas, 1995).

In this study, I assess the magnitude of nitrification processes within the euphotic zone at Station ALOHA, and the potential influence of nitrification in this part of the water column on new vs. regenerated production estimates and nitrous oxide generation. I also attempt to clarify the role of nitrification in the maintenance and variability of the PNM. The research has been performed primarily during the regular monthly HOT cruises and in the laboratory between cruises, and is intended as a contribution to the fulfillment of the goals of the HOT project. If nitrogen cycling in the oligotrophic central

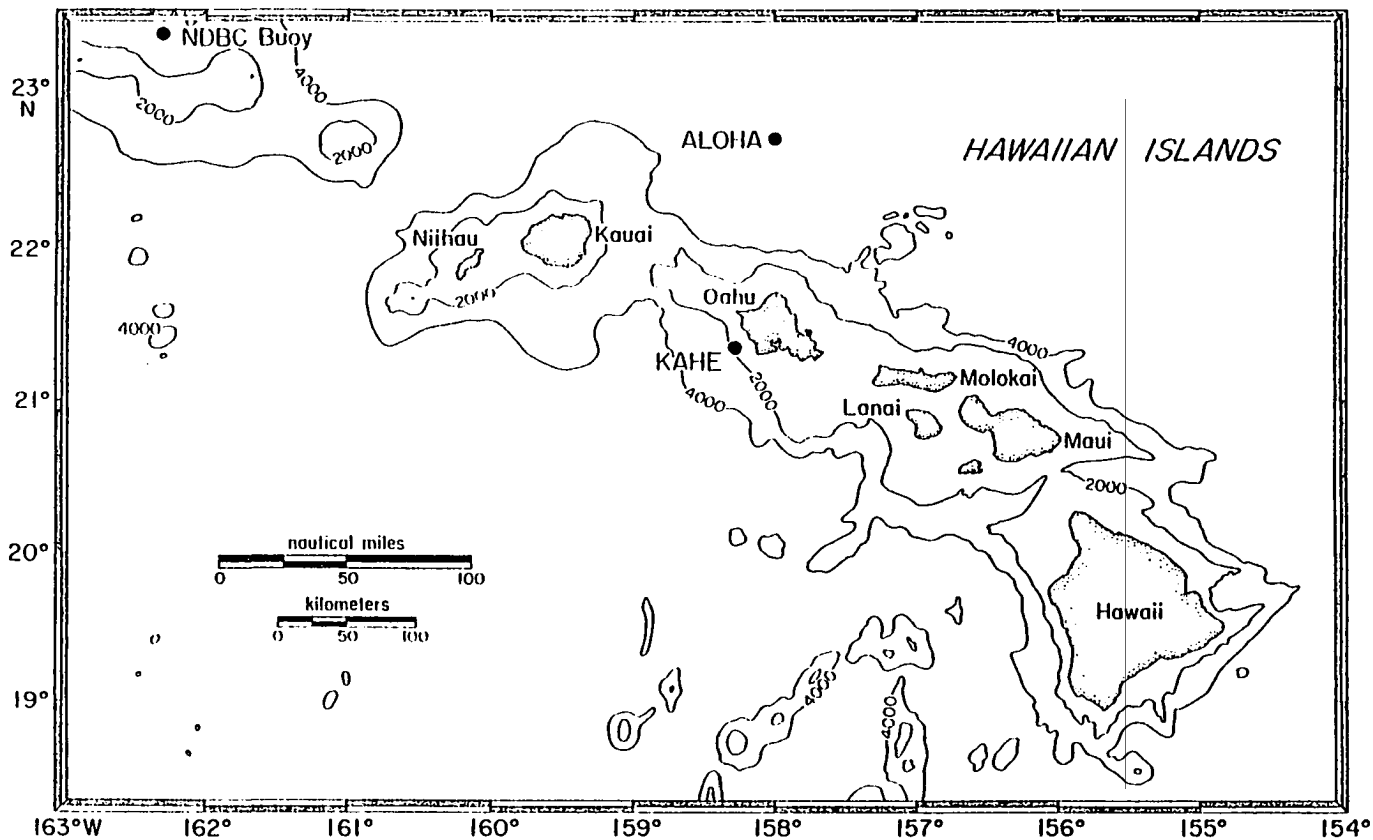


Fig. 1.3. Location of Station ALOHA north of the island of Oahu, Hawaii. The 2000 m and 4000 m isobaths are displayed as solid contour lines. Also shown are our nearshore Station Kahe and a weather buoy operated by the National Data Buoy Center from which we obtain sea surface temperature, wind speed and direction, wave height and wave spectrum data.

oceanic gyres is to be better understood, then the roles of nitrogen fixation, denitrification and nitrification must be analyzed in conjunction with established interdisciplinary programs at representative sites. The influence of N₂ fixation at Station ALOHA has already received some well-deserved attention (Karl et al., 1992; Letelier, 1994; Karl et al., 1995); the addition of the described nitrification study will help to fill in the gaps in our knowledge of oceanic nitrogen cycling.

This document is divided into six chapters, of which this introduction is the first. Chapter 2 deals with the issue of seawater nutrient sample preservation by freezing. Because most of the water samples collected in this study were preserved by freezing, an understanding of the potential effects of freezing on nutrient concentration determinations is critical. This chapter grew out of my own interests in preserving nitrite, nitrate and ammonium samples into a more comprehensive study of the use of freezing to preserve nutrient samples in general, including phosphate and silicate. Chapter 2 has been submitted for publication to *Marine Chemistry* under the authorship of J.E. Dore, T. Houlihan, D.V. Hebel, G. Tien, L. Tupas and D.M. Karl. The results of further experiments dealing with the effects of freezing on nitrite samples are to be found in Chapter 3.

Chapter 3 reports on the time-series study of nitrite distributions in the upper 200 m of the water column that I performed at Station ALOHA, and presents evidence for the vertical separation of the reductive and oxidative processes responsible for nitrite production within the PNM. Also to be found in this chapter are the results of experiments on frozen storage of nitrite samples, and discussion of the distribution of nitrite in deep water and its variability. Chapter 3 has been submitted to *Deep-Sea Research* under the authorship of J.E. Dore and D.M. Karl.

Chapter 4 expands the supporting evidence for the vertical separation hypothesis through the comparison of the upper water column distributions of nitrification rates with concentrations of nitrous oxide, nitrite and nitrate. Nitrous oxide is found to have both a nitrification-related source and an unknown source within the euphotic zone, contributing to its sea-air flux. The upward eddy-diffusive flux of N_2O from below the euphotic zone is found to be only a minor contributor to the mass balance of euphotic zone nitrous oxide. Also, in this chapter I suggest that the observed nitrification rates at Station ALOHA indicate that most nitrate-based production there is actually regenerated, not new, and I present a schematic model of the nitrogen cycle in the euphotic zone at Station ALOHA that includes the nitrification pathway. Chapter 4 is being prepared for submission to *Limnology and Oceanography* under the authorship of J.E. Dore and D.M. Karl.

Chapter 5 combines results from Chapters 3 and 4 into a mechanistic computer model of the primary nitrite maximum, compares the results of trial runs of the model with real data, and discusses the strengths and shortcomings revealed. Finally, Chapter 6 provides a summary of the results of this study and suggests directions for future research.

REFERENCES

- Allredge, A.L. and Y. Cohen. 1987. Can microscale chemical patches persist in the sea? Microelectrode study of marine snow, fecal pellets. *Science* **235**:689-691.
- Antia, N.J., B.R. Berland and D.J. Bonin. 1980. Proposal for an abridged nitrogen turnover cycle in certain marine planktonic systems involving hypoxanthine-guanine excretion by ciliates and their reutilization by phytoplankton. *Mar. Ecol. Prog. Ser.* **2**:97-103.
- Bock, E. 1965. Vergleichende untersuchngen über die wirkung sichtbaren lichtetes auf *Nitrosomonas europaea* and *Nitrobacter winogradskyi*. *Arch. Mikrobiol.* **51**:18-41.
- Brandhorst, W. 1959. Nitrification and denitrification in the eastern tropical North Pacific. *J. Cons. Perm. Int. Explor. Mer.* **25**:2-20.
- Caperon, J. and J. Meyer. 1972. Nitrogen-limited growth of marine phytoplankton II. Uptake kinetics and their role in nutrient limited growth of phytoplankton. *Deep-Sea Res.* **19**:619-632.
- Carlucci, A.F., E.O. Hartwig and P.M. Bowes. 1970. Biological production of nitrite in seawater. *Mar. Biol.* **7**:161-166.
- Carpenter, E.J. 1983. Nitrogen fixation by marine *Oscillatoria (Trichodesmium)* in the world's oceans. In: Nitrogen in the Marine Environment, E.J. Carpenter and D.G. Capone (eds), Academic Press, New York, pp. 65-104.
- Cicerone, R.J. 1989. Analysis of sources and sinks of atmospheric nitrous oxide (N₂O). *J. Geophys. Res.* **94**:18265-18271.
- Codispoti, L.A. and F.A. Richards. 1976. An analysis of the horizontal sequence of denitrification in the eastern tropical North Pacific. *Limnol. Oceanogr.* **21**:379-388.
- Dore, J.E. and D.M. Karl. 1993. RACER: Distribution of nitrite in the Gerlache Strait. *Antarctic J. U.S.* **27**:164-166.
- Dugdale, R.C. and J.J. Goering. 1967. Uptake of new and regenerated forms of nitrogen in primary productivity. *Limnol. Oceanogr.* **12**:196-206.
- Eppley, R.W. and W. Koeve. 1990. Nitrate use by plankton in the eastern subtropical North Atlantic, March-April 1989. *Limnol. Oceanogr.* **35**: 1781-1788.

- Eppley, R.W. and B.J. Peterson. 1979. Particulate organic matter flux and planktonic new production in the deep ocean. *Nature* **282**:677-680.
- Eppley, R.W., E.H. Renger, E.L. Venrick and M. Mullin. 1973. A study of plankton dynamics and nutrient cycling in the central gyre of the North Pacific Ocean. *Limnol. Oceanogr.* **18**: 534-551.
- Eppley, R.W., J.H. Sharp, E.H. Renger, M.J. Perry and W.G. Harrison. 1977. Nitrogen assimilation by phytoplankton and other microorganisms in the surface waters of the central North Pacific Ocean. *Mar. Biol.* **39**:111-120.
- Fiadeiro, M. and J.D.H. Strickland. 1968. Nitrate reduction and the occurrence of a deep nitrite maximum in the ocean off the west coast of South America. *J. Mar. Res.* **26**:187-201.
- French, D.P., M.J. Furnas and T.J. Smayda. 1983. Diel changes in nitrite concentration in the chlorophyll maximum in the Gulf of Mexico. *Deep-Sea Res.* **30**:707-722.
- Gundersen, K.R., J.S. Corbin, C.L. Hanson, M.L. Hanson, R.B. Hanson, D.J. Russell, A. Stollar and O. Yamada. 1976. Structure and biological dynamics of the oligotrophic ocean photic zone off the Hawaiian Islands. *Pac. Sci.* **30**:45-68.
- Hahn, J. 1975. N₂O measurements in the northeast Atlantic Ocean. "*Meteor*" *Forschungsergeb. Reihe A* **16**:1-14.
- Hahn, J. 1981. Nitrous oxide in the oceans. In: Denitrification, Nitrification, and Atmospheric Nitrous Oxide, C.C. Delwiche (ed), Wiley & Sons, New York, pp. 191-240.
- Harrison, W.G. 1983. Use of isotopes. In: Nitrogen in the Marine Environment, E.J. Carpenter and D.G. Capone (eds), Academic Press, New York, pp. 763-808.
- Harrison, W.G., J. McCarthy, B. von Bodungen and N. Owens. 1989. New production by ¹⁵N. In: SCOR JGOFS Report #6: Core Measurement Protocols. p.29.
- Hattori, A. and E. Wada. 1971. Nitrite distribution and its regulating processes in the equatorial Pacific Ocean. *Deep-Sea Res.* **18**:557-568.
- Herbland, A. and B. Voituriez. 1977. Production primaire, nitrate et nitrite dans l'Atlantique tropical II: distribution du nitrate et production de nitrite. *Cah. ORSTOM ser. Océanogr.* **15**:57-65.

Herbland, A. and B. Voituriez. 1979. Hydrological structure analysis for estimating the primary production in the tropical Atlantic Ocean. *J. Mar. Res.* **37**:87-101.

Houghton, J.T., G.J. Jenkins and J.J. Ephraums (eds). 1990. Climate Change: The IPCC Scientific Assessment, Intergovernmental Panel on Climate Change, Cambridge University Press, Cambridge, 365 pp.

Kaplan, W.A. 1983. Nitrification. In: Nitrogen in the Marine Environment, E.J. Carpenter and D.G. Capone (eds), Academic Press, New York, pp. 139-190.

Karl, D.M. 1986. Determination of in situ microbial biomass, viability, metabolism, and growth. In: Bacteria in Nature, Vol. 2, J.S. Poindexter (ed), Plenum Publishing, New York, pp. 85-176.

Karl, D.M., G.A. Knauer, J.H. Martin and B.B. Ward. 1984. Bacterial chemolithotrophy in the ocean is associated with sinking particles. *Nature* **309**:54-56.

Karl, D.M., R. Letelier, D.V. Hebel, D.F. Bird and C.D. Winn. 1992. *Trichodesmium* blooms and new nitrogen in the North Pacific Gyre. In: Marine Pelagic Cyanobacteria: Trichodesmium and other Diazotrophs, E.J. Carpenter, D.G. Capone and J.G. Rueter (eds), Kluwer Academic, Dordrecht, Netherlands, pp. 219-237.

Karl, D.M., R. Letelier, D. Hebel, L. Tupas, J. Dore, J. Christian and C. Winn. 1995. Ecosystem changes in the North Pacific subtropical gyre attributed to the 1991-92 El Niño. *Nature* **373**:230-234.

Karl, D.M. and R. Lukas. 1995. The Hawaii Ocean Time-series (HOT) program: Background, rationale and field implementation. *Deep-Sea Res.*, submitted.

Karl, D.M. and C.D. Winn. 1984. Adenine metabolism and nucleic acid synthesis: applications to microbiological oceanography. In: Heterotrophic Activity in the Sea, J.E. Hobbie and P.J. LeB. Williams (eds), Plenum Publishing, New York, pp. 197-215.

Kiefer, D.A., R.J. Olson and O. Holm-Hansen. 1976. Another look at the nitrite and chlorophyll maxima in the central North Pacific. *Deep-Sea Res.* **23**:1199-1208.

Kim, K. and H. Craig. 1990. Two-isotope characterization of N₂O in the Pacific Ocean and constraints on its origin in deep water. *Nature* **347**:58-61.

Letelier, R.M. 1994. Studies on the ecology of *Trichodesmium spp.* (Cyanophyceae) in the central North Pacific Gyre. Ph.D. Dissertation, University of Hawaii, Honolulu, Hawaii, 218 pp.

- Longhurst, A.R. and W.G. Harrison. 1989. The biological pump: profiles of plankton production and consumption in the upper ocean. *Prog. Oceanogr.* **22**:47-123.
- Miyazaki, T., E. Wada and A. Hattori. 1973. Capacities of shallow waters of Sagami Bay for oxidation and reduction of inorganic nitrogen. *Deep-Sea Res.* **20**:571-577.
- Miyazaki, T., E. Wada and A. Hattori. 1975. Nitrite production from ammonia and nitrate in the euphotic layer of the western North Pacific Ocean. *Mar. Sci. Comm.* **1**:381-394.
- Müller-Neuglück, M. and H. Engel. 1961. Photoinaktivierung von *Nitrobacter winogradskyi* Buch. *Arch. Mikrobiol.* **39**:130-138.
- Naqvi, S.W.A. and R.J. Noronha. 1991. Nitrous oxide in the Arabian Sea. *Deep-Sea Res.* **38**:871-890.
- Olson, R.J. 1980. Studies of biological nitrogen cycle processes in the upper waters of the ocean, with special reference to the primary nitrite maximum. Ph.D. Dissertation, University of California San Diego, San Diego, CA.
- Olson, R.J. 1981a. ¹⁵N tracer studies of the primary nitrite maximum. *J. Mar. Res.* **39**:203-226.
- Olson, R.J. 1981b. Differential photoinhibition of marine nitrifying bacteria: a possible mechanism for the formation of the primary nitrite maximum. *J. Mar. Res.* **39**:227-238.
- Olson, R.J., J.B. SooHoo and D.A. Kiefer. 1980. Steady state growth of the marine diatom *Thalassiosira pseudonana*: the uncoupled kinetics of nitrate uptake and nitrite production. *Plant Physiol.* **66**:383-389.
- Palenik, B. and F.M.M. Morel. 1991. Amine oxidases of marine phytoplankton. *Appl. Environ. Microbiol.* **57**:2440-2443.
- Paul, J.H. 1983. Uptake of organic nitrogen. In: Nitrogen in the Marine Environment, E.J. Carpenter and D.G. Capone (eds), Academic Press, New York, pp. 275-308.
- Platt, T., W.G. Harrison, M.R. Lewis, W.K.W. Li, S. Sathyendranath, R.E. Smith and A.F. Vezina. 1989. Biological production of the oceans: the case for a consensus. *Mar. Ecol. Prog. Ser.* **52**:77-88.
- Priscu, J.C. and M.T. Downes. 1985. Nitrogen uptake, ammonium oxidation and nitrous oxide (N₂O) levels in the coastal waters of western Cook Strait, New Zealand. *Estuarine Coastal Shelf Sci.* **20**:529-542.

- Rakestraw, N. W. 1936. The occurrence and significance of nitrite in the sea. *Biol. Bull. (Woods Hole)* 71:133-167.
- Ryther, J.H. 1959. Potential productivity of the sea. *Science* 130:602-608.
- Schön, G.H. and H. Engel. 1962. Der einfluß des lichtetes auf *Nitrosomonas europaea* Win. *Arch. Mikrobiol.* 42:415-428.
- Shaffer, G. 1993. Effects of the marine biota on global carbon cycling. In: The Global Carbon Cycle, M. Heimann (ed), NATO ASI ser. I vol. 15, Springer-Verlag, Berlin, pp. 431-455.
- Sharp, J.H. 1983. The distribution of inorganic nitrogen and dissolved and particulate organic nitrogen in the sea. In: Nitrogen in the Marine Environment, E.J. Carpenter and D.G. Capone (eds), Academic Press, New York, pp. 1-36.
- Vaccaro, R.F. and J.H. Ryther. 1960. Marine phytoplankton and the distribution of nitrite in the sea. *J. Cons. Perm. Int. Explor. Mer.* 25:260-271.
- Verjbinskaya, N. 1932. Observations on the nitrite changes in the Barents Sea. *J. Cons. Perm. Int. Explor. Mer.* 7:47-52.
- Vincent, W.F., M.T. Downes and C.L. Vincent. 1981. Nitrous oxide cycling in Lake Vanda, Antarctica. *Nature* 292:618-620.
- Wada, E. and A. Hattori. 1971. Nitrite metabolism in the euphotic layer of the central North Pacific Ocean. *Limnol. Oceanogr.* 16:766-772.
- Wada, E. and A. Hattori. 1972. Nitrite distribution and nitrate reduction in deep sea waters. *Deep-Sea Res.* 19:123-132.
- Wada, E. and A. Hattori. 1991. Nitrogen in the Sea: Forms, Abundances, and Rate Processes, CRC Press, Boca Raton, FL. 208 pp.
- Ward, B.B. 1982a. Marine ammonium-oxidizing bacteria: abundance and activity in the northeast Pacific Ocean. Ph.D. Dissertation, University of Washington, Seattle, WA.
- Ward, B.B. 1982b. Oceanic distribution of ammonium-oxidizing bacteria determined by immunofluorescent assay. *J. Mar. Res.* 40:1155-1172.
- Ward, B.B. 1986. Nitrification in marine environments. In: Nitrification, J.I. Prosser (ed), IRL Press, Oxford, pp. 157-184.

- Ward, B.B. 1987. Nitrogen transformations in the Southern California Bight. *Deep-Sea Res.* **34**:785-805.
- Ward, B.B. and A.F. Carlucci. 1985. Marine ammonia- and nitrite-oxidizing bacteria: serological diversity determined by immunofluorescence in culture and in the environment. *Appl. Environ. Microbiol.* **50**:194-201.
- Ward, B.B., K.A. Kilpatrick, E.H. Renger and R.W. Eppley. 1989. Biological nitrogen cycling in the nitracline. *Limnol. Oceanogr.* **34**:493-513.
- Ward, B.B., R.J. Olson and M.J. Perry. 1982. Microbial nitrification rates in the primary nitrite maximum off southern California. *Deep-Sea Res.* **29**:247-255.
- Watson, S.W. 1965. Characteristics of a marine nitrifying bacterium, *Nitrosocystis oceanus* sp.n. *Limnol. Oceanogr. (Suppl.)* **10**:R274-R289.
- Yoshida, N. 1988. ¹⁵N-depleted N₂O as a product of nitrification. *Nature* **335**:528-529.
- Yoshida, N., H. Morimoto, M. Hirano, I. Koike, S. Matsuo, E. Wada, T. Saino and A. Hattori. 1989. Nitrification rates and ¹⁵N abundances of N₂O and NO₃⁻ in the western North Pacific. *Nature* **342**:895-897.

CHAPTER 2

FREEZING AS A METHOD OF SAMPLE PRESERVATION FOR THE ANALYSIS OF DISSOLVED INORGANIC NUTRIENTS IN SEAWATER

ABSTRACT

The marine chemist is often faced with situations in which collected seawater samples for inorganic nutrient measurements may not be analyzed immediately. It is therefore of importance to establish preservation and storage techniques that will ensure sample integrity and not alter the precision or accuracy of analysis. For most oceanic waters, the immediate freezing of an unfiltered water sample in a clean polyethylene bottle is a suitable preservation method. This procedure is simple, it avoids potentially contaminating sample manipulations and chemical additions, and it adequately preserves the concentrations of nitrite, nitrate+nitrite, phosphate, silicate, and ammonium within a single water sample.

INTRODUCTION

Accurate measurements of dissolved nutrient concentrations in seawater are essential to the goals of many oceanographic research programs. Because the concentrations of the major nutrients in unpreserved seawater samples are altered, sometimes rapidly, by physical, chemical and biological processes, such samples must be analyzed immediately or preserved in a manner that successfully maintains the original concentrations of the species of interest until analyses can be performed. Unfortunately,

the nature of oceanographic research often prevents immediate at-sea chemical determinations from being made, whether due to heavy seas, inadequate lab space, improper electric power conditioning, hazard of contamination, lack of capable personnel or any of a myriad of other difficulties potentially encountered aboard a research vessel. Even when these problems can be solved, it may still be undesirable to perform at-sea analyses if the potential errors introduced as a result of working in a shipboard environment exceed the potential errors introduced through sample preservation and storage. It is therefore of great interest to marine chemists to find suitable preservation and storage methods for each of the major nutrients in seawater.

A successful preservation technique must maintain the original concentration of an analyte during storage to within the level of accuracy required by the particular program. Beyond this absolute requirement, there are a number of additional criteria to evaluate, including simplicity, relative ease of operation and rapid implementation. The ideal method would not require exposure of the sample to potentially contaminating materials or environments. If possible, chemical additions to the sample would be avoided. Finally, the optimal method will preserve all of the constituents of interest in a single sample without requiring different procedures for different chemical species.

For decades marine chemists have tested the suitability of various preservation techniques, considering the potential effects of filtration, storage container, temperature, chemical additions and radiation on samples of different water types. The considerable body of literature produced presents varied and often contradictory opinions on the effectiveness of preservation methods. Freezing of water samples in polyethylene containers is a very popular method, as it holds all of the desirable qualities listed above. Nevertheless, there is not total agreement as to whether freezing maintains the original nutrient concentrations within a sample to an acceptable degree of accuracy.

In this paper we will focus on the freezing method for the preservation of the concentrations in seawater of nitrite (NO_2^-), nitrate+nitrite (N+N), soluble reactive phosphate (SRP), soluble reactive silicate (SRSi) and ammonium (NH_4^+).

BACKGROUND

It will be instructive to first review the literature dealing with the preservation of nutrients by freezing (Table 2.1). Some general conclusions are evident:

- (1) Although slightly lower values of $[\text{NO}_2^-]$ have been noted after freezing (Thayer, 1970; Dore and Karl, 1995), such decreases are well within the analytical precision of both manual and automated analytical techniques, and only marginally detectable by highly sensitive chemiluminescent analyses.
- (2) Most studies agree that N+N concentrations are adequately preserved by freezing.
- (3) SRP appears to be problematic. Most investigators have found preservation by freezing to be effective, but some report a lowering of $[\text{SRP}]$ after prolonged frozen storage (Gilmartin, 1967; Clementson and Wayte, 1992).
- (4) It is generally agreed that $[\text{SRSi}]$ in seawater is adequately preserved by freezing except for losses to polymerization that occur when concentrations are high or pH is low. There are different opinions as to the SRSi concentration at which this effect becomes a problem (MacDonald et al., 1986; Chapman and Mostert, 1990).

Table 2.1. Chronology of research into the effects of sample freezing on dissolved nutrient assays of natural waters

Year	Reference	Methods ^a	Containers ^b	Recommendations ^c					Notes ⁱ
				N+N ^d	NO ₂ ^{-e}	SRP ^f	SRSi ^g	NH ₄ ^{+h}	
1953	Collier and Marvin	M	G	ND	ND	(+)	ND	ND	coastal seawater, filt. or unfilt.; quick-frozen
1962	Heron	M	PE	ND	ND	+	ND	ND	lake water, filt. or unfilt.; quick-frozen; bottles treated w/ iodine
1962	Proctor	M	PX	ND	+	ND	ND	ND	seawater, filt.; >7 mo storage
1965	Marvin and Proctor	M	G	ND	ND	ND	ND	+	estuarine water, filt.
1967	Fitzgerald and Faust	M	NS	ND	ND	(+)	ND	ND	algal cultures; filt. required
1967	Gilmartin	M	PE	ND	ND	(+)	ND	ND	estuarine water; phosphate ok if run immed. after thaw
1967	Kobayashi	NS	NS	(+)	ND	ND	(+)	ND	river and stream water; silicate losses from low salinity samples, recoverable by prolonged thaw; recommendation for nitrate made without direct comparison of fresh vs. frozen
1967	Newell	M	PE	ND	ND	ND	ND	(+)	Eng. Channel seawater; all low conc. (<1 μM, mean 0.3 μM); no def. trend but increased variability

Table 2.1. (Cont.) Chronology of research into the effects of sample freezing on dissolved nutrient assays of natural waters

1968	Jenkins	M	G, UP	(+)	-	(+)	ND	-	S.F. Bay estuarine water; glass used for SRP; nitrate and phosphate ok but preserved better when poisoned and refrigerated	
1969	Charpiot	AA	PE	(+)	-	-	-	ND	Mediterranean seawater; no SRP data (just suggestion); nitrate ok except losses from one deep sample	
1970	Burton et al.	M	PE	ND	ND	ND	+	ND	seawater, filt.; all low conc (<30 μM)	
27	1970	Thayer	M	PE	(+)	(+)	+	ND	(+)	estuarine water; nitrate and nitrite results depend on time of year; ammonium stable but 6% low
1971	Truesdale	M	NS	ND	ND	ND	ND	ND	-	seawater, unfiltered; large ammonium increases (contamination?)
1972	Strickland and Parsons	RO	RO	+	(+)	+	(+)	(+)	(+)	no data, just review; suggest no prolonged nitrite storage; silicate losses at high conc.; prefer not to store ammonium samples; suggest filt. for DOC
1973	Degobbis	M	G, PE	ND	ND	ND	ND	ND	+	offshore and inshore seawater; slow freezing; filtered

Table 2.1. (Cont.) Chronology of research into the effects of sample freezing on dissolved nutrient assays of natural waters

	1975	Johnson et al.	M	G	ND	ND	-	ND	ND	streamwater; phosphate losses, esp. when particles present; formation of calcite residue noted
	1975	Carpenter and McCarthy	NS (Man?)	NS	ND	ND	ND	ND	-	seawater; no direct comparison, just suggestion that erroneously high values may have been due to freezing of samples
	1975	Riley	RO	RO	(+)	(+)	(+)	(+)	(+)	no data, just review; suggest freezing ok but point out contradictions in literature
28	1976	Klingaman and Nelson	Man	UP	(+)	ND	(+)	ND	(+)	river/runoff water, filt. or unfilt.; phosphate ok if filt.; nitrate and ammonium, better results if frozen w/chem. preservative
	1977	Eppley et al.	NS (M?)	NS	ND	ND	ND	ND	-	oligo. N. Pac. seawater; no data, just suggestion that erroneously high values may be due to freezing
	1981	Perry and Eppley	M	NS	ND	ND	ND	ND	-	oligo. N. Pac. seawater; no data, just suggestion that erroneously high values may be due to freezing

Table 2.1. (Cont.) Chronology of research into the effects of sample freezing on dissolved nutrient assays of natural waters

1981	Ryle et al.	AA	PE	+	+	+	ND	ND	tropical seawater; 1 mo. storage
1982	MacDonald and McLaughlin	AA	G, PS	+	ND	(+)	(+)	ND	coastal and estuarine water; suggest filt. for phosphate; silicate losses at low salinity
1982	Morse et al.	AA, M	G, PE, T	-	ND	-	-	-	Gulf Stream seawater; find > 30% changes after 1-7 days freezing to be common, even in deep samples; no other study shows such poor preservation
1983	Grasshoff et al.	RO	RO	+	-	+	+	(+)	recommendations only, no data; suggest filt. for DOC, unfilt. for ammonium; insist on immed. analysis for nitrite
1984	Parsons et al.	RO	RO	+	-	(+)	(+)	+	no data, just review; insist nitrite be run immed.; suggest analyst check freezing for phosphate changes; silicate losses at high conc. (> 50 μM)
1985	Venrick and Hayward	AA	PE, PS	-	ND	-	-	ND	seawater; find freezing to be best preservation method but deny that it is suitable; insist fresh analyses essential
1986	Kremling and Wenck	AA	PP	+	ND	+	+	ND	100 and 2000 m N. Atlantic seawater

Table 2.1. (Cont.) Chronology of research into the effects of sample freezing on dissolved nutrient assays of natural waters

1986	MacDonald et al.	AA, M	UP	ND	ND	ND	(+)	ND	estuarine and seawater; silicate losses at high conc.
1986	Salley et al.	AA, M	NS	+	+	+	-	+	estuarine samples; 7-28 d storage
1986	Smith et al.	AA	PE	+	ND	+	ND	+	N. Pac. seawater, filt.; do not show data but mention "repeated controlled experiments"
1989	Walsh	AA	NS	+	ND	+	(+)	+	coastal and offshore seawater; silicate losses at high conc. (> 80 μ M), recoverable by prolonged thaw
1990	Chapman and Mostert	AA, M	HDPE, PX	+	ND	-	(+)	ND	subtropical seawater, 8 wk storage; silicate losses at high conc.
1990	Sakamoto et al.	AA	NS	ND	ND	ND	(+)	ND	seawater; silicate losses at high conc. (> 65 μ M), recoverable by warming sample after thaw
1992	Clementson and Wayte	AA	HDPE, PP	+	ND	(+)	ND	ND	open ocean seawater, filt.; probs. w/long-term phosphate storage, short-term ok
1992	Karl and Tien	MAGIC	HDPE	ND	ND	(+)	ND	ND	no data, just suggestion that freezing adequately preserves phosphate

Table 2.1. (Cont.) Chronology of research into the effects of sample freezing on dissolved nutrient assays of natural waters

1992	Takenaka et al.	IC	G, PE, SS	(+)	-	ND	ND	ND	found nitrite oxidation to nitrate accelerated by freezing in dilute acidic water samples; does not affect sum of nitrate+nitrite
1993	Avanzino and Kennedy	AA	HDPE, LDPE	+	ND	+	ND	+	streamwater; long-term storage (up to 8 yr); problems only w/ precip.-forming waters
1993	Dore et al.	AA, M	HDPE	ND	ND	ND	ND	(+)	Antarctic seawater, filt.; fresh and frozen ammonium equivalent except at low end where fresh>froz.; suggest contam. in fresh samples
1993	Gordon et al.	RO	RO	(+)	(+)	(+)	(+)	ND	seawater; no data, just suggestions; insist freezing samples be used only as last resort; insist quick-thaw necessary; suggest silica re-runs after 24 hr for samples > 40 µM
1995	Dore and Karl	C	HDPE	ND	+	ND	ND	ND	0-4800 m oligo. N. Pac. seawater; low levels (< 100 nM)

a) Analysis methods used: AA = automated colorimetric analysis; C = chemiluminescence; IC = ion chromatography; MAGIC = magnesium-induced co-precipitation; M = manual colorimetric analysis; NS = method not specified in reference; RO = recommendations only, reference may review several published data sets using various methods.

Table 2.1. (Cont.) Chronology of research into the effects of sample freezing on dissolved nutrient assays of natural waters

b) Container material used: G = glass; HDPE = high-density polyethylene; LDPE = low-density polyethylene; NS = container material not specified in reference; PE = polyethylene (density unspecified); PP = polypropylene; PS = polystyrene; PX = Pyrex; RO = recommendations only, reference may review several published data sets using various container materials; SS = stainless steel; T = Teflon; UP = unspecified plastic.

c) Recommendations: "+" = freezing recommended for storage; "(+)" = freezing conditionally recommended for storage (see notes); "-" = freezing not recommended for storage; ND = no discussion of the freezing of this constituent in reference.

d) N+N = nitrate plus nitrite, measured as nitrite after reduction of nitrate.

e) NO_2^- = nitrite

f) SRP = soluble reactive phosphate

g) SRSi = silicate, measured as dissolved reactive monosilicic acid

h) NH_4^+ = ammonium (plus ammonia)

i) Notes concerning the analytes for which conditional recommendation is given, and/or other information vital to the interpretation of the cited literature.

- (5) Although increases in variability may occur upon freezing ammonium samples, these are generally on the same order as the analytical variability. The elevated ammonium concentrations reported by Carpenter and McCarthy (1975), Eppley et al. (1977) and Perry and Eppley (1981) were never conclusively traced to the freezing process.

- (6) Two frequently cited investigations (Morse et al., 1982; Venrick and Hayward, 1985) conclude that no nutrients may be adequately preserved by freezing. We will discuss each of these in some detail later in this paper, as they comprise the bulk of the results that do not support freezing as a preservation method.

It is our intention to clarify some of the ambiguities encountered in the literature on this subject through the re-examination of published data and the presentation of our own data on sample preservation by freezing. We believe that for oxic oceanic waters of low particulate load all of the above referenced constituents may be preserved to a level of accuracy consistent with the goals of most oceanographic programs through the use of a single preservation method: slow freezing of unfiltered samples in clean polyethylene bottles in the dark at -20°C, with continued storage under the same conditions.

MATERIALS AND METHODS

Sample collection

The Hawaii Ocean Time-series (HOT) project has maintained a deep water oceanic station dubbed ALOHA (A Long-term Oligotrophic Habitat Assessment; Karl and Lukas,

1995) since October 1988 (Fig. 1.3). Station ALOHA, located at 22°45' N, 158° W, is occupied at approximately monthly intervals for the collection of physical, chemical and biological data relevant to the goals of the U.S.-JGOFS and U.S.-WOCE programs. Discrete water samples are collected from hydrocasts using a CTD-rosette system outfitted with 24 twelve liter PVC sampling bottles with Teflon-coated springs. During each HOT cruise, samples for a suite of inorganic and organic constituents are collected over the entire 4750 m water column.

All water samples analyzed for this study were collected at Station ALOHA during regular HOT cruises, with the following exceptions. Because ammonium concentrations at Station ALOHA are near or below the approximate analytical detection limit of 0.1 μM by the standard manual colorimetric method, storage experiments were not conducted. An ammonium storage experiment was carried out at Station 500.080 (65°21.41' S, 66°27.84' W) of the Palmer Long-Term Ecological Research (LTER) grid, near Renaud Island off the Antarctic Peninsula. A storage experiment for nitrite was also carried out at the same site. These samples were collected during cruise NBP93-02 of the RVIB Nathaniel B. Palmer using a twelve-place CTD-rosette system with external-closure PVC Niskin bottles (General Oceanics).

Depending upon the individual experiment, samples analyzed for this study were collected either in 125 or 500 ml high-density polyethylene (HDPE) bottles, or in 4 l polycarbonate (PC) bottles from which subsamples were decanted into individual HDPE bottles. Collection bottles were always acid-washed (3x with 1 M HCl), rinsed 3x with deionized distilled water (DDW) and completely dried before use. Each bottle was also rinsed 3x with sample before collection. No samples were prefiltered except those indicated in the filtration experiments, which were vacuum filtered through acid-washed Whatman GF/F filters using polycarbonate Millipore filtration manifolds. All freezing was

done in 125 or 500 ml HDPE bottles, filled about 2/3 full and stored upright so as to prevent the seawater from freezing out around the screw-cap. Freezing was achieved by immediate placement of samples into a -20°C walk-in or upright chest freezer. Samples remained frozen at -20°C in the dark until 4-12 hr before analysis, at which time they were completely thawed at room temperature in air or in a water bath, and allowed to achieve laboratory temperature.

Analytical methods

Most of the [N+N], [SRP] and all of the [SRSi] analyses in this study were carried out on a 4-channel continuous flow Technicon Autoanalyzer II® by Mr. Ted Walsh of Analytical Services, SOEST, University of Hawaii. The methods used follow those recommended by Technicon Industrial Systems (1973, 1977, 1979) with only slight modifications to surfactant concentrations, sampling rate and pump tube size (T. Walsh, pers. comm.). These analytical techniques are adaptations of the N+N method of Armstrong et al. (1967), the SRP method of Murphy and Riley (1962) and the SRSi method of Strickland and Parsons (1972). DDW is used as the diluent for all reagents and to establish the baseline. Seawater refractive index and turbidity blanks are used to correct each type of analysis. The SRP color reagent and all calibration standards are made fresh daily, the latter through dilution of high-concentration stocks with filtered low-nutrient seawater (usually surface water from Station ALOHA). Each standard is corrected for the absorbance of the seawater diluent and each sample is corrected for its blank absorbance at the appropriate wavelength. Accuracy was maintained through the use of internal standards and certified reference standards (CSK; Ambe, 1978). The detection limits and approximate analytical precisions for the autoanalyses are as follows:

N+N, detection limit = 0.03 μM , precision = $\pm 0.3\%$; SRP, detection limit = 0.02 μM , precision = $\pm 0.5\%$; SRSi, detection limit = 0.3 μM , precision = $\pm 1.5\%$. The stated precisions are for samples with N+N, SRP and SRSi concentrations $>0.2 \mu\text{M}$, $> 0.4 \mu\text{M}$ and $>2 \mu\text{M}$, respectively; for samples below these levels we estimate the precision to be on the order of the value of the detection limit.

Standard manual analyses were used for both ammonium and nitrite determinations. Ammonium determinations followed the phenol-hypochlorite method as described by Strickland and Parsons (1972), except that tightly-capped 50 ml polystyrene tubes were used as reaction flasks and color development was accelerated by keeping samples at 50 °C for 1 hr after reagent additions and then allowing them to return to room temperature before reading their absorbances. The detection limit for ammonium is about 0.10 μM and the approximate precision is $\pm 0.07 \mu\text{M}$. Nitrite was determined using the azo dye method as described by Strickland and Parsons (1972), again using polystyrene tubes for color development, but without heating. The detection limit for nitrite is about 0.01 μM and the approximate precision is $\pm 0.02 \mu\text{M}$.

Selected samples for nitrate+nitrite were also analyzed using the chemiluminescent technique developed by Cox (1980) and modified for seawater by Garside (1982). This method involves wet chemical reduction of the species of interest to nitric oxide with subsequent detection in a commercial chemiluminescent nitrogen detector (Antek model 720). No major modifications to the Garside procedure were used. The detection limit for N+N has been estimated to be approximately 1-2 nM, with a precision of $\pm 0.5 \text{ nM}$ for samples with $[\text{N+N}] \leq 50 \text{ nM}$ and $\pm 1.6\%$ for higher concentrations (Dore and Karl, 1995).

Selected samples were analyzed for [SRP] using the magnesium-induced coprecipitation (MAGIC) method developed by Karl and Tien (1992). This method involves the pre-concentration of SRP through co-precipitation with brucite ($\text{Mg}(\text{OH})_2$),

followed by analysis using the standard molybdenum blue color reaction. The detection limit is about 1 nM and the approximate precision of the analysis is $\pm 3\%$.

Experiments on the effects of freezing samples

We performed a series of experiments to assess sample integrity of unfiltered seawater samples during a freeze-thaw cycle. These experiments were designed to simulate normal HOT sampling procedures and therefore analysis of stored samples was made within one month of collection, usually considerably sooner.

In the N+N experiment, samples were taken from a number of depths from 0-150 m into replicate HDPE bottles. One set was immediately placed into the freezer and the other was analyzed at-sea using the chemiluminescent method. All at-sea analyses were completed within 8 hr of collection, and during this time the bottles were stored in the dark at 4°C. Frozen samples were analyzed 26 d later at our shore-based laboratory.

The experiments for nitrite and ammonium were conducted simultaneously on the same samples at a station near the Antarctic Peninsula. Water from a number of depths in the upper 200 m was collected, split and stored as described above for N+N. Both fresh and frozen analyses were performed aboard ship, the latter occurring after 3 d of frozen storage. No prefiltration was used. Standard manual methods were used for analyses (Strickland and Parsons, 1972). Additional experiments on the frozen storage of nitrite samples using chemiluminescent $[\text{NO}_2^-]$ determinations have been reported elsewhere (Dore and Karl, 1995).

The SRP experiment was performed in a similar manner, except fresh analyses were not performed at-sea. Several depths at Station ALOHA were sampled and from each a 4 l polycarbonate bottle was filled. These bottles were maintained in the dark at

4°C until the day of the fresh analyses, at which time triplicate subsamples were taken in HDPE bottles. Two sets were then frozen immediately and the third analyzed using the MAGIC procedure. The frozen sets were analyzed one week and two weeks later. Because no at-sea determinations were made, the phosphate concentrations in these samples cannot be related to the in situ values. However, because the fresh analyses occurred immediately upon sample splitting, the results accurately reflect the potential freezing effects on SRP determinations.

The SRSi data represent a compilation of several experiments designed to determine the extent of silica polymerization due to freezing. The experiments compare frozen and refrigerated samples analyzed on shore within one week of their collection at Station ALOHA. Because the "control" samples were not analyzed immediately but rather kept at 4°C for several days, these experiments do not directly assess the fresh vs. frozen question, but instead focus on the polymerization problem. Autoanalytical methods were used for the SRSi determinations in these experiments.

Statistical analysis of each of the experiments on freezing samples was accomplished using Model II reduced major axis (geometric mean) linear regression following the recommendations of Ricker (1973, 1975). The confidence intervals of the slope and y-intercept were calculated based on the recommendations of Jolicoeur and Mossimann (1968) and York (1966), respectively.

Experiments on the filtration of samples

We performed experiments on N+N, SRP and SRSi to determine if filtration resulted in any differences in the frozen sample results. Samples were vacuum filtered through acid-washed 47 mm glass fiber filters (Whatman GF/F) into acid-washed DDW-

rinsed Millipore polycarbonate filtration manifolds. Filtered sample was used to rinse the manifold reservoir 3x, then to rinse the HDPE sample bottles 3x. Replicate HDPE bottles were immediately frozen and returned to the shore, where within one week they were thawed and measured by autoanalysis. As with the freezing experiments, statistical analysis of each of the experiments on filtering samples was accomplished using Model II linear regression.

Experiments on the long-term frozen storage of samples

We performed experiments on N+N, SRP and SRSi to determine if the long-term (>1 mo) frozen storage of seawater samples would affect nutrient concentrations beyond any effect of the freezing process itself. From three depths at Station ALOHA, a large number of replicate samples were collected and immediately frozen. Several were measured by autoanalysis after 4 d frozen storage to establish the initial nutrient concentrations and variability. At approximately monthly intervals thereafter, an individual sample from each depth was thawed and re-analyzed, until no more samples remained. Statistical analysis of the N+N, SRP and SRSi long-term frozen storage experiments was accomplished with a Student's t-test (Sokal and Rohlf, 1981), by comparing the set of initial replicates with the combined replicates from later time points.

RESULTS

Experiments on the effects of freezing samples

Model II regression analyses of the frozen onto the fresh (or refrigerated in the case of SRSi) results reveal no significant deviation from a 1:1 correspondence based on the 99% confidence intervals of slope and y-intercept for NO_2^- , N+N, SRP, SRSi (<120 μM), and NH_4^+ (Figs. 2.1 and 2.2, Table 2.2). The same holds true when the 95% confidence intervals are applied, except for a slight significant increase in slope for the chemiluminescent nitrate+nitrite analyses. Some loss of precision after freezing is evident for SRP, as 4 of 16 SRP samples exhibit changes after freezing of more than twice the precision of the MAGIC analysis; however, none of these differences exceeds twice the precision of the autoanalytic method. In addition, if we examine individual replicates for the other analyses, we find that there are very few samples falling outside of the envelopes defined by twice the analytical precision of each analysis (for NH_4^+ , 1 of 8; for < 120 μM SRSi, 1 of 110; for NO_2^- , 0 of 8; for N+N, 0 of 8).

Experiments on the filtration of samples

Model II regression analyses of the filtered onto the unfiltered results reveal no significant deviation from a 1:1 correspondence using the 95% confidence intervals of slope and intercept for N+N and SRP (Fig. 2.3 and Table 2.2). A slight positive intercept for SRSi suggests leaching of silicate from the glass fiber filters. Because the volume filtered is constant, this amount tends to be constant, as indicated by the near-perfect slope of the regression line. None of the SRP samples (n=11) or SRSi samples (n=11), and

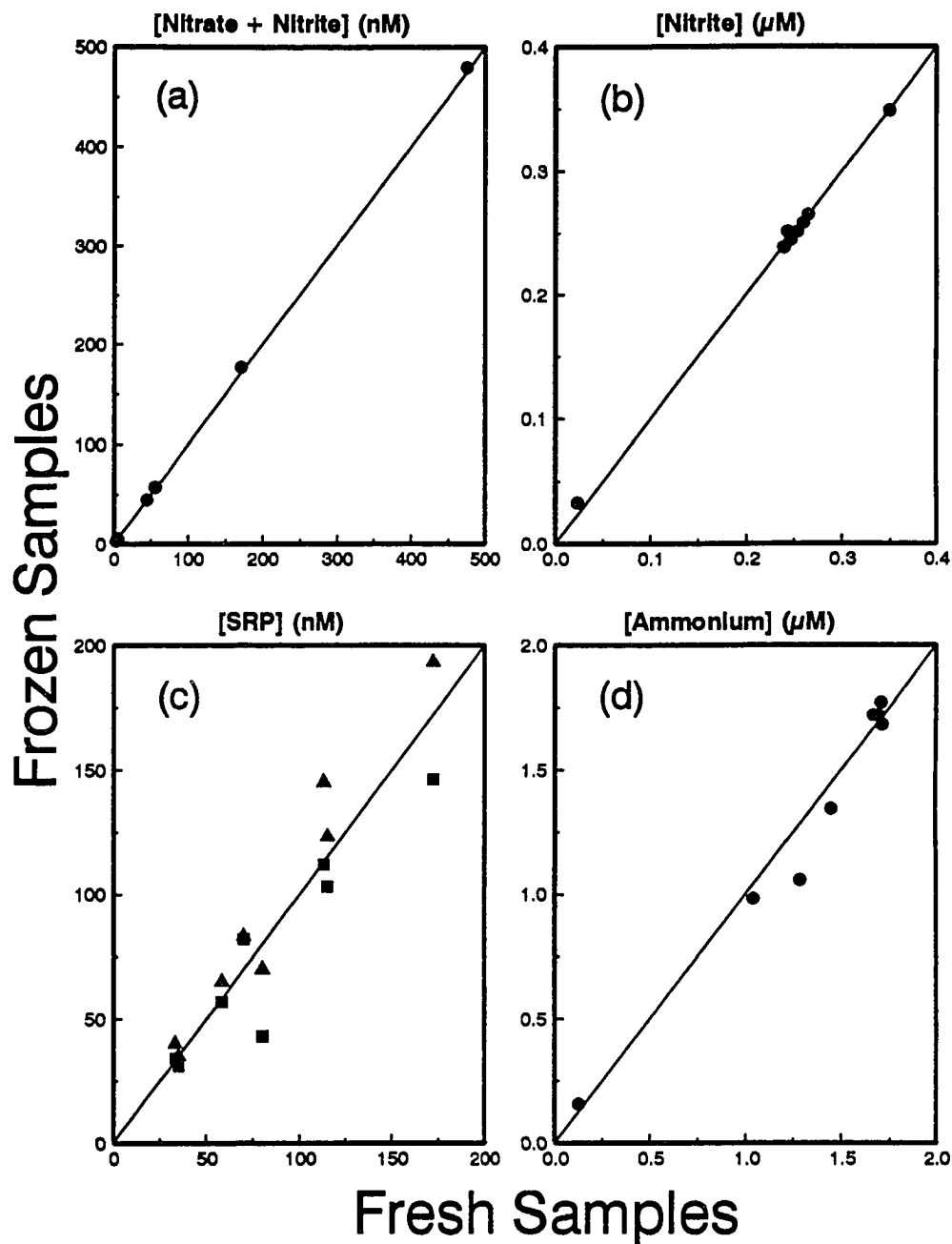


Fig. 2.1. Plots of frozen vs. fresh concentration determinations on unfiltered samples: (a) nitrate+nitrite as determined by chemiluminescence, (b) nitrite as determined by manual colorimetry, (c) soluble reactive phosphate as determined by MAGIC, (d) ammonium as determined by manual colorimetry. The solid line in each plot represents a perfect 1:1 relationship for comparison. Linear regression statistics are listed in Table 2.2.

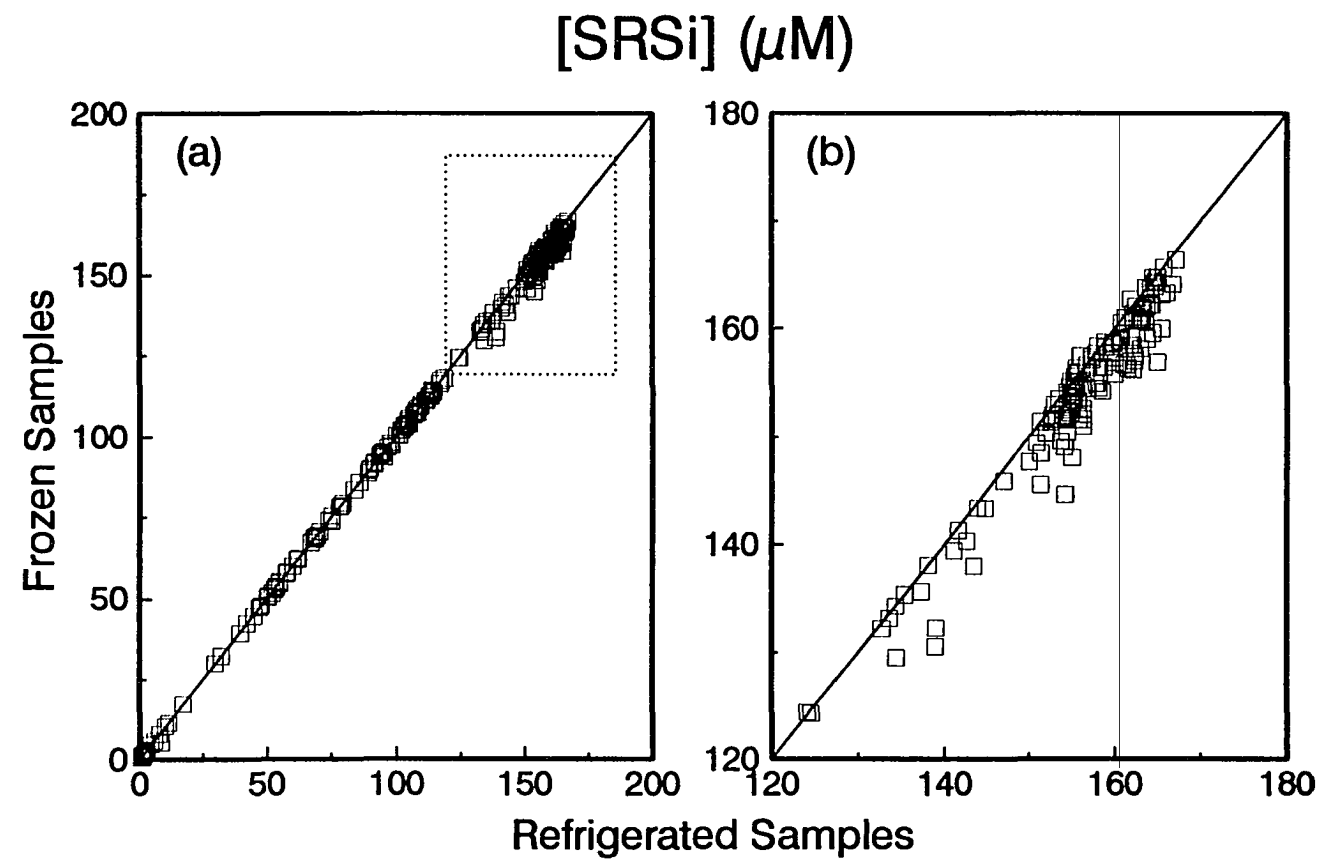


Fig. 2.2. Plot of frozen vs. refrigerated concentration determinations on unfiltered samples: (a) soluble reactive silicate as determined by autoanalysis, full range of data shown, (b) soluble reactive silicate, only values $>120 \mu\text{M}$ shown to emphasize polymerization losses. The solid line in each plot represents a perfect 1:1 relationship for comparison. Linear regression statistics are listed in Table 2.2.

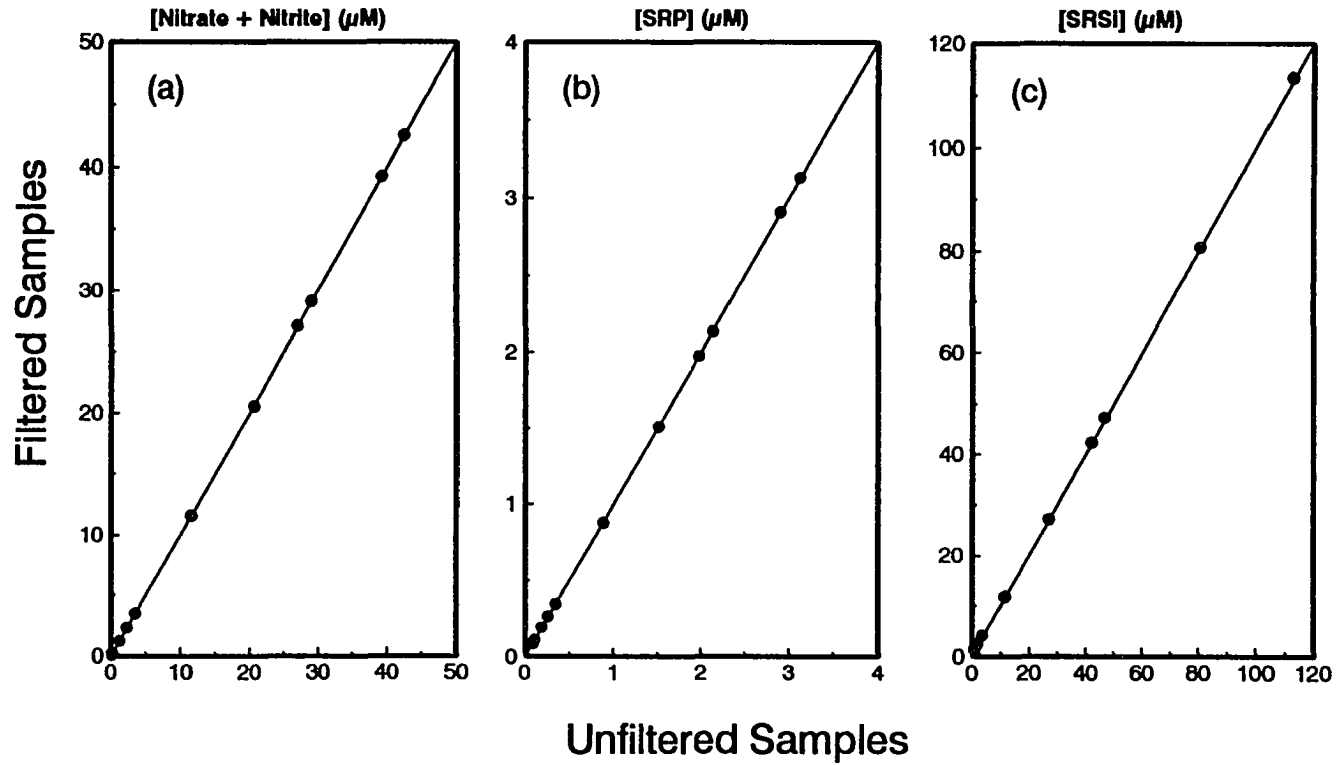


Fig. 2.3. Plots of filtered vs. unfiltered concentration determinations (all samples frozen): (a) nitrate+nitrite as determined by autoanalysis, (b) soluble reactive phosphate as determined by autoanalysis, (c) soluble reactive silicate as determined by autoanalysis. The solid line in each plot represents a perfect 1:1 relationship for comparison. Linear regression statistics are listed in Table 2.2.

Table 2.2. Model II reduced major axis linear regression statistics for seawater sample storage experiments

Analyte ^a	Method ^b	Unit ^c	Control ^d	Treatment ^e	n ^f	r ^g	slope ^h	95% conf. interval ⁱ	99% conf. interval ^j	Y-int. ^k	95% conf. interval ^l	99% conf. interval ^m
N+N	C	nM	Fresh	Froz.	8	1.000	1.011	1.002 - 1.020	0.997 - 1.025	0.45	(1.04) - 1.94	(1.80) - 2.71
NO ₃ ⁻	M	μM	Fresh	Froz.	8	0.999	0.966	0.930 - 1.003	0.912 - 1.022	0.01	0.00 - 0.02	0.00 - 0.02
SRP	MAGIC	nM	Fresh	Froz.	16	0.937	1.060	0.869 - 1.294	0.806 - 1.395	(4.48)	(23.61) - 14.65	(31.03) - 22.07
SRSi (full range)	AA	μM	Refrig.	Froz.	277	1.000	1.015	1.011 - 1.018	1.010 - 1.019	(0.42)	(0.83) - (0.01)	(0.97) - 0.12
SRSi (<120 μM)	AA	μM	Refrig.	Froz.	139	1.000	1.001	1.000 - 1.003	0.999 - 1.003	0.11	(0.02) - 0.23	(0.06) - 0.27
NH ₄ ⁺	M	μM	Fresh	Froz.	8	0.985	1.011	0.863 - 1.222	0.791 - 1.333	(0.04)	(0.29) - 0.16	(0.40) - 0.27
N+N	AA	μM	Froz. Unfilt.	Froz. Filt.	11	1.000	1.000	0.999 - 1.002	0.998 - 1.003	(0.02)	(0.06) - 0.01	(0.08) - 0.03
SRP	AA	μM	Froz. Unfilt.	Froz. Filt.	11	1.000	1.000	0.997 - 1.004	0.995 - 1.005	(0.01)	(0.01) - 0.00	(0.01) - 0.00
SRSi (full range)	AA	μM	Froz. Unfilt.	Froz. Filt.	11	1.000	1.000	0.996 - 1.004	0.994 - 1.006	0.22	0.04 - 0.40	(0.03) - 0.47

Table 2.2. (Cont.) Model II reduced major axis linear regression statistics for seawater sample storage experiments

- a) Analytes as listed in footnotes d-h of Table 2.1. For SRSi, either the full range of available data, or a subset containing only those values below 120 μM are used, as indicated.
- b) Analytical methods used as listed in footnote a of Table 2.1.
- c) Concentration units are μM except where chemiluminescence and MAGIC methods are used, in which case units are nM.
- d) Control measurements used as X values in regression calculations. Froz. = frozen, Unfilt. = unfiltered.
- e) Storage conditions considered as treatments; measurements used as Y values in regression calculations. Froz. = frozen, Filt. = filtered.
- f) Number of observations.
- g) Correlation coefficient.
- h) Slope of regression line (unitless).
- i) 95% confidence interval of the regression slope.
- j) 99% confidence interval of the regression slope.
- k) Y-intercept of regression line in μM or nM (see units). Negative values indicated with parentheses.
- l) 95% confidence interval of regression Y-intercept. Negative values indicated with parentheses.
- m) 99% confidence interval of regression Y-intercept. Negative values indicated with parentheses.

only one of the N+N samples (n=11) deviate from the 1:1 line by more than twice the analytical precision of their respective analyses.

Experiments on the long-term frozen storage of samples

The results of the long-term frozen storage experiments for N+N, SRP and SRSi indicate no significant deviation from the initial values for periods of up to one year (Fig. 2.4), except for three sample sets (Table 2.3). These conclusions are based on a Student's t-test of the initial replicates with the grouped time>0 replicates. The three differences found significant are all less than twice the analytical precisions of the respective analyses.

DISCUSSION

Our results indicate that for oligotrophic oceanic waters, slow freezing of unfiltered samples in HDPE bottles is an adequate preservation method for all of the analytes tested. The only experiments which reveal consistent significant deviation from control values of a magnitude more than twice the estimated analytical precision are the MAGIC-SRP fresh vs. frozen comparison and the full range SRSi refrigerated vs. frozen comparison. In the case of SRP, while the results suggest a slight increase in variability caused by freezing, they also show that this effect is of a magnitude small enough to be neglected when using standard manual or automated colorimetric methods. The silicate "problem" is restricted to samples with high SRSi concentrations, as evidenced by the lack of significant effect when only <120 μM samples are tested. The polymerized silicate in the frozen high-concentration samples can be reconverted to SRSi by prolonged thawing and/or warming of the sample (Walsh, 1989; Sakamoto et al., 1990). Alternatively, if the time lag

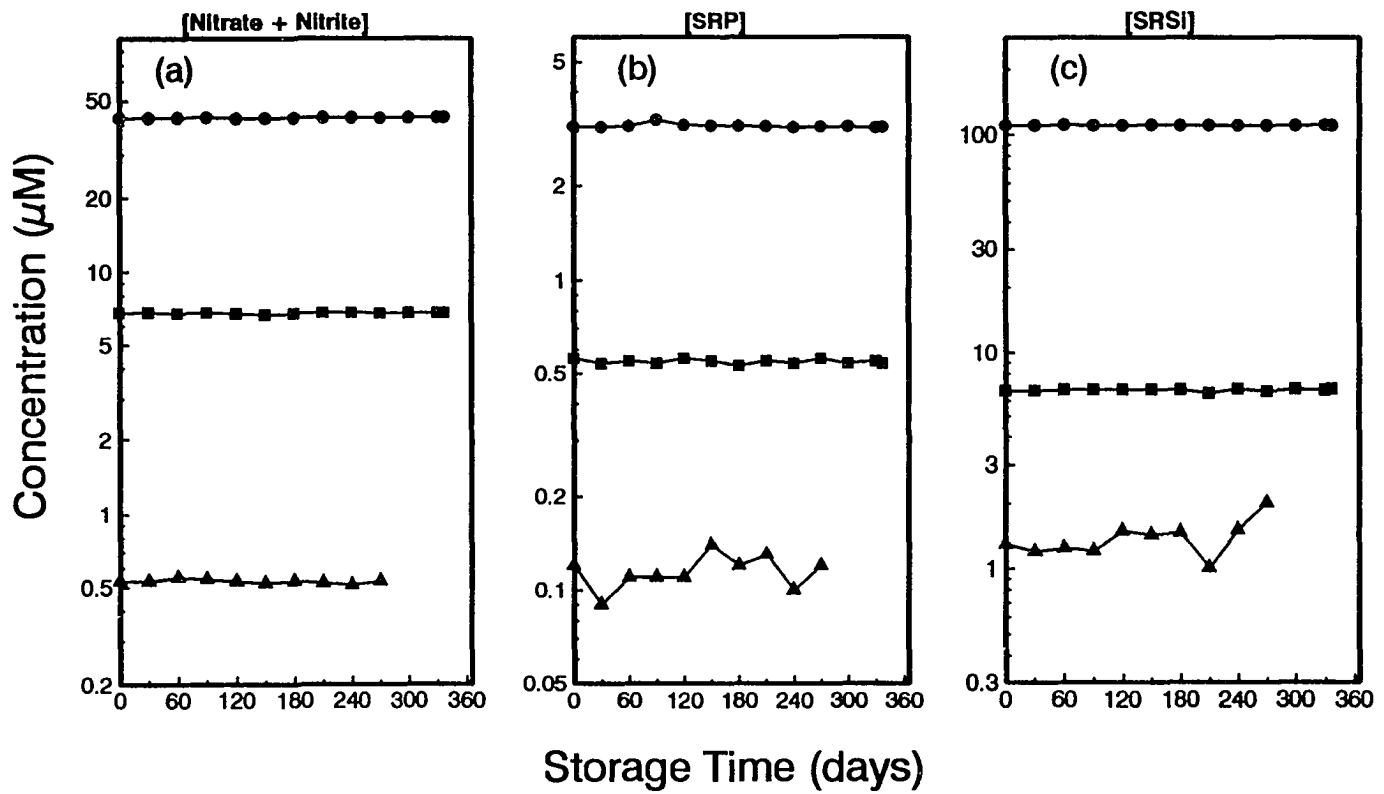


Fig. 2.4. Results of long-term frozen storage experiments: (a) time-course of nitrate+nitrite concentration during frozen storage as determined by autoanalysis, (b) as in (a) except for soluble reactive phosphate, (c) as in (a) except for soluble reactive silicate. The solid line represents a perfect 1:1 relationship for comparison. Student's t-test statistics are listed in Table 2.2.

Table 2.3. Student's t-test statistics for long-term frozen storage experiments

Analyte ^a	Depth ^b	Controls ^c				Treatments ^d				Diff. Means ⁱ	Sig. Level ^j
		storage ^e	n ^f	mean ^g	std. dev. ^h	storage	n	mean	std. dev.		
N+N	150	Froz. 4 d	13	0.526	0.010	Froz. 34 - 274 d	9	0.529	0.017	-0.003	0.554
	250	Froz. 4 d	16	6.791	0.022	Froz. 34 - 341 d	12	6.772	0.002	0.020	0.130
	1000	Froz. 4 d	16	42.364	0.046	Froz. 34 - 341 d	12	42.535	0.123	-0.171	***0.000
SRP	150	Froz. 4 d	13	0.122	0.017	Froz. 34 - 274 d	9	0.114	0.015	0.008	0.285
	250	Froz. 4 d	16	0.562	0.017	Froz. 34 - 341 d	12	0.546	0.009	0.016	**0.007
	1000	Froz. 4 d	16	3.099	0.013	Froz. 34 - 341 d	12	3.113	0.046	-0.014	0.269
SRSi	150	Froz. 4 d	13	1.295	0.239	Froz. 34 - 274 d	9	1.400	0.288	-0.105	0.360
	250	Froz. 4 d	16	6.638	0.102	Froz. 34 - 341 d	12	6.713	0.090	-0.075	*0.055
	1000	Froz. 4 d	16	110.412	0.338	Froz. 34 - 341 d	12	110.432	0.239	-0.019	0.869

a) Analytes as listed in footnotes d, f and g of Table 2.1.

b) Approximate depth at Station ALOHA from which the samples were collected. All three analytes listed were determined from the same replicate subsamples collected at each depth. All depths are in m.

Table 2.3. (Cont.) Student's t-test statistics for long-term frozen storage experiments

- c) A number of replicates were initially analyzed in a single run to determine the control values.
- d) The additional replicates were analyzed at approximately 1 month intervals and constitute the treatment group.
- e) The duration of frozen storage before analysis.
- f) Number of observations.
- g) Mean analyte concentration for the replicates within each group. All concentrations in μM .
- h) Standard deviation of the mean analyte concentrations for the replicates within each group.
- i) The difference in the mean analyte concentrations between the treatment group and the control group.
- j) The significance level of a Student's t-test comparing the treatment and control groups. * = significant difference at the 0.1 level, ** = significance at the 0.01 level, *** = significance at the 0.001 level.

between collection and analysis is to be short, replicate sample splits can be refrigerated instead of being frozen.

The question thus arises: why have various investigators disagreed on whether nutrient samples are adequately preserved by freezing? There are several potential reasons why such disputes appear in the literature. One reason is that the analytical requirements of scientific studies are often quite different. We contend that if a vast majority of preserved samples yield values that are within twice the analytical precision of the fresh values then the preservation is adequate; other investigators may not require this level of reproducibility. Similarly, investigators may conclude that if statistical significance can be ascertained between fresh and preserved values, the preservation is inadequate, as did Venrick and Hayward (1985). The problem with this approach is that sometimes statistical tests may find significant differences when such differences are no larger than the normal analytical and field variability. A re-examination of the data from Venrick and Hayward (1985), focusing only on the mean values for samples frozen for one month in polyethylene bottles, shows that the results were fairly good, with the exception of one set of SRP analyses and one set of high-end SRSi measurements (Fig. 2.5). The low values for the high-end [SRSi] can be explained by polymerization. The high [SRP] values cannot be readily explained, but one outlier should not be enough to cause us to dismiss freezing as a method of SRP preservation, given that many "unknown" factors other than the preservation process itself may contribute to the final measured value, and considering the excellent fit of the rest of the data points to the 1:1 line.

Another reason that freezing may have been dismissed in the past is the wide array of water types that have been used in preservation studies. Our endorsement of freezing for nutrient preservation is restricted to oxygenated seawater of low particulate load, such as that found at central gyre sites like Station ALOHA, where total suspended loads in

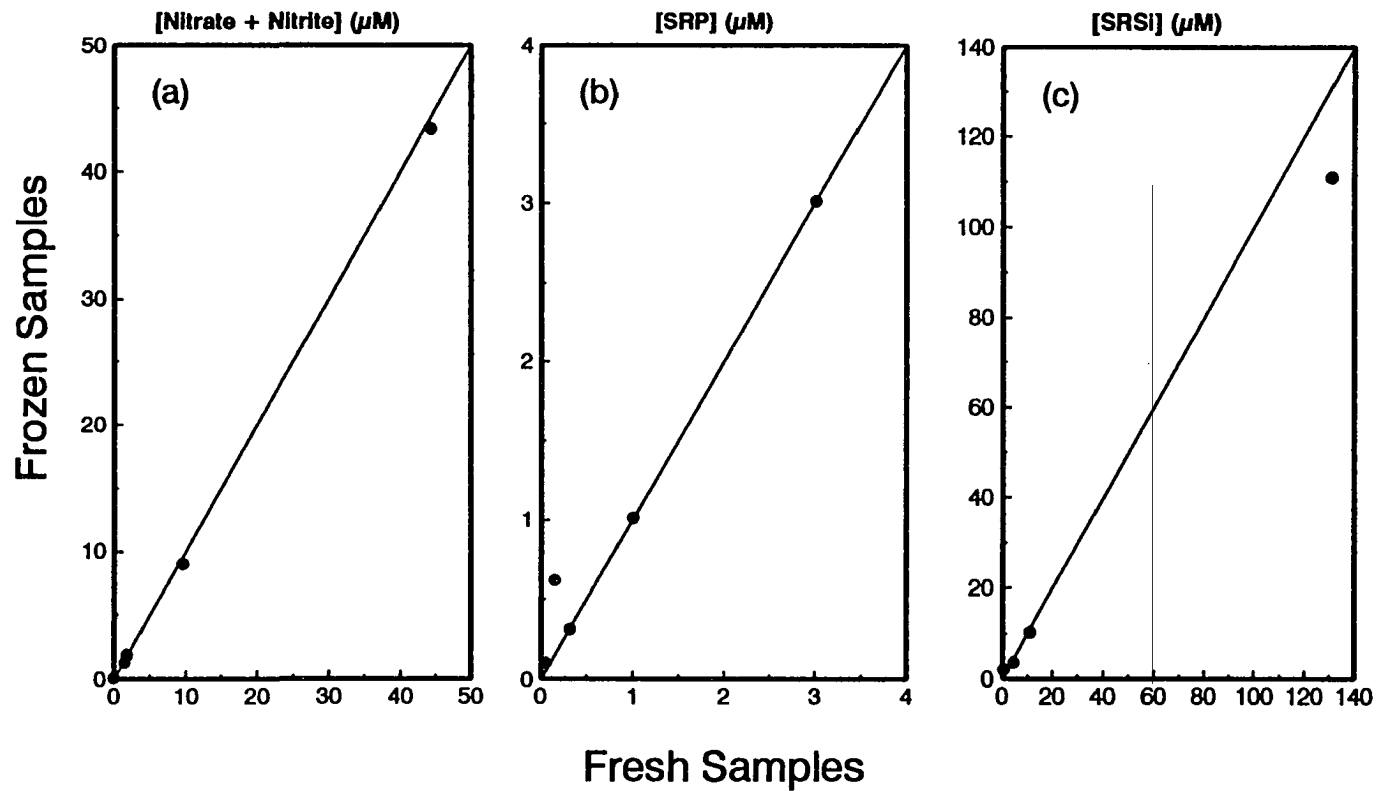


Fig. 2.5. Plots of frozen vs. fresh determinations; data taken from Venrick and Hayward (1985). Only the mean values for samples frozen one month in polyethylene bottles are presented. Each mean value represents 4 or 5 replicate samples. (a) nitrate+nitrite, (b) soluble reactive phosphate, (c) soluble reactive silicate. All determinations were made by autoanalysis. The solid line represents a perfect 1:1 relationship for comparison.

surface waters seldom exceed $200 \mu\text{g l}^{-1}$ and are usually $<50 \mu\text{g l}^{-1}$. Preservation of nutrients in freshwater, anoxic water or water with low pH may be hampered by precipitate formation and/or silicate polymerization, and measurements of nutrients in waters with high suspended loads may suffer from adsorption problems, turbidity interferences and rapid biological alterations. If working in these environments, investigators are advised to assess the validity of their preservation methods.

A third and underappreciated reason for discrepancies between fresh and frozen replicates is poor quality control in sampling, storage and analytical procedures during the experiment. Even excellent analysts can make mistakes. For this reason, we must in deciding upon a storage method look to the large group of studies that show little or no effect of freezing on nutrient concentrations, rather than the handful that show unexplained anomalies. For example, we strongly suspect that some "unknown" quality control problems entered the experiments conducted by Morse et al. (1982). It is difficult to explain how a $20 \mu\text{M}$ nitrate sample after storage for one day at -20°C in a polyethylene bottle can have $44 \mu\text{M}$ nitrate, then after six more days at -20°C have $32 \mu\text{M}$ nitrate (Morse et al., 1982). These extreme changes are an order of magnitude greater than any changes observed by other investigators, even those who do not recommend freezing nitrate samples.

Lastly, misunderstandings about the quality of sample preservation can arise from inaccurate citations of the primary literature. Papers containing inaccurate citations may in turn be cited, perpetuating the misconception. An example of this phenomenon is found in the literature on the preservation of ammonium in seawater samples. Upon finding that their frozen samples yielded suspiciously high ammonium concentrations, Carpenter and McCarthy (1975) suggested that perhaps "some aspect of freezing, storage, or thawing resulted in NH_4^+ contamination." They went on to say that "one possibility is that

ammonium was liberated through cellular rupture as samples were frozen." They did not present any data comparing fresh and frozen ammonium determinations. Nevertheless, Eppley et al. (1977), upon finding suspiciously high ammonium concentrations in their samples, stated that "as noted by Carpenter and McCarthy (1975), the preservation of water samples by freezing results in contamination and high estimates." This misconception led Perry and Eppley (1981) to conclude that their high ammonium values resulted from freezing the samples as well, while citing both of the above papers. When one examines those studies involving the direct comparisons of fresh and frozen seawater ammonium samples, however, one finds that most agree that freezing is an adequate method of preservation.

CONCLUSIONS

Inorganic nutrient concentrations in oxic oceanic seawater samples of low particulate load are adequately maintained for several months if immediately frozen and stored at -20 °C in clean high-density polyethylene bottles. Previous studies finding fault with freezing as a preservation method for nutrients either dealt with very different water types, used different containers, focused on statistically significant differences of a similar magnitude to normal analytical and field variability, misinterpreted published results or possibly suffered from unidentified analytical errors. Of all the analytes tested, only SRSi samples >120 µM are appreciably affected by the freezing process, and this effect appears to be reversible.

REFERENCES

- Ambe, M. 1978. Note of the experience in the preparation of CSK standard solutions and the ICES-SCOR intercalibration experiment, 1969-1970. *Mar. Chem.* **6**:171-178.
- Armstrong, F.A., C.R. Stearns and J.D.H. Strickland. 1967. The measurement of upwelling and subsequent biological processes by means of the Technicon Autoanalyzer® and associated equipment. *Deep-Sea Res.* **14**:381-389.
- Avanzino, R.J. and V.C. Kennedy. 1993. Long-term frozen storage of stream water samples for dissolved orthophosphate, nitrate plus nitrite, and ammonia analysis. *Wat. Resources Res.* **29**:3357-3362.
- Burton, J.D., T.M. Leatherland and P.S. Liss. 1970. The reactivity of dissolved silicon in some natural waters. *Limnol. Oceanogr.* **15**:473-476.
- Carpenter, E.J. and J.J. McCarthy. 1975. Nitrogen fixation and uptake of combined nitrogenous nutrients by *Oscillatoria (Trichodesmium) thiebautii* in the western Sargasso Sea. *Limnol. Oceanogr.* **20**:389-401.
- Chapman, P. and S.A. Mostert. 1990. Does freezing of nutrient samples cause analytical errors? *S. Afr. J. Mar. Sci.* **9**:239-247.
- Charpiot, R. 1969. Technique de conservation des echantillons d'eau de mer pour le dosage de phosphates, nitrites, nitrates, silice et bore. *Cah. Oceanogr.* **21**:773-793.
- Clementson, L.A. and S.E. Wayte. 1992. The effect of frozen storage of open-ocean seawater samples on the concentration of dissolved phosphate and nitrate. *Wat. Res.* **26**:1171-1176.
- Collier, A.W. and K.T. Marvin. 1953. Stabilization of the phosphate ratio of sea water by freezing. *Fish. Bull. U.S.* **79**:71-76.
- Cox, R.D. 1980. Determination of nitrate and nitrite at the parts per billion level by chemiluminescence. *Anal. Chem.* **52**:332-335.
- Degobbis, D. 1973. On the storage of seawater samples for ammonia determination. *Limnol. Oceanogr.* **18**:146-150.
- Dore, J.E. and D.M. Karl. 1995. Nitrite distributions and dynamics at Station ALOHA. *Deep-Sea Res.*, submitted.

Dore, J.E., G. Tien, R. Letelier, G. Parrish, J. Szyper, J. Burgett and D.M. Karl. 1993. RACER: Distributions of nitrogenous nutrients near receding pack ice in Marguerite Bay. *Antarctic J. U.S.* 27:177-179.

Eppley, R.W., J.H. Sharp, E.H. Renger, M.J. Perry and W.G. Harrison. 1977. Nitrogen assimilation by phytoplankton and other microorganisms in the surface waters of the central North Pacific Ocean. *Mar. Biol.* 39:111-120.

Fitzgerald, G.P. and S.L. Faust. 1967. Effect of water sample preservation methods on the release of phosphorus from algae. *Limnol. Oceanogr.* 12:332-334.

Garside, C. 1982. A chemiluminescent technique for the determination of nanomolar concentrations of nitrate and nitrite in seawater. *Mar. Chem.* 11:159-167.

Gilmartin, M. 1967. Changes in inorganic phosphate concentration occurring during seawater sample storage. *Limnol. Oceanogr.* 12:325-328.

Gordon, L.I., J.C. Jennings, Jr., A.A. Ross and J.M. Krest. 1993. A suggested protocol for continuous flow automated analysis of seawater nutrients (phosphate, nitrate, nitrite and silicic acid) in the WOCE Hydrographic Program and the Joint Global Ocean Fluxes Study, OSU Coll. of Oc. Descriptive Chem. Oc. Grp. Tech. Rpt. 93-1, Oregon State University, Corvallis, OR, 52 pp.

Grasshoff, K., M. Ehrhardt and K. Kremling (eds). 1983. Methods of Seawater Analysis (2nd edn.), Verlag Chemie, Weinheim, Ger., 419 pp.

Heron, J. 1962. Determination of phosphate in water after storage in polyethylene. *Limnol. Oceanogr.* 7:316-321.

Jenkins, D. 1968. The differentiation, analysis, and preservation of nitrogen and phosphorus forms in natural waters. In: Advances in Chemistry Series, No. 73: Trace Inorganics in Water, R.F. Gould (ed), American Chemical Society, Washington, D.C., pp. 265-280.

Johnson, A.H., D.R. Bouldin and G.W. Hergert. 1975. Some observations concerning preparation and storage of stream samples for dissolved inorganic phosphate analysis. *Wat. Resources Res.* 11:559-562.

Jolicoeur, P. and J.E. Mossimann. 1968. Intervalles de confiance pour la pente de l'axe majeur d'une distribution normale bidimensionnelle. *Biom. Praxim.* 9:121-140.

Karl, D.M. and R. Lukas. 1995. The Hawaii Ocean Time-series (HOT) program: Background, rationale and field implementation. *Deep-Sea Res.*, submitted.

- Karl, D.M. and G. Tien. 1992. MAGIC: A sensitive and precise method for measuring dissolved phosphorus in aquatic environments. *Limnol. Oceanogr.* **37**:105-116.
- Klingaman, E.D. and D.W. Nelson. 1976. Evaluation of methods for preserving the levels of soluble inorganic phosphorus and nitrogen in unfiltered water samples. *J. Environ. Qual.* **5**:42-46.
- Kobayashi, J. 1967. Silica in fresh water and estuaries. In: Chemical Environment in the Aquatic Habitat, H.L. Golterman and R.S. Clymo (eds), North-Holland, Amsterdam, pp. 41-55.
- Kremling, K. and A. Wenck. 1986. On the storage of dissolved inorganic phosphate, nitrate and reactive silicate in Atlantic Ocean water samples. *Meeresforschung* **31**:69-74.
- Macdonald, R.W. and F.A. McLaughlin. 1982. The effect of storage by freezing on dissolved inorganic phosphate, nitrate and reactive silicate for samples from coastal and estuarine waters. *Wat. Res.* **16**:95-104.
- Macdonald, R.W., F.A. McLaughlin and C.S. Wong. 1986. The storage of reactive silicate samples by freezing. *Limnol. Oceanogr.* **31**:1139-1142.
- Marvin, K.T. and R.R. Proctor, Jr. 1965. Stabilizing the ammonia-nitrogen content of estuarine and coastal waters by freezing. *Limnol. Oceanogr.* **10**:288-290.
- Morse, J.W., M. Hunt, J. Zullig, A. Mucci and T. Mendez. 1982. A comparison of techniques for preserving dissolved nutrients in open ocean seawater samples. *Ocean Sci. Eng.* **7**:75-106.
- Murphy, J. and J.P. Riley. 1962. A modified single solution method for the determination of phosphate in natural waters. *Anal. Chim. Acta* **27**:31-36.
- Newell, B.S. 1967. The determination of ammonia in sea water. *J. Mar. Biol. Ass. U.K.* **47**:271-280.
- Parsons, T.R., Y. Maita and C.M. Lalli. 1984. A Manual of Chemical and Biological Methods for Seawater Analysis, Pergamon Press, Oxford, 173 pp.
- Perry, M.J. and R.W. Eppley. 1981. Phosphate uptake by phytoplankton in the central North Pacific Ocean. *Deep-Sea Res.* **28**:39-49.
- Proctor, R.R., Jr. 1962. Stabilization of the nitrite content of sea water by freezing. *Limnol. Oceanogr.* **7**:479-480.

- Ricker, W.E. 1973. Linear regression in fishery research. *J. Fish. Res. Board Can.* **30**:409-434.
- Ricker, W.E. 1975. A note concerning Professor Jolicoeur's comments. *J. Fish. Res. Board Can.* **32**:1494-1498.
- Riley, J.P. 1975. Analytical chemistry of sea water. In: Chemical Oceanography, vol. 3 (2nd edn.), J.P. Riley and G. Skirrow (eds), Academic Press, New York, pp. 193-514.
- Ryle, V.D., H.R. Mueller and P. Gentien. 1981. Automated analysis of nutrients in tropical sea waters, Austral. Inst. Mar. Sci. Tech. Bull., Oceanogr. Ser. No. 3, 24 pp.
- Sakamoto, C.M., G.E. Friederich and L.A. Codispoti. 1990. MBARI procedures for automated nutrient analyses using a modified Alpkem Series 300 Rapid Flow Analyzer, Monterey Bay Aquarium Research Institute Tech. Rpt. no. 90-2, 84 pp.
- Salley, B.A., J.G. Bradshaw and B.J. Neilson. 1986. Results of comparative studies of preservation techniques for nutrient analysis on water samples, U.S. Environmental Protection Agency, Chesapeake Bay Program, Annapolis, MD, 32 pp.
- Smith, S.V., W.J. Kimmerer and T.W. Walsh. 1986. Vertical flux and biogeochemical turnover regulate nutrient limitation of net organic production in the North Pacific Gyre. *Limnol. Oceanogr.* **31**:161-167.
- Sokal, R.R. and F.J. Rohlf. 1981. Biometry (2nd edn.), W. H. Freeman and Co., San Francisco, 859 pp.
- Strickland, J.D.H., and T.R. Parsons. 1972. A Practical Handbook of Seawater Analysis, Bull. Fish. Res. Board Can., 167 (2nd edn.), 310 pp.
- Takenaka, N., A. Ueda and Y. Maeda. 1992. Acceleration of the rate of nitrite oxidation by freezing in aqueous solution. *Nature* **358**:736-738.
- Technicon Industrial Systems. 1973. Orthophosphate in water and seawater, Autoanalyzer II® Industrial Method No. 155-71W. Tarrytown, New York, 3 pp.
- Technicon Industrial Systems. 1977. Silicates in water and seawater. Autoanalyzer II® Industrial Method No. 186-72W. Tarrytown, New York, 2 pp.
- Technicon Industrial Systems. 1979. Nitrate and nitrite in water and seawater. Autoanalyzer II® Industrial Method No. 158-71W. Tarrytown, New York, 4 pp.

Thayer, G.W. 1970. Comparison of two storage methods for the analysis of nitrogen and phosphorus fractions in estuarine water. *Chesapeake Sci.* **11**:155-158.

Truesdale, V.W. 1971. A modified spectrophotometric method for the determination of ammonia (and amino-acids) in natural waters, with particular reference to sea water. *Analyst* **96**:584-590.

Venrick, E.L. and T.L. Hayward. 1985. Evaluation of some techniques for preserving nutrients in stored seawater samples. *Rep. Calif. Coop. Oceanic Fish. Invest.* **26**:160-168.

Walsh, T.W. 1989. Total dissolved nitrogen in seawater: a new high-temperature combustion method and a comparison with photo-oxidation. *Mar. Chem.* **26**:295-311.

York, D. 1966. Least-squares fitting of a straight line. *Can. J. Phys.* **44**:1079-1086.

CHAPTER 3

NITRITE DISTRIBUTIONS AND DYNAMICS AT STATION ALOHA

ABSTRACT

We used a chemiluminescence method to measure nitrite concentrations in the water column at the U.S.-JGOFS/WOCE time-series Station ALOHA (22°45' N, 158° W) from September 1989 to November 1993. We present a detailed time-series of nitrite in the upper 200 m in order to examine the dynamics of the primary nitrite maximum. Our results reveal a double-peaked structure to this feature that is consistent with a vertical separation of the reductive and oxidative microbial processes responsible for nitrite production. The possibility of using the nitrite content of this upper layer as an indicator of nitrogen export from the euphotic zone is explored and rejected.

Midwater nitrite profiles (200-1000 m) show a supra-exponential decrease in concentration with depth and reveal month-to-month variability. Nitrite concentrations in deep waters (1000-4800 m) are in the nanomolar to subnanomolar range, and are similar to Atlantic data, arguing against significant basin scale differences in the deep nitrite pool. Deep profiles also show measurable variability on both monthly and annual timescales.

INTRODUCTION

Nitrite, because of its intermediate redox position between ammonium and nitrate, is a useful indicator of the equilibrium state of the oxidative and reductive pathways of the marine nitrogen cycle. Accumulations of nitrite in certain marine strata mark the locations

where biologically mediated changes in combined nitrogen occur (Rakestraw, 1936; Vaccaro and Ryther, 1960). Marine biological processes known to produce nitrite include: (1) incomplete assimilatory reduction of nitrate by phytoplankton (Vaccaro and Ryther, 1960; Kiefer et al., 1976) and bacteria (Wada and Hattori, 1972), (2) chemoautotrophic oxidation of ammonium by nitrifying bacteria (Brandhorst, 1959; Olson, 1981), and (3) dissimilatory reduction of nitrate by denitrifying bacteria (Brandhorst, 1959; Fiadeiro and Strickland, 1968; Codispoti and Richards, 1976). In well-oxygenated oceanic waters the latter process is not thought to be significant in nitrite production, however its relative contribution may increase in the midwater oxygen minimum layer and within the interiors of large particles (Karl et al., 1984).

Despite the long-recognized importance of nitrite as a nitrogen cycle intermediate, methodological constraints have prevented the acquisition of detailed water column nitrite profiles. The standard colorimetric assay (Strickland and Parsons, 1972) is inaccurate at concentrations below about 50 nM, while nitrite levels in the open ocean typically exceed this value only within a narrow layer near the base of the euphotic zone (the primary nitrite maximum or PNM). Wada and Hattori (1971) developed a sample pre-concentration method capable of extending measurements down to nanomolar levels, but the large sample volumes (500-1000 ml) and multiple manipulations required by their method are undesirable. Routine measurements of the nanomolar and often sub-nanomolar concentrations of nitrite in oceanic surface and sub-PNM waters have only recently become possible with the advent of the chemiluminescent technique, developed by Cox (1980) and modified for seawater samples by Garside (1982). The chemiluminescent method offers excellent precision and accuracy, as well as a low detection limit. This technique has been successfully used to measure low-level nitrite in the Sargasso Sea

(Brzezinski, 1988; Zafiriou et al., 1992) and in the Northwest Atlantic and the Caribbean Sea (Zafiriou et al., 1992).

The PNM found in oxic oligotrophic seawaters has been traditionally described as a narrow, symmetric peak located near the base of the euphotic layer, with undetectable nitrite concentrations above and below. More recently, the PNM was discovered to be asymmetric, with a pronounced upper peak that slowly decays with depth as a "tail" into deep water (Zafiriou et al., 1992). Variations of the upper PNM structure have also been described, including enigmatic double maxima, and smooth vertically-mixed profiles (Wada and Hattori, 1991). Through repeated measurements covering both daily and yearly time scales at a single location, we hoped to elucidate the "normal" structure of the PNM and the types of variability that could be expected.

We report here on the water-column nitrite distributions measured at the US-JGOFS/WOCE time-series station ALOHA in the North Pacific subtropical gyre over the period September 1989 to November 1993. Though some deep profiles (to between 1000 m and the seafloor at about 4800 m) are presented, most of the data are from the upper 200 m, where we have extensively examined the structure and variability of the PNM. For correlative purposes, we include some data on [nitrite+nitrate] distributions as well. We are aware of only one other low-level nitrite data set from the North Pacific (Wada and Hattori, 1972), and believe the present nitrite data represent both the first from this region utilizing the chemiluminescent technique and the first multiyear time-series study of nitrite in the Pacific.

MATERIALS AND METHODS

Station location

All sampling was performed during the regular monthly cruises of the Hawaii Ocean Time-series (HOT) project to the deep water Station ALOHA (A Long-term Oligotrophic Habitat Assessment; Karl and Lukas, 1995). Station ALOHA is defined as a six nautical mile radius circle centered at 22° 45' N, 158° 00' W, about 100 km north of Kahuku Pt., Oahu, Hawaii (Fig. 1.3); every effort is made to sample only within this circle. The site was chosen to be representative of the oligotrophic gyre of the North Pacific Ocean. Between September 1989 and November 1993 the HOT project completed 41 cruises to Station ALOHA. We obtained at least one upper water column (0-200 m) profile of nitrite from 31 of these cruises, and multiple profiles from eight of them. Midwater profiles (200-1000 m) and deep profiles (1000-4800 m) were obtained from seven cruises. Cruise dates and vessels are listed elsewhere (Karl and Lukas, 1995).

Sampling

Sample collection was performed using a 24-place rosette with 12-liter PVC bottles, equipped with a SeaBird CTD, a Beckman polarographic oxygen sensor and a SeaTech flash fluorometer. Light levels and attenuation were determined using a Licor on-deck cosine collector and a Biospherical underwater profiling natural fluorometer. CTD protocols followed WOCE standards as described in Bingham and Lukas (1995).

Individual water samples were drawn using clean Tygon tubing into 125-ml acid-washed polyethylene bottles. For each rosette position sampled, the tubing was

thoroughly flushed, and each sample bottle was rinsed three times with sample before filling. Particulate matter for chlorophyll-a determinations was concentrated by filtration and extracted in acetone for later analysis by fluorometry as described in Letelier et al. (1995). Nitrite and other nutrient samples were immediately placed in a -20 °C freezer without filtration and kept frozen until the day of analysis. Details of our standard nutrient analyses are given in Dore et al. (1995). A free-floating sediment trap array was used for the collection of sinking particulate matter. Details of our sediment trap protocols and particulate analyses are presented in Karl et al. (1995a).

Chemiluminescent analyses

Frozen samples were thawed slowly in a bath of room-temperature water a few hours before analysis. Subsamples (10 ml) were introduced into the reaction apparatus using a clean syringe. Nitrite concentration ($[\text{NO}_2^-]$) was determined through wet chemical reduction using sodium iodide and glacial acetic acid, and subsequent detection of the nitric oxide (NO) produced with an Antek model 720 chemiluminescent nitrogen analyzer. Similarly, nitrite+nitrate concentration ($[\text{NO}_2^- + \text{NO}_3^-]$) was determined after reduction to NO using ferrous ammonium sulfate, ammonium molybdate and concentrated sulfuric acid. Reagents were pre-sparged with the Ar carrier gas and so introduced no blank. Both procedures followed the methods described by Garside (1982) with no major modifications. Occasionally, chemiluminescent $[\text{NO}_2^- + \text{NO}_3^-]$ analyses were not performed; in these cases standard automated colorimetric analyses were used instead (Dore et al., 1995). All nitrite data presented here were determined by chemiluminescence.

Detection limits, precision and accuracy

Standards were prepared fresh by volumetric serial dilutions of a primary 10 mM stock (NaNO_2 or KNO_3) with distilled deionized water (DDW). Accuracy was maintained by including dilutions of CSK certified reference standards (Ambe, 1978) in each analytical run; these always agreed with our standards to within about $\pm 2\%$.

For $[\text{NO}_2^-]$ analyses, the lowest concentration of standard to reliably give a readable signal was 0.2 nM. At the same time, our DDW diluent, many samples from the surface mixed layer and some from deep waters produced zero counts on the detector (i.e., the system blank was zero and indistinguishable from some samples). From this we estimate the absolute detection limit to be approximately 0.1-0.2 nM. Quantification of samples below 1 nM is questionable, though, because the precision (standard deviation of duplicate or triplicate analyses of individual standards or samples) at concentrations < 50 nM averaged ± 0.5 nM. We cannot therefore directly compare individual samples below 1 nM, but we can with some confidence compare multi-point trends at these low levels. At concentrations above 50 nM, the average precision was $\pm 1.6\%$.

For $[\text{NO}_2^- + \text{NO}_3^-]$ analyses, the lowest standard used was 1.0 nM. Although for these analyses DDW consistently gave a signal (i.e., the system blank was nonzero), the signal from the 1 nM standard was always significantly higher. Average precision was similar to that for nitrite alone, but low-end variability leads us to estimate our detection limit at about 1-2 nM.

Precautions

Because the concentrations of nitrite in these waters are often at or near detection limits, care must be taken to avoid contamination. On board a research vessel, stack gases containing NO and nitrogen dioxide (NO₂) can cause interference (Zafiriou et al., 1992). We were careful to minimize possible exposure of the samples to ambient air on deck, and fortunately did not encounter noticeable contamination problems. Natural NO levels in oxic sea waters are too low to interfere with the analyses of nitrite and nitrate (Ward and Zafiriou, 1988).

To avoid wear and tear on the chemiluminescent analyzer and the associated reaction apparatus and to ensure the high quality of the data, we performed analyses at our land-based laboratory, requiring the preservation and storage of samples. We therefore conducted experiments comparing methods of preservation and shipboard analyses of fresh samples vs. later laboratory analyses of stored samples. In the first of these experiments, a 20 liter polyethylene carboy was filled with water from just below the PNM (130 m) and returned to our laboratory. Six sets of four replicate 125 ml polyethylene bottles were filled from this carboy; one set was analyzed immediately while the others were subjected to different treatments before analysis. The treatments included freezing at -20°C (slow), freezing at -70°C (quick), acidification with HCl to a pH of 2.5, and combinations thereof. All unfrozen samples were analyzed within six hours of the sample splitting. All frozen samples were analyzed after being stored 19 days at -20°C and thawed in a room temperature water bath.

In the second experiment, thirty-four depths from near-bottom to near-surface were sampled over the course of two casts. From each rosette bottle two or four samples were drawn; half of these were immediately placed in the -20°C freezer. The others were

maintained at 4°C and withdrawn a few at a time about one hour before analysis; all of these at-sea analyses were performed within about ten hours of collection. The frozen samples were returned to land and analyzed one week later.

RESULTS AND DISCUSSION

Storage experiments

The results of our first storage experiment confirmed the observation of Takenaka et al. (1992) that at low pH, the freezing of an aqueous sample dramatically reduces its nitrite concentration; however, we found no significant differences (at $\alpha=0.05$) in nitrite concentration between fresh and slow frozen samples at normal seawater pH (Table 3.1). Quick freezing at -70 °C is not recommended, as we found a slight but significant reduction in nitrite concentration when samples were preserved in this manner (Table 3.1). Takenaka et al. (1992) reported that the rate of oxidation of nitrite to nitrate in acidic solutions is accelerated by an increased rate of freezing; it is likely that our observed nitrite loss upon quick freezing is a result of the same process, but is less pronounced due to the higher pH of the seawater medium. We conclude that there is no discernable effect of the freezing process itself when performed at -20 °C on a natural seawater sample stored in polyethylene.

In our second storage experiment, we compared shipboard analysis with laboratory analysis of samples stored frozen, and found the agreement to be excellent (Fig. 3.1). The largest difference between fresh and frozen samples was 2.1 nM. All samples with fresh values below 10 nM gave frozen values that differed by 1.0 nM or less; those below 1 nM differed by at most 0.6 nM. A model II reduced major axis (geometric mean) linear

Table 3.1. Results of an experiment to determine the effects of several sample storage methods on the concentration of nitrite. See text for details of experiment.

Treatment	Nitrite Concentration* nM
Fresh	30.2 (± 1.0)
Slow Frozen (-20°C)	29.5 (± 0.6)
Quick Frozen (-70°C)	28.6 (± 0.8)
Acidified (pH = 2.5)	26.2 (± 0.6)
Acidified & Slow Frozen	0.7 (± 0.4)
Acidified & Quick Frozen	1.1 (± 0.4)

* Mean (± 1 Standard Deviation), n = 4.

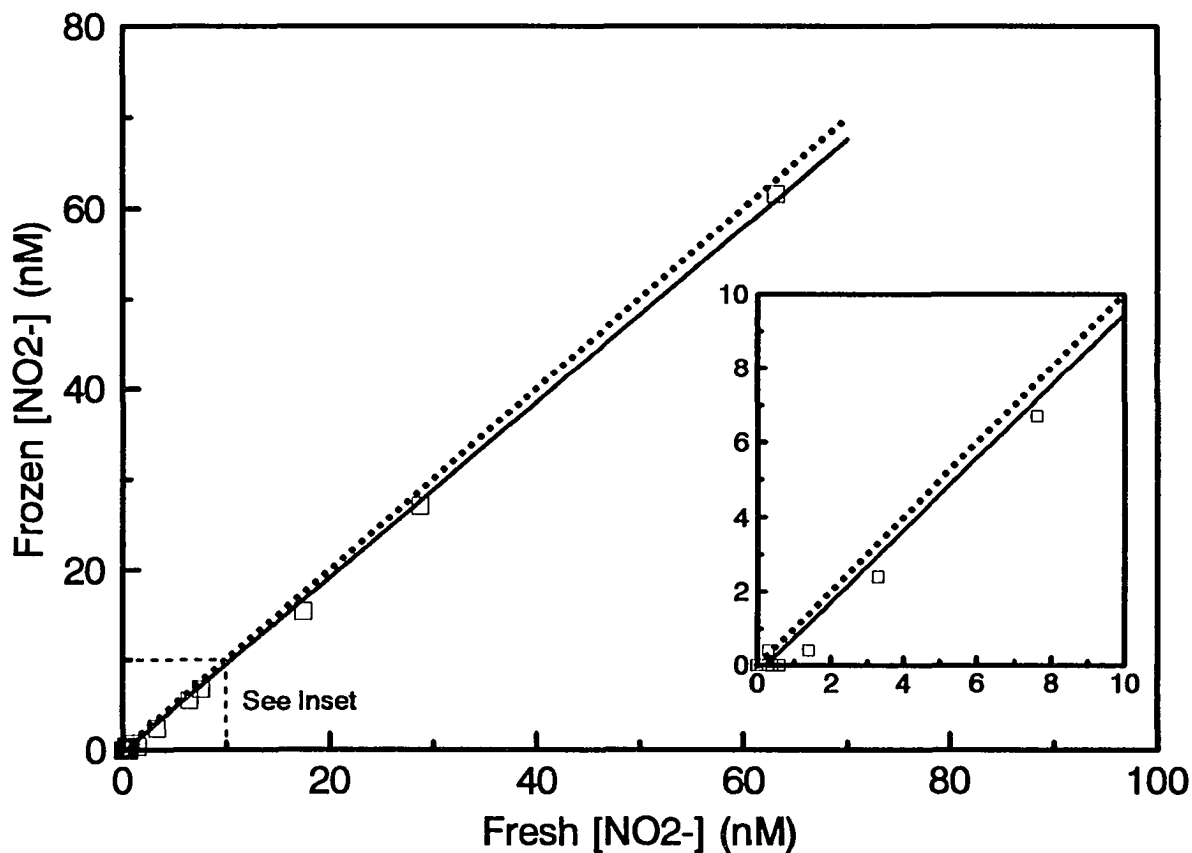


Fig. 3.1. Results of an experiment to determine the effects of frozen storage of nitrite samples with respect to samples analyzed at sea. The horizontal axis gives the concentration of nitrite in nM as measured at sea; the vertical axis represents the measured concentration of replicate samples frozen and returned to the laboratory for analysis, also in nM. The inset plot is an expansion of the main plot emphasizing those samples with concentrations less than 10 nM. The dotted line is the theoretical 1:1 relation in the absence of treatment effect ($y = x$). The solid line is a reduced major axis model II linear regression of the 34 data points ($y = -0.23 + 0.97x$, $r = 0.999$).

regression (Ricker, 1973) of the frozen data onto the fresh data indicates that there was a slight tendency for the fresh values to exceed the frozen values. Furthermore, the three samples exhibiting differences >1.0 nM were from within the PNM. Biological activity can rapidly alter nitrite concentration in unpreserved samples (Wada and Hattori, 1972; Zafiriou et al., 1992). Considering this observation and our failure to observe a significant "freezing effect" in the first experiment, we suspect that at least part of the slight discrepancy between fresh and frozen analyses is due to increases in nitrite in the fresh samples while they are stored under refrigeration awaiting analysis. Given the above and the difficulties involved in at-sea analyses, we believe that the analysis of nitrite in seawater is best performed on samples immediately frozen at -20 °C and returned to a land-based laboratory.

Nitrite in the upper water column

The upper 200 m of the water column includes the nitrite-impooverished surface layer, the "classical" PNM, and the upper reaches of the nitrite tail. An example of what we consider to be a "typical" upper water column nitrite profile under calm conditions is shown in Fig. 3.2. This profile, taken during HOT-41 (Oct. 1992), shows the major structural features of the PNM that we will focus on throughout this paper. First, we see a nitrite-poor surface layer, with concentrations <2 nM and often at or below the 0.1-0.2 nM detection limit. Second, there is an abrupt increase to an upper primary nitrite maximum (UPNM), where concentrations reach 60-200 nM; this is the "classical" PNM made evident by colorimetric techniques, and is invariably closely associated with the top of the $[\text{NO}_2^- + \text{NO}_3^-]$ gradient or "nitracline" (Herbland and Voituriez, 1979). The nitracline itself is located within the deep chlorophyll maximum layer (DCML). Third,

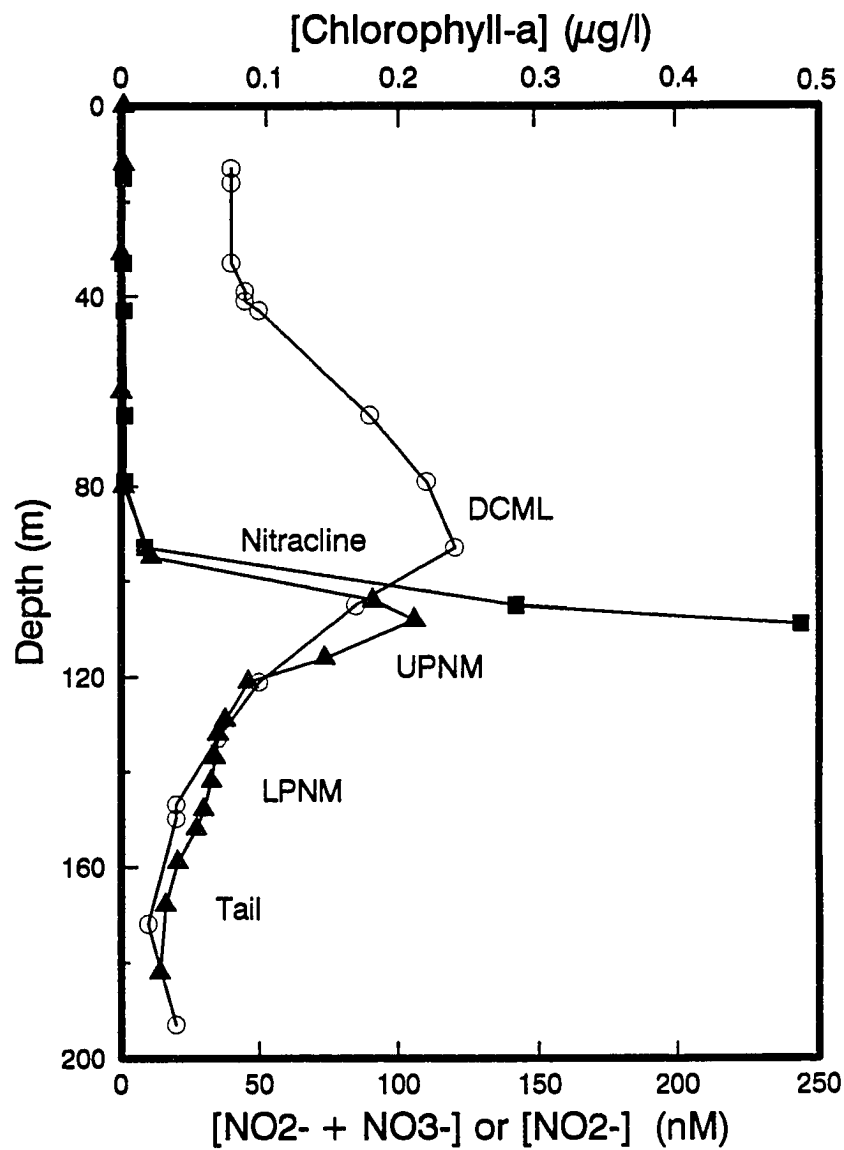


Fig. 3.2. Upper water column profiles of [nitrite], [nitrite+nitrate] and [chlorophyll-a] taken during HOT-41 (Oct. 1992). The bottom horizontal axis shows [nitrite] or [nitrite+nitrate] in nM, the upper horizontal axis shows [chlorophyll-a] in $\mu\text{g l}^{-1}$ and the vertical axis gives the density-averaged depth in m (see text). Concentrations are expressed in nM. Solid squares are [nitrite+nitrate], solid triangles are [nitrite] and open circles are [chlorophyll-a]. Major features associated with the primary nitrite maximum are labeled and discussed in the text.

we find the depth-decaying nitrite tail described by Zafiriou et al. (1992), with concentrations of around 50 nM at the base of the UPNM dropping to about 5-20 nM at 200 m. Lastly we see a second nitrite peak below the UPNM, in this case between about 135 and 155 m. This lower primary nitrite maximum (LPNM) varies greatly in magnitude. In the present case it is only barely discernable, but it is often more pronounced, at times rivaling the UPNM in magnitude. We have found a clearly defined LPNM in approximately one third of the cruises we have examined, and it arguably exists in others; we believe that the double-peaked PNM is not an anomaly, but that the maintenance of two distinct maxima is an indication of a vertical separation of nitrogen-cycle processes in this portion of the water column.

Let us now examine the types of temporal variability seen in the typical upper water column nitrite structure. First, we will look at variability on short timescales (hours to days); changes in nitrite profiles on such timescales can be quite dramatic (e.g., see French et al., 1983). We assume that within the circle defining Station ALOHA horizontal variability of upper water column nitrite during any given three-day period is small. While we cannot entirely dismiss the presence of spatial heterogeneity, a published 0-200 m nitrite section (using colorimetric techniques) along 28° N shows little variability between 162°30' W and 180° W, supporting our assumption (Schulenberger, 1978). Similarly, the section along 155° W presented by Wada and Hattori (1972) shows a strong degree of homogeneity in the vertical distribution of upper water column nitrite between about 15° N and 35° N. Nevertheless, minor spatial differences capable of complicating our temporal study could be masked by the 50 nM contour intervals used by the above authors, and so cannot be completely ruled out.

Given our assumption of relative spatial homogeneity, however, apparent changes in the vertical nitrite structure observed while on station must be the combined result of

two phenomena: changes in the positions of features due to physical motions or mixing of the water column, and changes of concentration within features due to biological and chemical transformations of nitrogen species. An example from HOT-19 (July, 1990) illustrates both types of alterations. Fig. 3.3a shows two nitrite profiles from casts sampled about 12 hours apart, plotted as $[\text{NO}_2^-]$ vs. depth (for clarity, only the 60-180 m range is shown). The offset between the upper slope of the UPNM in the two casts is due to the vertical displacement of isopycnals by an internal wave. In order to filter such short-term vertical motions of the PNM, we employ a density-averaging technique, in which a sampled isopycnal is related to its average depth during the three days on station (Fig. 3.3b). When plotted against this density-averaged depth, the correspondence in the positioning of features in the nitrite profiles is evident. The remaining disparities between the two profiles must be due to in situ sources and sinks of nitrite. In this particular case, what is observed is a decrease in integrated nitrite (0-200 m) of 1.2 mmol m^{-2} in 12 hours, which corresponds to a turnover time of about 2.6 days. We do not always see such rapid changes between profiles on a single cruise; however, since nitrification, phytoplankton nitrate reduction and phytoplankton nitrite assimilation are all strongly affected by light, and since internal waves can move organisms and substrates at a particular isopycnal vertically tens of meters through the light field in a few hours, it is not surprising that these short-term variations do occur.

Next let us examine nitrite variability on seasonal and longer timescales. Fig. 3.4 is a contour plot of nitrite concentration covering the upper 200 m from HOT-10 (Sept. 1989) to HOT-50 (Nov. 1993). To filter the short-term depth fluctuations of isopycnals caused by internal wave motions we again use density-averaged depth, rather than the actual in situ depth at the time of the bottle trip. This filtering allows us to use multiple profiles from a single cruise (when available), and to examine longer-term trends without

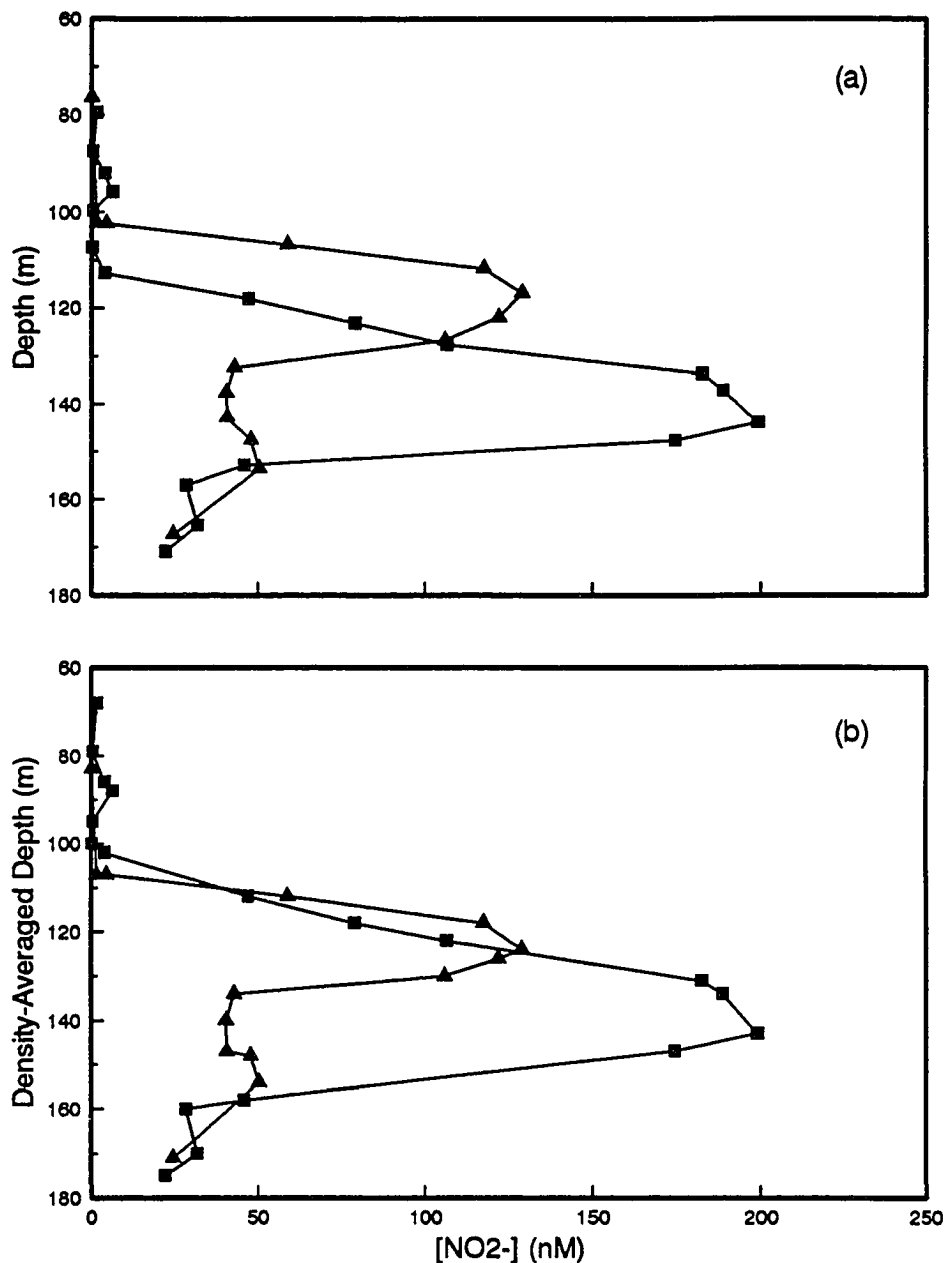


Fig. 3.3. Upper water column profiles of nitrite sampled twelve hours apart during HOT-19 (July 1990). Horizontal axis is nitrite concentration in nM. Solid squares are from a cast begun at 0400 hr local time, solid triangles are from a cast begun that evening at 1600 hr. (a) Vertical axis shows in situ depth in m, emphasizing vertical displacement of features. (b) Vertical axis shows depth in m after employing density-averaging (as explained in the text), emphasizing concentration changes within features.

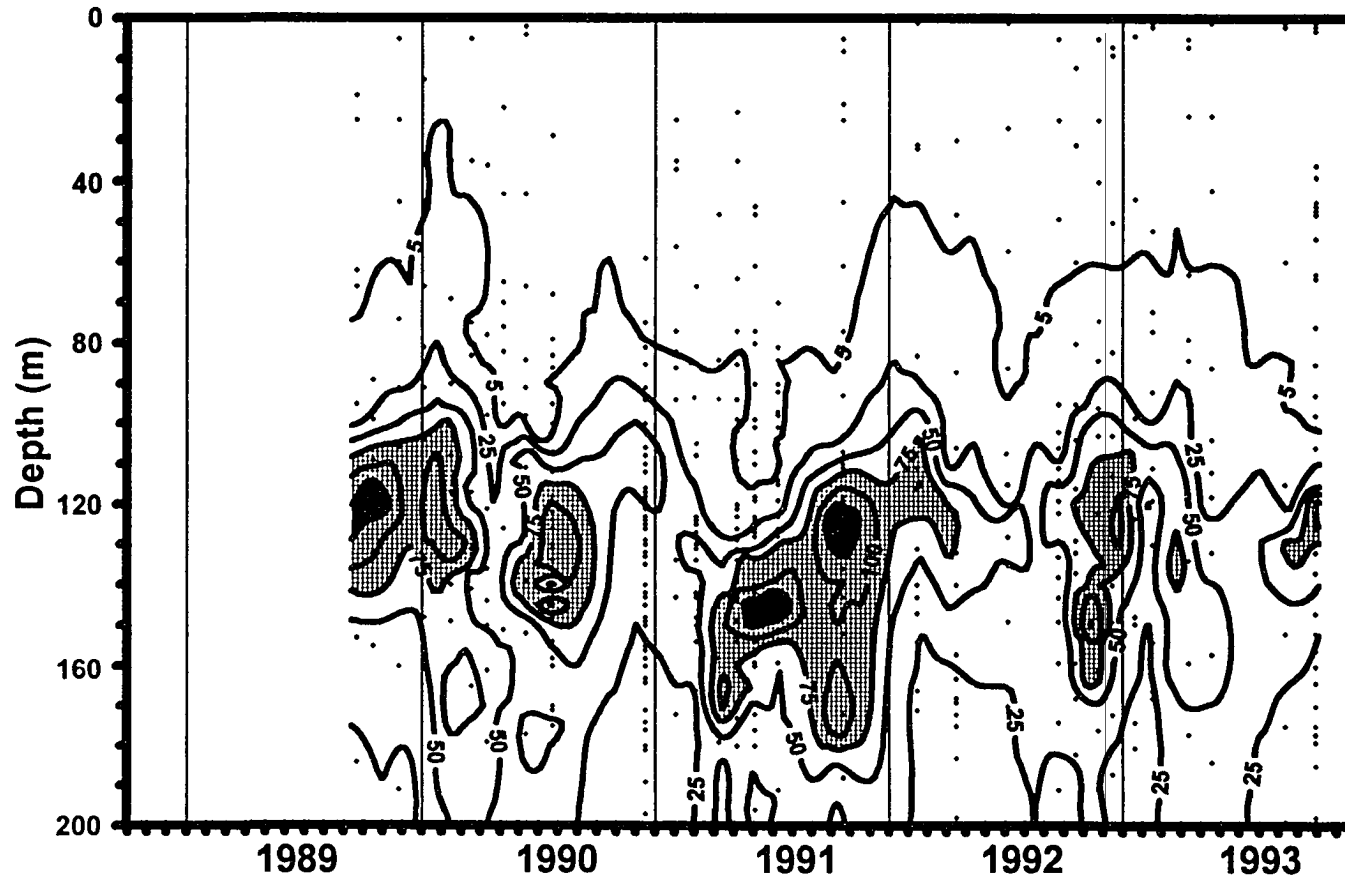


Fig. 3.4. Time-series contour plot of nitrite concentration in the upper 200 m at Station ALOHA during the first five years of the HOT program. Nitrite analyses were not begun until HOT-10 (Sept. 1989). The horizontal axis represents time in calendar years, the vertical axis shows density-averaged depth in m (see text). Contours show $[\text{NO}_2^-]$ in nM. Contour lines are located at 5 nM, 25 nM and every 25 nM thereafter. Hatching is included where values exceed 75 nM and solid shading indicates values >125 nM. Solid diamonds indicate where samples were collected.

undo short-term aliasing. Because the UPNM is an extremely sharp feature, the smoothing introduced by contouring yields a slightly lower maximum nitrite concentration than actually measured in an individual profile; nevertheless, a number of important trends in the smoothed data are evident.

We observe a distinct seasonality in the 5 and 25 nM contours, which can be used as an indicator of vertical mixing of nitracline waters into the surface layer. Upward excursions of these contours can be seen each year, and are associated with winter water column instability; in a particularly strong event during HOT-14 (Feb. 1990), the 5 nM contour nearly reached the sea surface. These observations are consistent with the hypothesized seasonality of mixing in the North Pacific gyre presented by Venrick (1993). The deepening of these contours in summer and early fall appears to be associated with the seasonal increase in light penetration. An abrupt deepening of the 25 nM contour is seen to some degree in the spring or early summer of each year, and is pronounced in 1990. This feature does not seem to be associated with wind-driven mixing from the surface downward, but instead with some sort of density instability in the thermocline, perhaps as a result of the passage of a mesoscale eddy.

Finally let us look at the positions of the UPNM and LPNM. We see three distinct times of year when the UPNM is intensified. Each winter, a shallow maximum develops, associated with vertical mixing; it is well-defined in 1989-90 and 1992-93, and discernable in 1990-91 and 1991-92. In spring, the UPNM deepens with the instability in the thermocline, clearly so in 1991 and 1993, less obviously in 1990 and 1992. Each summer/fall, slightly lagging the June maxima in light intensity, a robust UPNM develops. This feature is distinct in three of the years shown, but is not evident in 1992. Seasonality in the LPNM is not noted in this data set. In fact, because the LPNM is usually only a few nM in magnitude, its existence is masked by the large contour intervals used in Fig. 3.4.

Only during HOT-19 (summer 1990) and HOT-31 (fall 1991) does a distinct LPNM appear in the plot below the UPNM, yet within individual profiles a LPNM is often discernable (as in Figs. 3.2 and 3.3).

PNM structure and the nitracline

The nitrite profiles in the upper 200 m at Station ALOHA show the traditional features: a depleted surface layer with nanomolar to subnanomolar concentrations, a primary nitrite maximum, and a decrease into deeper waters. When examined in more detail, however, they reveal that the PNM is actually segregated into two layers: a large narrow UPNM which begins abruptly with the onset of the nitracline, and a low, broad LPNM, which rises above the depth-decaying nitrite tail. We suspect that the UPNM is maintained by the incomplete reduction of nitrate during assimilation by phytoplankton, and that the LPNM is the result of differential photoinhibition of the processes of ammonium oxidation and nitrite oxidation by nitrifying bacteria.

Herbland and Voituriez (1979) have compiled statistics on the relative vertical positions of the nitracline (which they defined as the first non-zero nitrate value as determined by standard colorimetric methods) and of the PNM at 123 stations across the tropical and subtropical Atlantic. They found a tight relationship, the PNM being on average about 11 m below the top of the nitracline. We use a slightly different procedural definition of the nitracline: we find the first sample that has $[\text{NO}_2^- + \text{NO}_3^-] > 100 \text{ nM}$, then take the midway depth between it and the previous sample above, and relate the isopycnal at that depth to the average depth that the isopycnal was at during the cruise. This density-averaging filters out much of the effect of internal waves, allowing correlation of PNM depth and nitracline depth when the two constituents were not sampled from the

same cast. Our data, a model II linear regression thereof, and the Herbland and Voituriez (1979) regression are all shown in Fig. 3.5. Those authors used data from many different areas, with nitracline depths varying from about 15 to 105 m. Our data are from a single location over several years, thus cover less range in nitracline depths. Nevertheless, we see from Fig. 3.5 that over long times, large areas and different ocean basins, the strong correlation between the onset of the nitracline and the appearance immediately below of the UPNM is never compromised. Such a relationship is consistent with the direct measurements of nitrate assimilation rate made by Eppley and Koeve (1990), whose data show a distinct maximum in this rate about 10-15 m below the top of the nitracline. Consider now the position of the nitrite maximum that is predicted by the nitrification model of Olson (1981). For waters with such clarity as at Station ALOHA ($k_{\text{par}} \approx 0.036\text{-}0.044 \text{ m}^{-1}$) the Olson model predicts a low broad peak centered at about 130-140 m. Because internal wave motions frequently move isopycnals at Station ALOHA vertically 20 m or more in a single day, the average light level at a given isopycnal is higher than that measured at its average reference depth. The layer in which differential nitrification occurs is thus expected to be deeper than that predicted by the static model. We believe that the addition of 10 m to the depth of the Olson PNM is reasonable and conservative. Thus the Olson PNM should be located at about 140-150 m, which is not consistent with the shallow depth of the UPNM. Nor is the low, broad shape of the Olson peak consistent with the strong, steep UPNM that we observe. Fig. 3.6 presents a time-series of UPNM position and nitracline position, showing their coherence and offset, and showing their average (\pm sd) depths to be 126 ± 18 m and 115 ± 18 m, respectively. Also shown is the position of the LPNM on eleven occasions when it was distinctly present. Its average depth is 149 ± 15 m, which is much more consistent with the feature predicted by the modified Olson model.

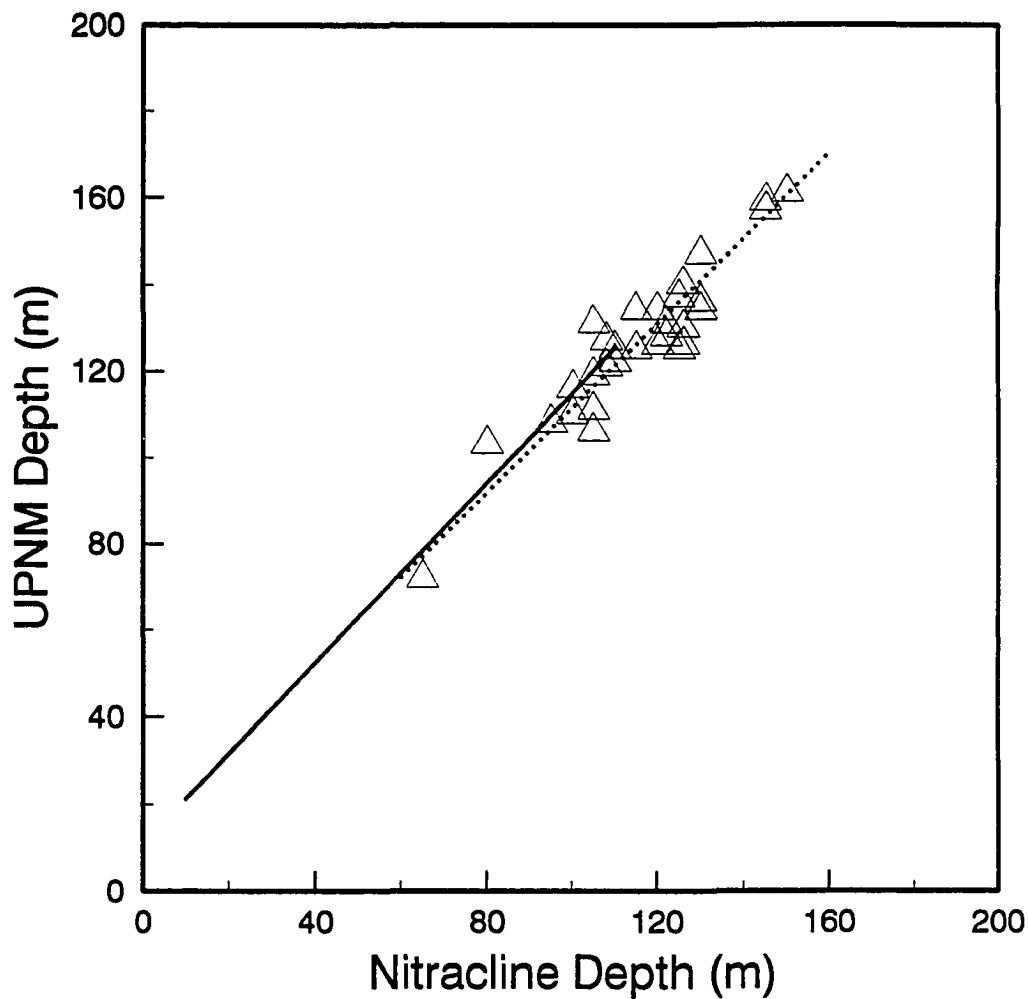


Fig. 3.5. Relationship between the positions of the upper primary nitrite maximum (UPNM) and the nitracline at Station ALOHA. The horizontal axis displays the depth associated with the nitracline, the vertical axis shows the depth associated with the UPNM. Both depths are density-averaged (see text) and in m. Open triangles are the actual data points from the 31 HOT cruises from which nitrite profiles were obtained. The dotted line is a reduced major axis model II linear regression of the data. The relationship determined by Herbland and Voituriez (1979) using data from 123 stations in the Atlantic is shown as a solid line.

The PNM and particle flux

Both nitrite-forming processes within the PNM, the excretion of nitrite by phytoplankton and the oxidation of ammonium to nitrite by nitrifying bacteria, can be associated with the gravitational export of particulate organic matter. Phytoplankton nitrite excretion is a result of nitrate assimilation in the lower euphotic zone, representing new production that is available for export. Nitrification is fueled by the ammonium regenerated from organic nitrogen, which may in turn have particle-associated nitrogen as a source. We therefore hypothesized that the integrated 0-200 m nitrite and the sinking particulate nitrogen collected in our 150 m sediment traps may co-vary in time.

During the period from HOT-10 (Sept. 1989) through HOT-28 (July 1991), the integrated nitrite and the particulate nitrogen flux were fairly well correlated, as expected (Fig. 3.7). The peaks and valleys in the time-series of nitrogen flux are either contemporaneous with or lag slightly the corresponding features in the nitrite record. However, from HOT-28 (July 1991) to HOT-50 (Nov. 1993) the relationship breaks down. Nitrite still shows considerable temporal variability, while particle flux decreases in both magnitude and variability and ceases to vary with nitrite.

The mechanism responsible for the observed changes in the characteristics of the particle flux is not entirely clear, but this and other equally dramatic changes in ecosystem parameters at Station ALOHA have been noted over the same time period, and may be related to the 1991-92 ENSO event (Karl et al., 1995a, 1995b). It is clear, though, that the integrated nitrite cannot under all conditions be used as an indicator of nitrogen export as we had originally hypothesized.

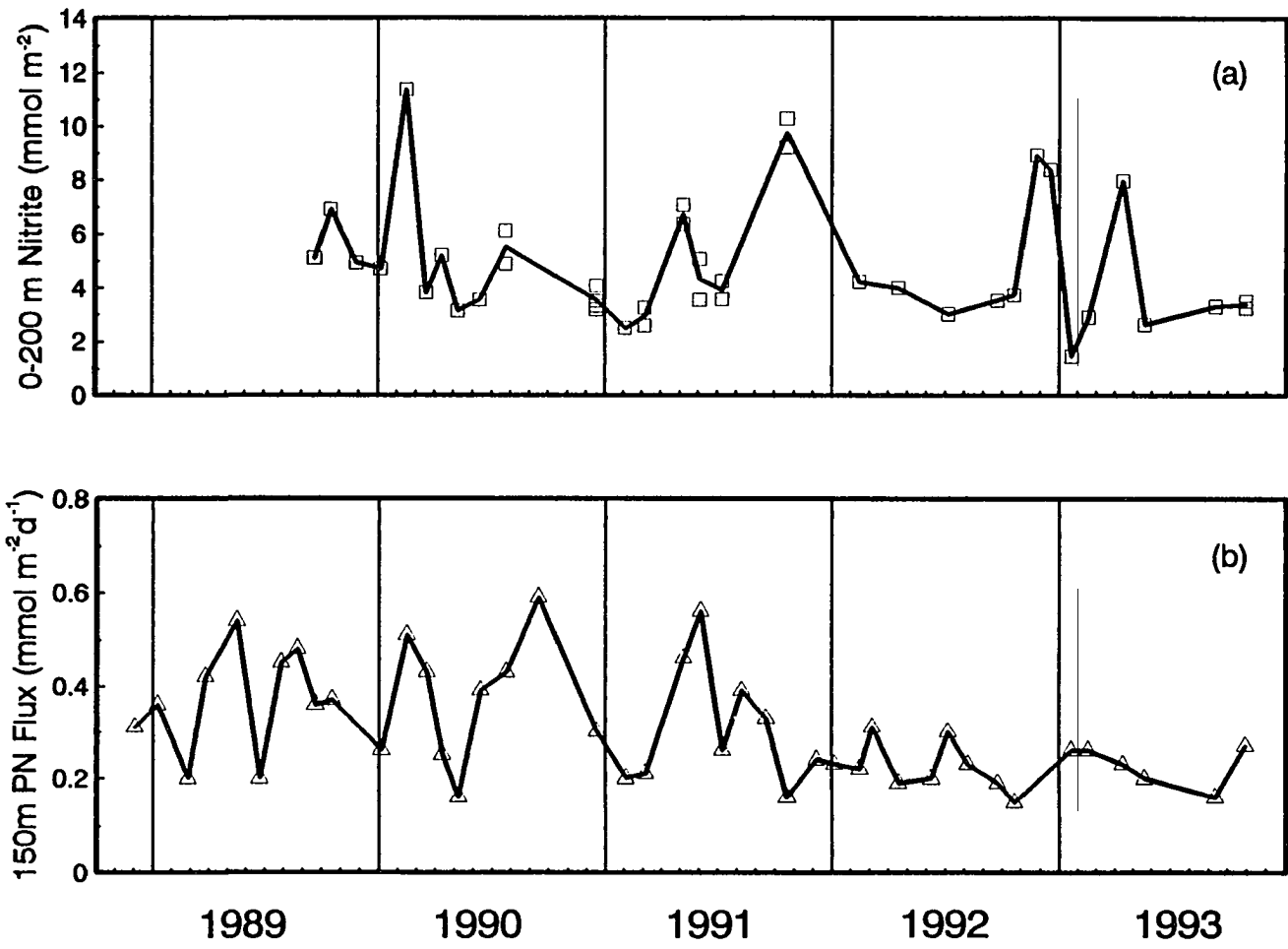


Fig. 3.7. Time-series of (a) 0-200 m depth-integrated nitrite and (b) mean particulate nitrogen flux at 150 m as collected by sediment traps at Station ALOHA. Integrated nitrite is expressed in mmol m⁻² along the vertical axis, nitrogen flux in mmol m⁻² d⁻¹. Horizontal axis displays time in calendar years.

Midwater and deep nitrite profiles

Nitrite distributions from seven HOT cruises measured over the 200-1000 m range show a supra-exponential decay from levels >5 nM to levels <1 nM over this depth interval (Fig. 3.8). An exception to this is the two-point maximum observed around 815 to 825 m during HOT-25 (Apr. 1991). This part of the water column is within the oxygen minimum zone (Bingham and Lukas, 1995) and the elevated nitrite may be an expression of nitrification and/or denitrification processes occurring at low oxygen tension. It is not clear why this feature appears during only one of the seven cruises examined. Also shown in Fig. 3.8 is part of a published profile from the NW Atlantic (Columbus Iselin 8816, Sta. No. 1; Zafiriou et al., 1992). Within the 200-1000 m range we find similar nitrite distributions to those measured in the Atlantic, both in shape and absolute magnitude. We also see concentration changes of a factor of two or more between cruises, indicating substantial variability on monthly timescales. These observations tend to support the hypothesis of rapid nitrite turnover in this part of the water column proposed by Zafiriou et al. (1992).

Fig. 3.9 shows our measured nitrite concentrations from 1000 m to within a few meters of the bottom at 4800 m from the same seven cruises as above. Note the change in nitrite concentration scale. Atlantic deep water nitrite data from the same cast of Zafiriou et al. (1992) mentioned above are presented for comparison. Concentrations of nitrite in these waters are low and with the exception of the near-bottom sample from HOT-25, all of these samples are ≤ 2 nM. Our values are substantially lower than those shown in the section presented by Wada and Hattori (1972), who reported concentrations up to 12 nM in waters deeper than 1000 m yet well above the seafloor. As their section passed within about 300 km of our study site, we must conclude either that horizontal or temporal nitrite

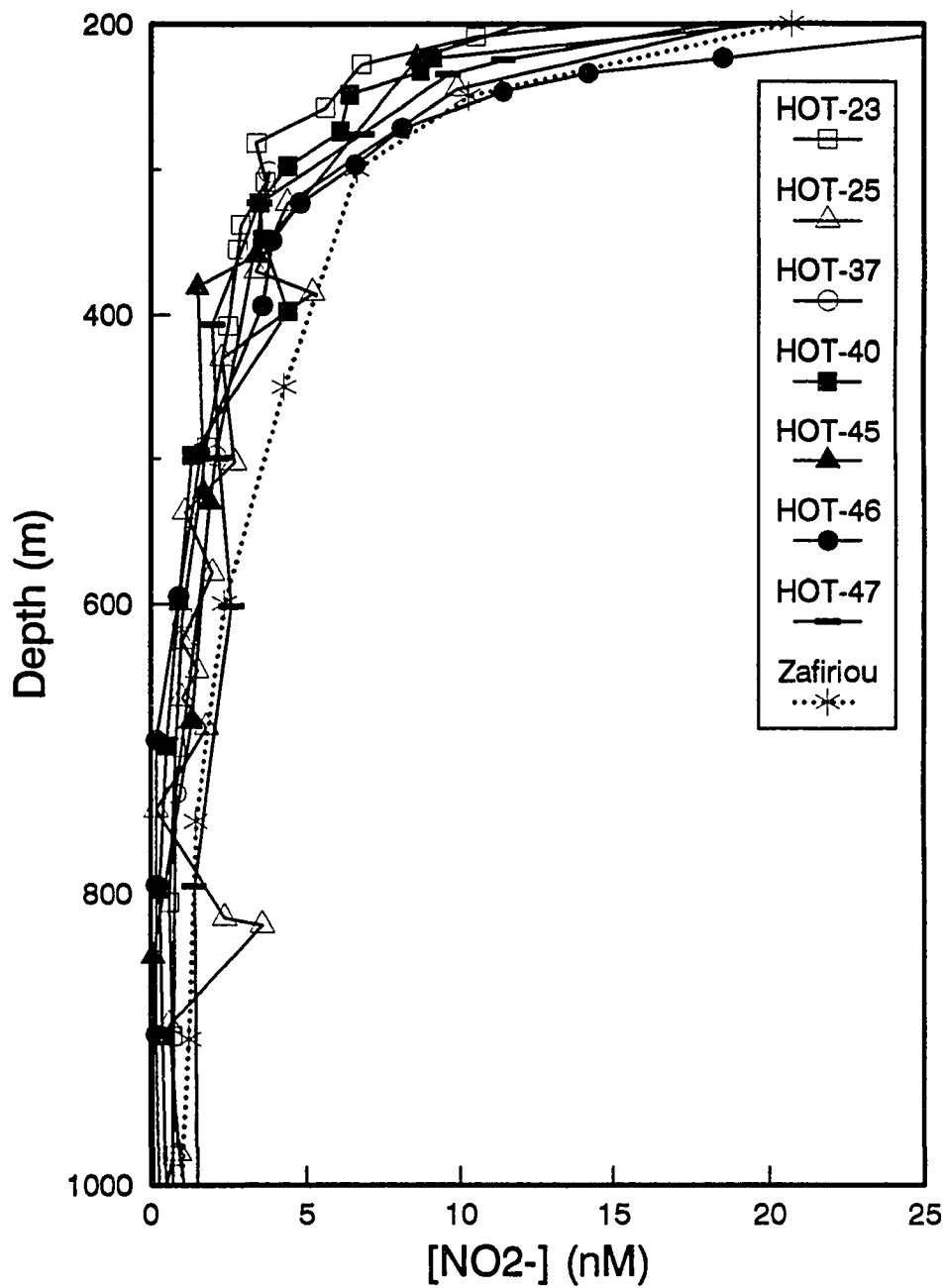


Fig. 3.8. Midwater profiles of nitrite from Station ALOHA. Horizontal axis is nitrite concentration in nM, vertical axis is depth in m. Individual cruises are as labeled. The asterisks and dotted line show for comparison data from the NW Atlantic published by Zafiriou et al. (1992).

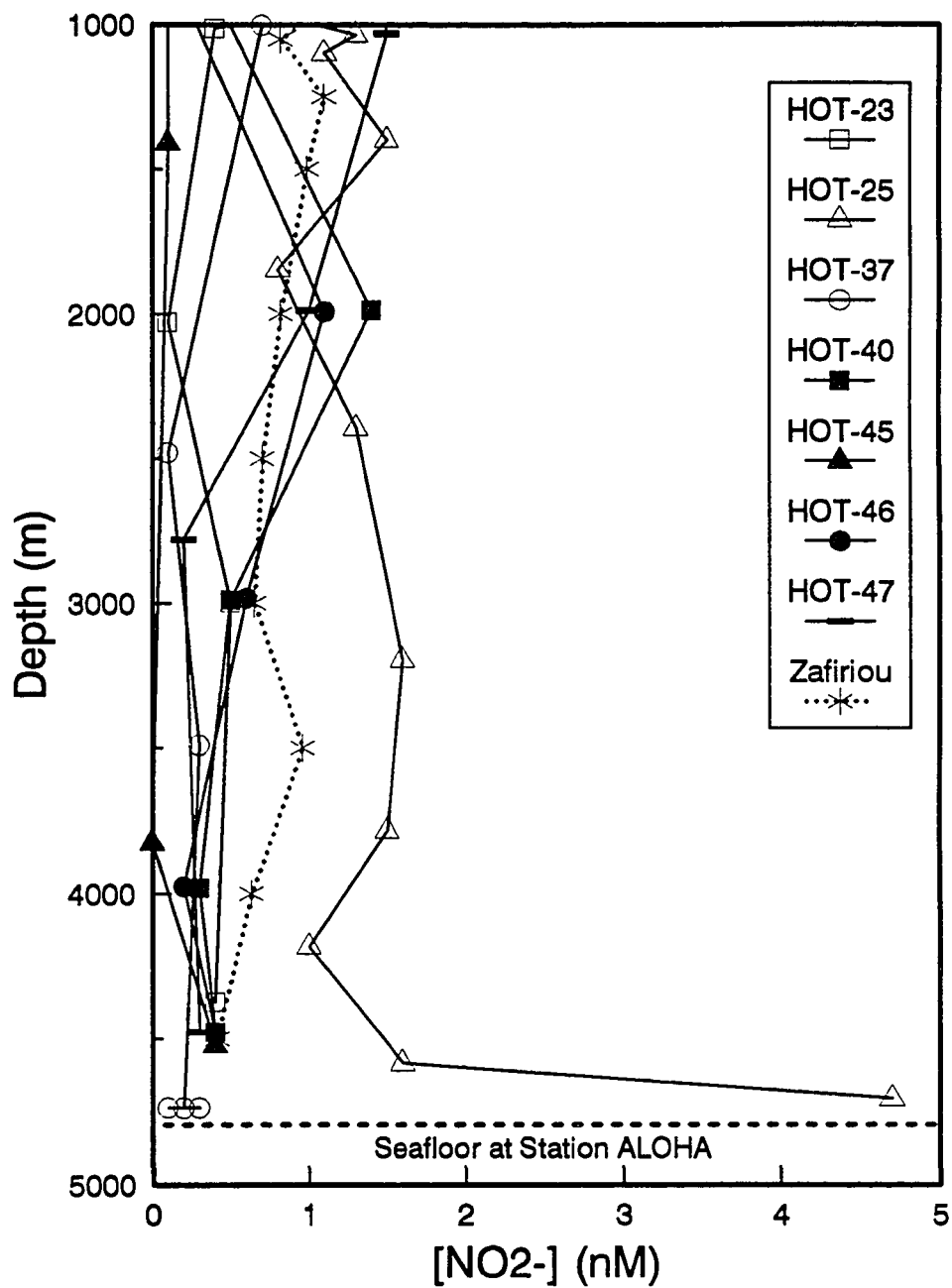


Fig. 3.9. Deep water profiles of nitrite from Station ALOHA. Horizontal axis is nitrite concentration in nM, vertical axis is depth in m. Individual cruises are as labeled. The asterisks and dotted line show for comparison data from the NW Atlantic published by Zafiriou et al. (1992).

variability in the deep ocean is large enough to account for these differences or that the analytical method used by these investigators suffered from difficulties at the low end of the concentration range. Because our values are much more consistent with those from the Atlantic, which Zafiriou et al. (1992) obtained using methods similar to ours, we suspect the latter is at least partly responsible for the discrepancy.

Four of our seven deep nitrite profiles show enrichments in the 4500-4800 m range with respect to their concentrations in the 3800-4300 m range above. In the HOT-25 profile this near-bottom enrichment is especially pronounced. Such enrichments have also been documented in the tropical Atlantic and Caribbean by Zafiriou et al. (1992). Rather than being anomalous, they may be a common feature of the deep ocean sediment-water interface. Because these bottom effects extend up 300 m or more from the ocean floor, and because they vary in magnitude, they may be indicators of variability in the intensity of sedimentary or nepheloid layer nitrogen cycle processes.

In deep waters above the potential influence of the sediments, the rates of nitrogen cycle process are expected to be very slow. However, we see up to 2 nM changes in deep nitrite on monthly to yearly timescales (Fig. 3.9). While this concentration change is small, when integrated over a 4000 m layer it represents a total nitrite change of 8 mmol m⁻², more than is usually found within the entire euphotic zone. This indicates that substantial month-to-month variability in the rates of deep nitrogen cycle processes and/or in the rate of supply of nitrogenous substrates exists in the deep Pacific.

CONCLUSIONS

We have measured the distribution of nitrite and its variability at Station ALOHA over a four year period using chemiluminescent measurement techniques. In the upper

200 m of the water column, we consistently find a depleted surface layer, a primary nitrite maximum (PNM) and a supra-exponential decay into deeper waters. Upon closer inspection, we find that the PNM is actually a two-peaked structure: it is comprised of a large upper maximum (UPNM) associated at all times with the nitracline, and a lower peak (LPNM) which is not always discernable but at times may rival the UPNM in magnitude. We believe that the former is maintained by the reduction of nitrate during its assimilation by phytoplankton, and that the latter is maintained by differential nitrification. We also find that, despite initially favorable results, the nitrite content of the upper 200 m is not a consistent indicator of particulate nitrogen export.

Below 200 m, the concentration of nitrite continues to decay to nanomolar and often sub-nanomolar levels. The magnitude and curvature of the distribution below 200 m closely resemble those measured in the Atlantic, arguing against significant basin-to-basin differences in the deep nitrite pool. As in the Atlantic, near-bottom nitrite enrichments are at times noted at Station ALOHA. Substantial temporal nitrite variability exists on monthly to yearly timescales in the 200-4800 m layer, indicating dynamic nitrogen cycling even at great depths.

REFERENCES

- Ambe, M. 1978. Note of the experience in the preparation of CSK standard solutions and the ICES-SCOR intercalibration experiment, 1969-1970. *Mar. Chem.* **6**:171-178.
- Bingham, F. and R. Lukas. 1995. Seasonal cycles of temperature, salinity and dissolved oxygen observed in the Hawaii Ocean Time-series. *Deep-Sea Res.*, submitted.
- Brandhorst, W. 1959. Nitrification and denitrification in the eastern tropical North Pacific. *J. Cons. Perm. Int. Explor. Mer.* **25**:2-20.
- Brzezinski, M.A. 1988. Vertical distribution of ammonium in stratified oligotrophic waters. *Limnol. Oceanogr.* **33**:1176-1182.
- Codispoti, L.A. and F.A. Richards. 1976. An analysis of the horizontal regime of denitrification in the eastern tropical North Pacific. *Limnol. Oceanogr.* **21**:379-388.
- Cox, R.D. 1980. Determination of nitrate and nitrite at the parts per billion level by chemiluminescence. *Anal. Chem.* **52**:332-335.
- Dore, J.E., T. Houlihan, D.V. Hebel, G. Tien, L. Tupas, and D.M. Karl. 1995. Freezing as a method of sample preservation for the analysis of dissolved inorganic nutrients in seawater. *Mar. Chem.*, submitted.
- Eppley, R.W. and W. Koeve. 1990. Nitrate use by plankton in the eastern subtropical North Atlantic, March-April 1989. *Limnol. Oceanogr.* **35**:1781-1788.
- Fiadeiro, M. and J.D.H. Strickland. 1968. Nitrate reduction and the occurrence of a deep nitrite maximum in the ocean off the west coast of South America. *J. Mar. Res.* **26**:187-201.
- French, D.P., M.J. Furnas and T.J. Smayda. 1983. Diel changes in nitrite concentration in the chlorophyll maximum in the Gulf of Mexico. *Deep-Sea Res.* **30**:707-722.
- Garside, C. 1982. A chemiluminescent technique for the determination of nanomolar concentrations of nitrate and nitrite in seawater. *Mar. Chem.* **11**:159-167.
- Herbland, A. and B. Voituriez. 1979. Hydrological structure analysis for estimating the primary production in the tropical Atlantic Ocean. *J. Mar. Res.* **37**:87-101.

Karl, D.M., J.R. Christian, J.E. Dore, D.V. Hebel, R. M. Letelier, L.M. Tupas and C.D. Winn. 1995a. Seasonal and interannual variability in primary production and particle flux at Station ALOHA. *Deep-Sea Res.*, submitted.

Karl, D.M., G.A. Knauer, J.H. Martin and B.B. Ward. 1984. Bacterial chemolithotrophy in the ocean is associated with sinking particles. *Nature* **309**:54-56.

Karl, D.M., R. Letelier, D. Hebel, L. Tupas, J. Dore, J. Christian and C. Winn. 1995b. Ecosystem changes in the North Pacific subtropical gyre attributed to the 1991-92 El Niño. *Nature* **373**:230-234.

Karl, D.M. and R. Lukas. 1995. The Hawaii Ocean Time-series (HOT) program: Background, rationale and field implementation. *Deep-Sea Res.*, submitted.

Kiefer, D.A., R.J. Olson and O. Holm-Hansen. 1976. Another look at the nitrite and chlorophyll maxima in the central North Pacific. *Deep-Sea Res.* **23**:1199-1208.

Letelier, R.M., J.E. Dore, C.D. Winn and D.M. Karl. 1995. Temporal variability in photosynthetic carbon assimilation efficiencies at Station ALOHA. *Deep-Sea Res.*, submitted.

Olson, R.J. 1981. Differential photoinhibition of marine nitrifying bacteria: a possible mechanism for the formation of the primary nitrite maximum. *J. Mar. Res.* **39**:227-238.

Rakestraw, N. W. 1936. The occurrence and significance of nitrite in the sea. *Biol. Bull. (Woods Hole)* **71**:133-167.

Ricker, W.E. 1973. Linear regression in fishery research. *J. Fish. Res. Board Can.* **30**:409-434.

Schulenberger, E. 1978. The deep chlorophyll maximum and mesoscale environmental heterogeneity in the western half of the North Pacific central gyre. *Deep-Sea Res.* **25**:1193-1208.

Strickland, J.D.H., and T.R. Parsons. 1972. A Practical Handbook of Seawater Analysis. (Bulletin No. 167, 2nd ed.) Ottawa: Fisheries Research Board of Canada.

Takenaka, N., A. Ueda and Y. Maeda. 1992. Acceleration of the rate of nitrite oxidation by freezing in aqueous solution. *Nature* **358**:736-738.

Vaccaro, R.F. and J.H. Ryther. 1960. Marine phytoplankton and the distribution of nitrite in the sea. *J. Cons. Perm. Int. Explor. Mer.* **25**:260-271.

Venrick, E.L. 1993. Phytoplankton seasonality in the central North Pacific: The endless summer reconsidered. *Limnol. Oceanogr.* **38**:1135-1149.

Wada, E. and A. Hattori. 1971. Spectrophotometric determination of traces of nitrite by concentration of azo dye on an ion-exchange resin, application to sea waters. *Anal. Chim. Acta* **56**:233-240.

Wada, E. and A. Hattori. 1972. Nitrite distribution and nitrate reduction in deep sea waters. *Deep-Sea Res.* **19**:123-132.

Wada, E. and A. Hattori. 1991. Nitrogen in the Sea: Forms, Abundances, and Rate Processes, CRC Press, Boca Raton, FL. 208 pp.

Ward, B.B. and O.C. Zafiriou. 1988. Nitrification and nitric oxide in the oxygen minimum of the eastern tropical North Pacific. *Deep-Sea Res.* **35**:1127-1142.

Zafiriou, O.C., L.A. Ball and Q. Hanley. 1992. Trace nitrite in oxic waters. *Deep-Sea Res.* **39**:1329-1347.

CHAPTER 4

NITRIFICATION IN THE EUPHOTIC ZONE AS A SOURCE FOR NITRITE, NITRATE AND NITROUS OXIDE AT STATION ALOHA

ABSTRACT

We measured chemoautotrophic bacterial nitrification rates in the euphotic zone at the North Pacific time-series Station ALOHA using clean incubations, high-precision chemical assays and inhibitor-sensitive radiocarbon uptake experiments. Ammonium and nitrite oxidation rates above 125 m were usually $<4 \mu\text{mol m}^{-3} \text{d}^{-1}$, but between 125 and 175 m the rates were variable and generally substantial, with a maximum ammonium oxidation rate of $122.6 \mu\text{mol m}^{-3} \text{d}^{-1}$ and a mean of $37.9 \mu\text{mol m}^{-3} \text{d}^{-1}$. Nitrite oxidation rates over this depth range averaged $28.8 \mu\text{mol m}^{-3} \text{d}^{-1}$ with a maximum of $106.8 \mu\text{mol m}^{-3} \text{d}^{-1}$. The highest nitrification rates were found below the large upper primary nitrite maximum (UPNM), coincident with a local nitrous oxide maximum. The distributions suggest that significant contribution of euphotic zone ammonium oxidation to the nitrite pool occurs below but not within the UPNM.

Euphotic zone nitrification appears to be a significant source for nitrous oxide, exceeding on an areal basis the eddy-diffusive flux of this gas from the deep water pool by at least an order of magnitude. However, sea-air gas flux calculations suggest that an additional source(s) of unknown nature dominates the production of nitrous oxide within the euphotic zone. A comparison of nitrous oxide profiles with nitrite profiles in the euphotic zone suggests that nitrous oxide may be produced during nitrite assimilation by

phytoplankton, although other potential sources such as denitrification cannot be ruled out.

Nitrification in the euphotic zone is also an important source of regenerated nitrate, at least several times greater on an areal basis than the rate of supply of nitrate from deep water via eddy-diffusion. This suggests that the traditional new production concept needs to be modified. We propose a conceptual model of the nitrogen cycle for the euphotic zone at Station ALOHA that includes important roles for both nitrification and nitrogen fixation.

INTRODUCTION

Nitrification, the microbiologically-mediated oxidation of ammonium to nitrite to nitrate, is a key process in the global nitrogen cycle (Ward, 1986). In the marine environment, the vertical flux into the euphotic zone of nitrate regenerated by nitrification in deep water is considered crucial to ecosystem stability through its support of new primary photosynthetic production (Eppley and Peterson, 1979). However, nitrifying bacteria are also active within the euphotic zone, especially within the primary nitrite maximum (Olson, 1981a; Ward et al., 1982), and in associations with sinking particles (Karl et al., 1984). Although primary production based on nitrate is usually equated with new production (Dugdale and Goering, 1967; Eppley and Peterson, 1979), if the nitrate is regenerated within the euphotic zone it must be considered recycled production. Consequently, if nitrification in an oceanic ecosystem proceeds at a substantial rate within the euphotic zone then nitrate uptake cannot be equated with new production for that ecosystem (Dugdale and Goering, 1967; Priscu and Downes, 1985; Ward et al., 1989b).

It has been suggested that bacterial nitrification is responsible for the maintenance of the primary nitrite maximum (PNM), an accumulation of nitrite found in the lower euphotic zone over much of the world's oceans (Rakestraw, 1936; Brandhorst, 1959; Olson, 1981b). However, the excretion of nitrite by phytoplankton during nitrate assimilation has also been implicated as a nitrite source (Vaccaro and Ryther, 1960; Kiefer et al., 1976; Herbland and Voituriez, 1979). At oligotrophic oceanic sites such as the Hawaii Ocean Time-series Station ALOHA (22°45' N, 158° W), the PNM is located well within the euphotic zone (Dore and Karl, 1995), hence knowledge of the relative importance of these oxidative and reductive processes is necessary for an accurate understanding of the nitrogen cycle in such areas.

Furthermore, nitrification produces the ozone-depleting greenhouse gas nitrous oxide as a by-product (Ritchie and Nicholas, 1972; Goreau et al., 1980; Poth and Focht, 1985). Euphotic zone nitrification represents a near-surface source of this trace gas (Capone, 1991), yet other processes potentially contribute to the generation of nitrous oxide within the euphotic zone as well.

The distribution and magnitude of euphotic zone nitrification processes are clearly important factors to consider in biogeochemical studies of marine primary production, nitrogen cycling and carbon cycling. We report here the results of a number of field observations and rate experiments designed to elucidate the extent of euphotic zone nitrification and its potential influence on recycled production, the sea-air flux of nitrous oxide and the distribution of nitrite at Station ALOHA.

MATERIALS AND METHODS

Station location

All sampling and experiments were performed at Station ALOHA (A Long-term Oligotrophic Habitat Assessment; Fig. 1.3), a North Pacific deep water (>4500 m) site visited at approximately monthly intervals as part of the Hawaii Ocean Time-series (HOT) project (Karl and Lukas, 1995). The HOT project is funded jointly by the U.S.-JGOFS and U.S.-WOCE programs, which primarily focus on biogeochemistry and hydrography, respectively. The oligotrophic waters at Station ALOHA are considered representative of the North Pacific subtropical gyre. Sampling is restricted to a circle with an 11 km radius centered at 22°45' N, 158° W, 100 km north of Kahuku Pt., Oahu, Hawaii.

Sampling

A CTD/rosette system equipped with 24 twelve-liter PVC bottles with Teflon-coated springs was used for sample collection. In addition to the CTD (SeaBird), the system uses a flash fluorometer (SeaTech) and a polarographic oxygen sensor (Beckman). The protocols for CTD operation, data analysis and sensor calibration are described elsewhere (Bingham and Lukas, 1995). The surface flux of photosynthetically available radiation (PAR; 400-700 nm) was measured with a Licor cosine collector. Underwater PAR was determined using a hand-lowered Biospherical profiling natural fluorometer.

Nutrients and dissolved oxygen

Water samples for nitrite (NO_2^-) and nitrate (NO_3^-) were drawn using clean Tygon tubing into acid-washed 125-ml polyethylene bottles and stored frozen as described in Dore and Karl (1995) for later analysis at our shore-based laboratory. $[\text{NO}_2^-]$ and $[\text{NO}_3^- + \text{NO}_2^-]$ were measured by the chemiluminescent methods developed by Cox (1980) and Garside (1982), which offer detection limits and precisions of 2 nM or less (Dore and Karl, 1995). $[\text{NO}_3^-]$ was calculated by difference. In all nitrification rate experiments, both $[\text{NO}_2^-]$ and $[\text{NO}_3^- + \text{NO}_2^-]$ were determined on the same samples, but some of the water column profiles of $[\text{NO}_3^- + \text{NO}_2^-]$ were determined on separate casts, thus water column $[\text{NO}_3^-]$ is not reported separately. In these cases, the depths at which $[\text{NO}_3^- + \text{NO}_2^-]$ samples were collected are adjusted using potential densities so that the relative positions of features are not altered by short-term internal wave motions, which have been shown to vertically displace isopycnals at Station ALOHA by tens of meters in a few hours (Dore and Karl, 1995).

Samples for dissolved oxygen were collected without aeration using clean Tygon tubing into 125 ml glass iodine flasks, immediately fixed and determined at sea using whole-bottle iodate titrations with a computer-assessed potentiometric endpoint, a slight variation of the whole-bottle Winkler method described by Carpenter (1965).

Nitrous oxide

Samples for nitrous oxide (N_2O) were collected in 300 ml glass BOD-type bottles with ground glass stoppers, which had been previously washed with HCl and combusted (450 °C for >5 hr). Clean Tygon tubing was used to rinse and fill each sample bottle from

the bottom, allowing at least two volumes of sample to overflow in the process and displacing all bubbles. Each sample was then aspirated to just below the neck and poisoned with 100 μl saturated mercuric chloride. The neck was dried with a clean Kimwipe and the stopper replaced after light lubrication with a carbon-based grease (Apiezon). The stoppers were secured with polyethylene tape and the samples were stored in the dark at laboratory temperature (appx. 20 $^{\circ}\text{C}$) until the day of analysis. N_2O samples stored in a similar manner have been demonstrated to be stable for at least 1.5 months (Elkins, 1980; Butler and Elkins, 1991). Furthermore, although the storage time for our samples ranged from a few days to several months, we found no trend in the relationship between measured surface $[\text{N}_2\text{O}]$ and storage time.

N_2O analysis was performed using a Varian model 3300 gas chromatograph (GC) outfitted with a ^{63}Ni electron capture detector held at 360 $^{\circ}\text{C}$. The protocol, briefly outlined here, was similar to that of Elkins (1980), except that our GC was configured for backflushing and we did not use multiple equilibrations. Separation was achieved on Chromosorb 102 (80/100 mesh) packed in a 3 m column of 3.2 mm diameter stainless steel tubing maintained at 55 $^{\circ}\text{C}$. The carrier gas was an ultra high purity 5% mixture of methane in argon; ultra high purity helium was used for sample equilibrations and backflushing. Both gases were further purified using molecular sieve 5A and an oxygen scrubber.

Upon opening an individual sample bottle, a gas-tight syringe was used to draw 10 ml of sample without aeration, then an additional 10 ml of helium. The syringe was capped and shaken for 2 min to equilibrate the solute and gas phases, then the headspace was flushed through a 5 ml stainless steel sample loop attached to a six-port zero-dead volume valve (Valco) and given 1 min to reach atmospheric pressure. A 1 m vent coil of 1.6 mm diameter tubing prevented introduction of ambient air into the sample loop as the

pressure equalized. Upon activating the valve, the carrier flow (25 ml min^{-1}) flushed the 5 ml sample by way of a second valve through a 30 cm pre-column of Poropak-T (80/100 mesh) and then on to the analytical column. After 1 min, the second valve was switched so that the pre-column was back-flushed with helium, preventing water and associated halocarbons from contaminating the analytical column and detector (Butler and Elkins, 1991).

N_2O peak area was determined using a Hewlett-Packard model 3396A integrator. Under the above conditions, the N_2O peak eluted at 2.4 min, well after the oxygen peak which eluted at 1.4 min. A small CO_2 peak, sometimes evident at 2.0 min, was well resolved from the N_2O peak. N_2O concentration and percent saturation were calculated using published equations for seawater (Weiss and Price, 1980) assuming an atmospheric mixing ratio of 312 ppbv. We have assumed this mixing ratio based on the world mean tropospheric N_2O concentration in 1990 (310 ppbv) extrapolated to 1993 assuming a yearly rise of 0.25% (Houghton et al., 1990). The same value is obtained independently from taking the mean of the extrapolated 1993 values of the atmospheric N_2O mixing ratio as measured in 1988 at Cape Meares, Oregon, and at Point Matatula, American Samoa, between which Hawaii is roughly equidistant (Boden et al., 1991).

The average precision of the N_2O assay, based on 15 samples that were run in duplicate, was $\pm 3.6\%$. Accuracy was maintained by comparing standards from two different vendors. Calibration slopes based on a 1.011 ppmv standard (Scott) and by dilutions of a 155 ppmv standard (Airco) agreed to within $<3\%$.

Nitrification rates

Chemoautotrophic ammonium oxidation rates were determined by an inhibitor-sensitive dark radiocarbon (^{14}C) uptake assay (Billen, 1976; Somville, 1978) and independently by a chemical assay. Chemoautotrophic nitrite oxidation rates were also measured using a chemical assay.

The ^{14}C -based assay relies upon measurement of the dark incorporation of $\text{H}^{14}\text{CO}_3^-$ into particulate organic matter within an incubated water sample with and without the addition of a metabolic inhibitor that is known to affect ammonium oxidizing bacteria. Incubations were conducted in the dark to prevent interference from photoautotrophic carbon assimilation, and were temperature controlled to simulate in situ conditions. The difference between the ^{14}C assimilated in the controls and that assimilated in the inhibited samples is a measure of the growth of ammonium oxidizing bacteria.

We used acetylene gas (C_2H_2) as an inhibitor of ammonium oxidation. C_2H_2 is known to be an effective inhibitor of NH_4^+ oxidation (Walter et al., 1979; Hynes and Knowles, 1981; Jones and Morita, 1984), and is highly water soluble. Acetylene also inhibits denitrification, but since denitrification is not an autotrophic process its inhibition should not appreciably affect the results of the ^{14}C based assay. Nitrapyrin (N-Serve; Dow Chemical Co.) is more commonly used as a nitrification inhibitor, however, it has been noted that in oligotrophic oceanic waters it can act as a general metabolic inhibitor (Ward, 1986). Nitrapyrin also must be introduced dissolved in a solvent, which itself can affect metabolism (Ward, 1986), while acetylene is introduced as an ultra high purity gas.

Details of the experimental protocol used changed slightly over time but the protocol essentially adhered to the following procedures. A nighttime rosette cast was made to collect samples from up to 24 depths within the upper 200 m. Nitrification rate

experiments were conducted on water from two to six of these depths. Up to 400 ml of sample were collected directly from the rosette bottles under subdued light into acid-washed incubation bottles, usually 500 ml polycarbonate bottles to which red rubber septa had been attached with silicone sealant. The sealant was aged to assure complete curing, and the septum was attached in such a way that the sealant never came in contact with the water sample. Using gas chromatography with flame ionization detection (Letelier, 1994) it was determined that less than 10% of the C_2H_2 in the headspace diffused through the polycarbonate container over the duration of a typical incubation.

From each depth, from two to four replicate incubation bottles were filled for controls and an equal number for the C_2H_2 treatments. Each bottle was inoculated with 75-200 μCi of $H^{14}CO_3^-$, then quickly treated with the inhibitor. Ultra high purity C_2H_2 (3 ml) was injected into the headspace through the septum with a syringe after an equal volume had been removed. Although in this protocol the final C_2H_2 concentration varied with sample and headspace volume it was always greater than the 3.8 μM required for complete inhibition of ammonium oxidation in pure cultures of the ammonium oxidizing bacterium *Nitrosomonas europaea* (Hynes and Knowles, 1981). The incubation bottles were then gently agitated to evenly distribute the radiocarbon and the inhibitor, covered with opaque bags, and placed in temperature controlled water baths for approximately 24 hr. The in situ temperatures were matched to within $\pm 1^\circ C$. After the incubations, the samples were vacuum filtered through 0.2 μm polycarbonate membrane filters (Nuclepore). The ^{14}C activity was determined using liquid scintillation counting as described in Letelier et al. (1995). Dissolved inorganic carbon concentrations, used in the calculation of carbon assimilation rates, were determined independently by coulometry (Winn et al., 1994).

Because the ^{14}C -based assay measures carbon incorporation as a surrogate for ammonium oxidation, a conversion factor must be applied to obtain the latter rate from the former. A number of studies have reported such factors for marine nitrifiers, ranging from 8.3 to 41.7 mol NH_4^+ oxidized per mol C fixed during ammonium oxidation (Carlucci and Strickland, 1968; Billen, 1976; Belser, 1984; Glover, 1985; Feliatra and Bianchi, 1993). The large range probably reflects both a lack of obligate coupling between the oxidation of ammonium and carbon fixation in nitrifying bacteria and a varied response of nitrifiers to different environmental parameters. We have adopted the lower value of 8.3 (Billen, 1976), owing to the observation of Feliatra and Bianchi (1993) that nitrifiers in seawater generally have the lowest N:C when compared to nitrifiers in other natural aquatic environments. The empirical N:C measured independently by combining our data from the ^{14}C experiments and the chemical assay (see below) confirmed that this was a reasonable conversion factor.

Our second method for the assessment of nitrification rates involves the direct measurement of the changes in $[\text{NO}_2^-]$ and $[\text{NO}_3^-]$ in incubated samples. Replicate samples were incubated in the dark in 500 ml acid-washed polycarbonate bottles without any additions for 24-36 hr. Ammonium oxidation was determined by the change of the total $[\text{NO}_3^- + \text{NO}_2^-]$ over the course of the incubation, and nitrite oxidation by the change in $[\text{NO}_3^-]$ alone. Although processes other than nitrification may alter $[\text{NO}_3^-]$ and $[\text{NO}_2^-]$ even in total darkness (e.g. phytoplankton nitrate reduction), nitrification is expected to dominate the conversions of these nitrogen species in the absence of light energy. Also, because much of the nitrate assimilated by phytoplankton in the dark is reduced only as far as nitrite (Laws and Wong, 1978), little error in the ammonium oxidation rate measurements would be introduced by this process, though underestimates of the nitrite oxidation rates may result. Heterotrophic nitrification, while it has not been conclusively

demonstrated to occur in seawater (Kaplan, 1983), would be included by the chemical measurements, but because it is not an autotrophic process it would have less effect on the ^{14}C -based measurements, and furthermore would cause the two independent estimates of nitrification to diverge. During one cruise we used both methods simultaneously in order to check the validity of the conversion factors chosen for the ^{14}C -based method.

Because our ^{14}C -based nitrification measurements are based upon the difference in carbon assimilation between control and treatment groups, which each have some natural variability associated with them, it is difficult to define an absolute detection limit for the assay. Based upon our lowest observed variability within groups, however, we estimate that ammonium oxidation rates $<2 \mu\text{mol m}^{-3} \text{d}^{-1}$ are not measurable using our protocol. Similarly, the chemical-based assays for ammonium and nitrite oxidation are limited by within-group variability; for these assays, we estimate that nitrification rates $<4 \mu\text{mol m}^{-3} \text{d}^{-1}$ are not measurable with our protocol.

RESULTS AND DISCUSSION

Nitrification rates

Nitrification rates in the upper 125 m were undetectable in all but one case (Table 4.1). Of seven ^{14}C -based ammonium oxidation rate measurements in this layer, only one exceeded the estimated $2 \mu\text{mol m}^{-3} \text{d}^{-1}$ detection limit for the assay ($17.8 \mu\text{mol m}^{-3} \text{d}^{-1}$ at 59 m during HOT-41), and the one chemical-based ammonium oxidation measurement above 125 m was below the estimated $4 \mu\text{mol m}^{-3} \text{d}^{-1}$ detection limit. The single nitrite oxidation rate measured in this upper layer was also $<4 \mu\text{mol m}^{-3} \text{d}^{-1}$. Between 125 and 175 m, however, ammonium oxidation rates were often substantial, reaching a maximum

Table 4.1. Nitrification rates at Station ALOHA†

Cruise	Date	Depth (m)	NH ₄ ⁺ Ox Rate		NO ₂ ⁻ Ox Rate
			(μmol m ⁻³ d ⁻¹)		(μmol m ⁻³ d ⁻¹)
			¹⁴ C-based	chem-based	chem-based
HOT-31	Oct. 1991	131	9.8	32.3	9.6
		152	*122.6	119.5	106.8
HOT-36	Apr. 1992	121	§<2	‡—	—
		151	21.8	—	—
		160	80.2	—	—
HOT-40	Sept. 1992	59	<2	—	—
		100	<2	—	—
		120	<2	—	—
		135	7.0	—	—
		152	<2	—	—
		173	5.3	—	—
HOT-41	Oct. 1992	59	17.8	—	—
		89	<2	—	—
		109	<2	—	—
		131	97.4	—	—
		151	<2	—	—
		174	32.6	—	—

Table 4.1. (Cont.) Nitrification rates at Station ALOHA

HOT-50	Oct. 1993	106	—	[□] <4	<4
		135	—	*6.8	<4
		155	—	*23.3	*18.6
		175	—	10.5	8.8

† Nitrification rates are given as the daily rates of microbial ammonium and nitrite oxidation as measured using an inhibitor-sensitive radiocarbon uptake assay (¹⁴C-based) and by a chemical assay (chem-based).

‡ = No data.

§ = Measured rate is below the estimated 2 μmol m⁻³ d⁻¹ detection limit of the ¹⁴C-based assay.

□ = Measured rate is below the estimated 4 μmol m⁻³ d⁻¹ detection limit of the chemical-based assay.

* Indicates statistically significant difference between treatment and control groups at the α = 0.05 level using a Student's t-test.

of $122.6 \mu\text{mol m}^{-3} \text{d}^{-1}$ (mean = $37.9 \mu\text{mol m}^{-3} \text{d}^{-1}$, median = $21.8 \mu\text{mol m}^{-3} \text{d}^{-1}$, $n = 15$). Nitrite oxidation rates were also elevated within this depth range, with a maximum of $106.8 \mu\text{mol m}^{-3} \text{d}^{-1}$ (mean = $28.8 \mu\text{mol m}^{-3} \text{d}^{-1}$, median = $9.6 \mu\text{mol m}^{-3} \text{d}^{-1}$, $n = 5$). Because values below the estimated analytical detection limits were treated as zero for these calculations, the mean and median rates reported above should be considered minimum estimates.

These vertical distributions of nitrifying activity are consistent with photoinhibition of nitrifying bacteria in the upper layer and a release from inhibition below 125 m (Fig. 4.1). Also of note is that ammonium oxidation only slightly exceeds nitrite oxidation in this data set (Table 4.1), suggesting that although nitrite oxidizers may suffer greater photoinhibition than ammonium oxidizers (Olson, 1981b), the net production of nitrite by nitrification is not as large as might be expected if only ammonium oxidation data were available. At the same time, this implies that the net production rate of nitrate by nitrification is only slightly below the rate of ammonium oxidation.

Previous measurements of nitrification rates in the lower euphotic zone of the North Pacific subtropical gyre are few, and range from 2.24 - $7.30 \mu\text{mol m}^{-3} \text{d}^{-1}$ (Olson, 1981a). However, this entire data set of five measurements, made with ^{15}N tracer techniques, was from a single cruise over a time period of only two weeks, and no more than one depth was sampled on any given day. Because ammonium oxidation rates in our study varied considerably with depth and between cruises, and given that rates of over $200 \mu\text{mol m}^{-3} \text{d}^{-1}$ have been measured or estimated in other marine environments (Ward, 1982; Priscu and Downes, 1985; Feliatra and Bianchi, 1993), we consider our results to be more representative of this oceanic habitat. Furthermore, the good agreement between the independent ^{14}C -based and chemical-based ammonium oxidation rate measurements made during HOT-31 (Table 4.1) gives us additional confidence in our results.

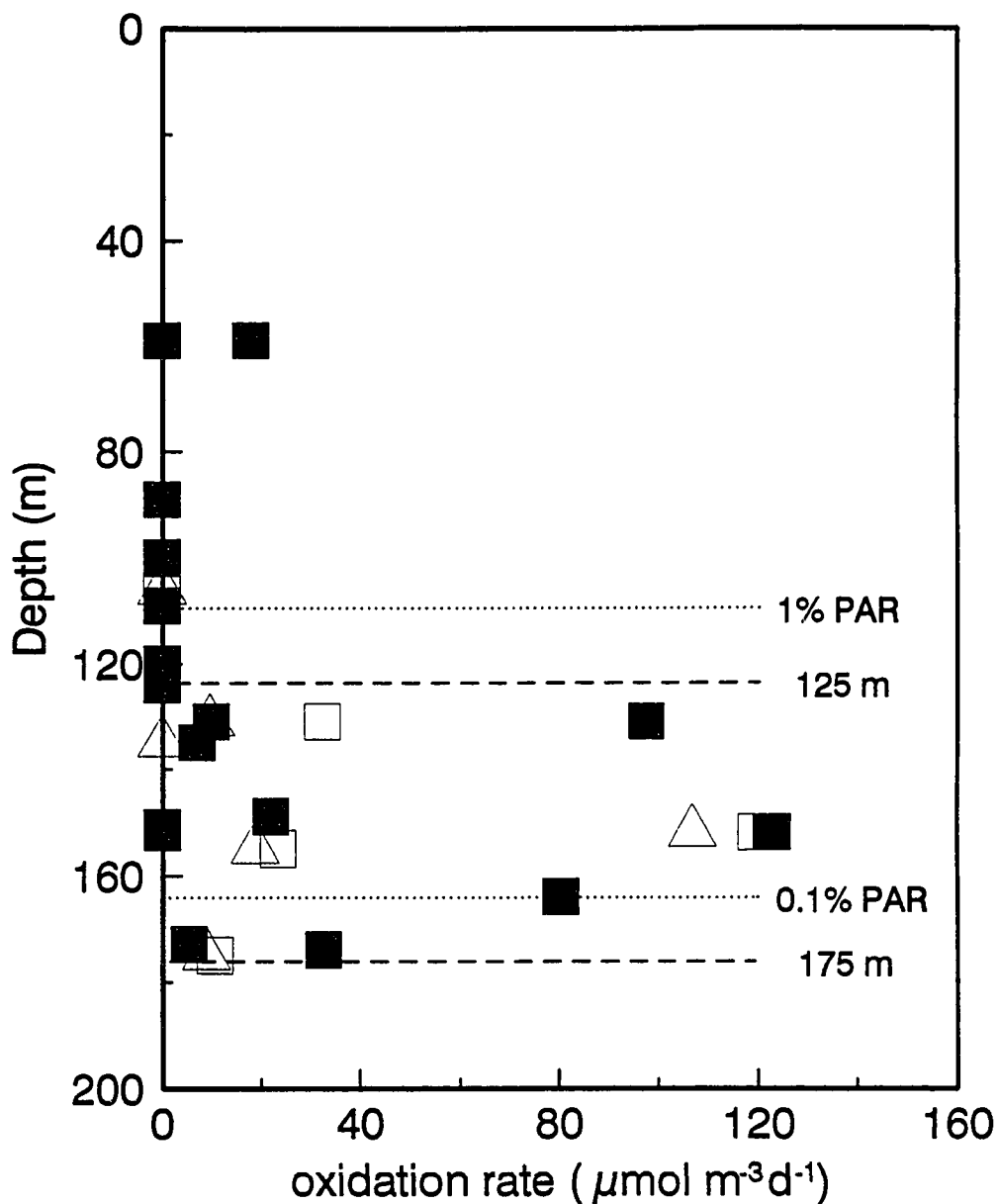


Fig. 4.1. Depth distribution (0-200 m) of nitrification rates from five cruises at Station ALOHA. Solid and open squares represent ammonium oxidation rates based on ¹⁴C and chemical assays, respectively. Open triangles represent chemical-based nitrite oxidation rates. The lower euphotic zone is designated as the 125-175 m layer (dashed lines). Approximate depths of the 1% and 0.1% PAR levels are also indicated (dotted lines). Data are from HOT-31 (Oct. 1991), HOT-36 (Apr. 1992), HOT-40 (Sept. 1992), HOT-41 (Oct. 1992) and HOT-50 (Oct. 1993).

Nitrification and the primary nitrite maximum

Water column profiles of $[\text{NO}_2^-]$ and $[\text{NO}_3^- + \text{NO}_2^-]$ in all of the seven HOT cruises discussed here show a primary nitrite maximum (PNM) beginning a few meters beneath the top of the nitrate gradient or nitracline (Figs. 4.2-4.8). In all five of the cruises for which we have nitrification rate measurements, both ammonium oxidation rates and (where available) nitrite oxidation rates within the large upper peak of the primary nitrite maximum are lower than a few meters below within the "tail" of the nitrite distribution (Figs. 4.2-4.5 and 4.7). This finding is consistent with our earlier hypothesis that this upper primary nitrite maximum (UPNM) is maintained by algal reduction of nitrate rather than by bacterial ammonium oxidation (Dore and Karl, 1995). A lower primary nitrite maximum (LPNM) below 125 m depth is clearly evident in three cases (HOT-31, HOT-40 and HOT-57; Figs. 4.2, 4.4 and 4.8) and less apparent in a fourth profile (HOT-41; Fig. 4.5). The LPNM may be a result of the differential photoinhibition of ammonium oxidizing and nitrite oxidizing bacteria (Olson, 1981b), and we do find high nitrification rates in this part of the water column and an excess of ammonium oxidation over nitrite oxidation (Table 4.1). However, the maximum ammonium oxidation rates are not always precisely coincident with the LPNM. The nitrite distribution in HOT-45 (Fig. 4.6) is unusual, as is the shallow depth of the nitracline. We believe that this distribution is a result of restratification after a mixing event, and that it shows the development of a new UPNM a few meters below the unusually shallow nitracline, a remnant UPNM at 120 m and a LPNM at 140 m.

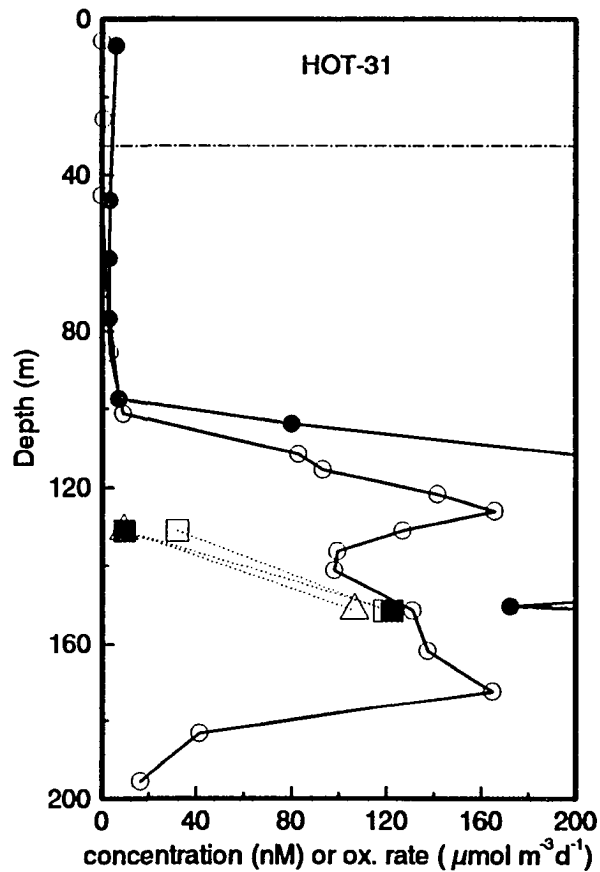


Fig. 4.2. Depth profiles (0-200 m) of selected parameters at Station ALOHA during HOT-31 (Oct. 1991). Solid and open circles represent $[\text{NO}_3^- + \text{NO}_2^-]$ and $[\text{NO}_2^-]$, respectively. Solid and open squares represent ammonium oxidation rate as measured by ^{14}C and chemical assays, respectively. Open triangles represent nitrite oxidation rate based on chemical assay. Horizontal dashed line shows cruise mean depth of the mixed layer ($\Delta\sigma_\theta/\Delta z < 5 \text{ g m}^{-4}$).

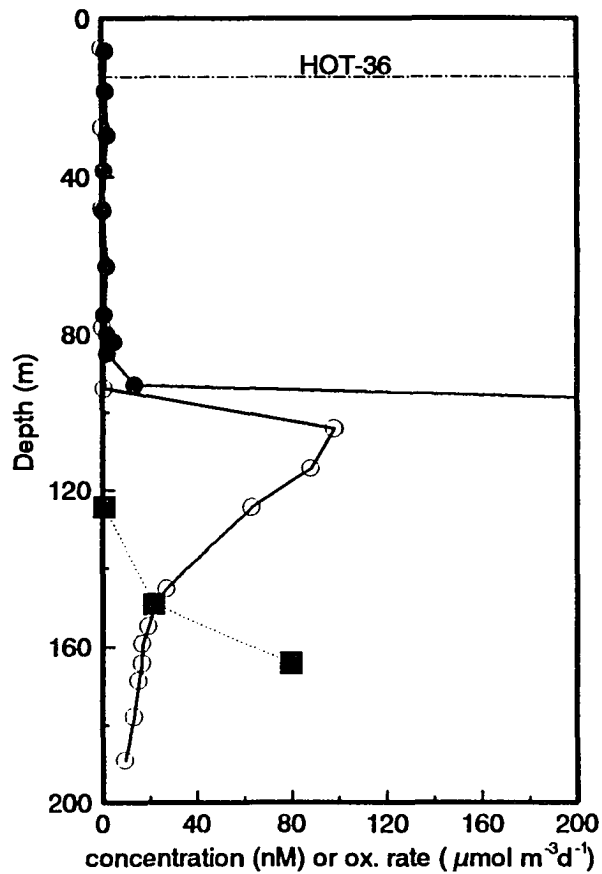


Fig. 4.3. Depth profiles (0-200 m) of selected parameters at Station ALOHA during HOT-36 (Apr. 1992). Solid and open circles represent $[\text{NO}_3^- + \text{NO}_2^-]$ and $[\text{NO}_2^-]$, respectively. Solid squares represent ammonium oxidation rate as measured by ^{14}C assay. Horizontal dashed line shows cruise mean depth of the mixed layer ($\Delta\sigma_\theta/\Delta z < 5 \text{ g m}^{-4}$).

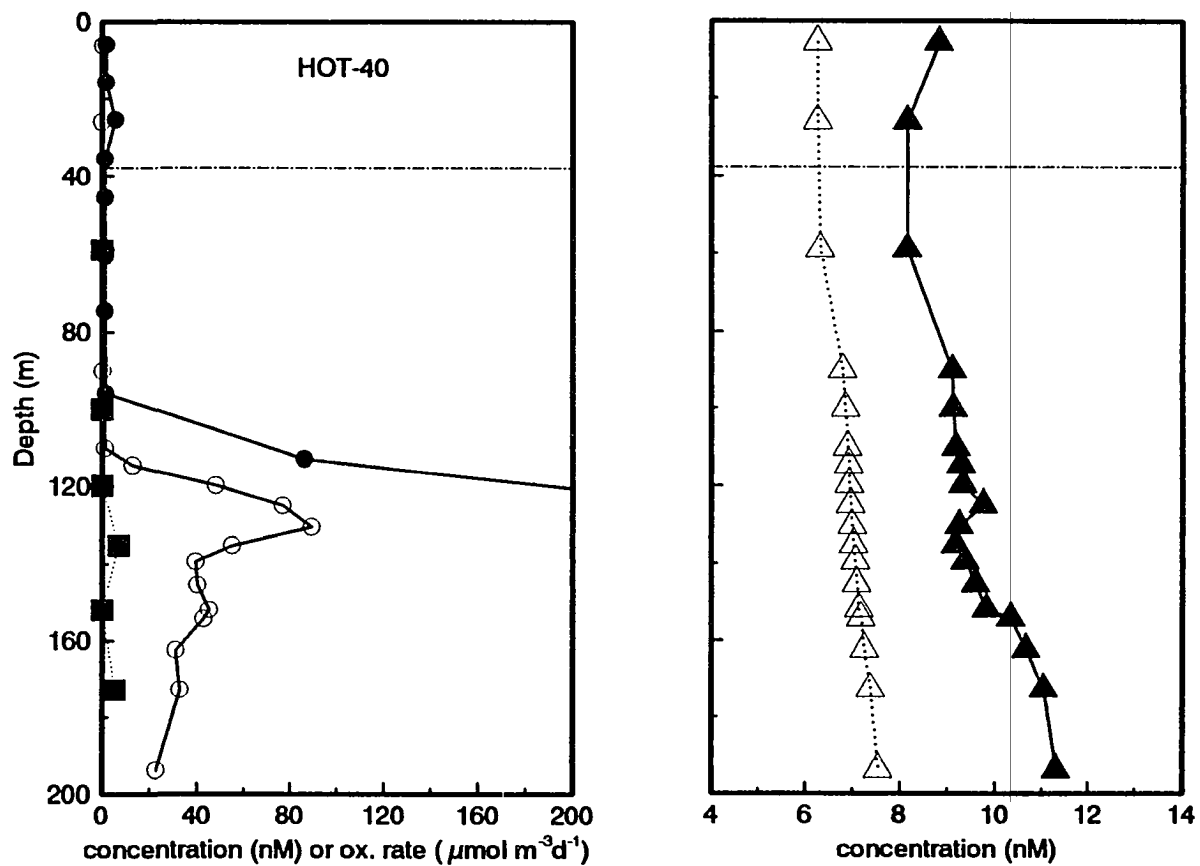


Fig. 4.4. Depth profiles (0-200 m) of selected parameters at Station ALOHA during HOT-40 (Sept. 1992). Left panel: solid and open circles represent $[\text{NO}_3^- + \text{NO}_2^-]$ and $[\text{NO}_2^-]$, respectively; solid squares represent ammonium oxidation rate as measured by ^{14}C assay. Right panel: solid triangles represent $[\text{N}_2\text{O}]$, open triangles represent saturation values of $[\text{N}_2\text{O}]$. Horizontal dashed lines in each panel show cruise mean depth of the mixed layer ($\Delta\sigma_\theta/\Delta z < 5 \text{ g m}^{-4}$).

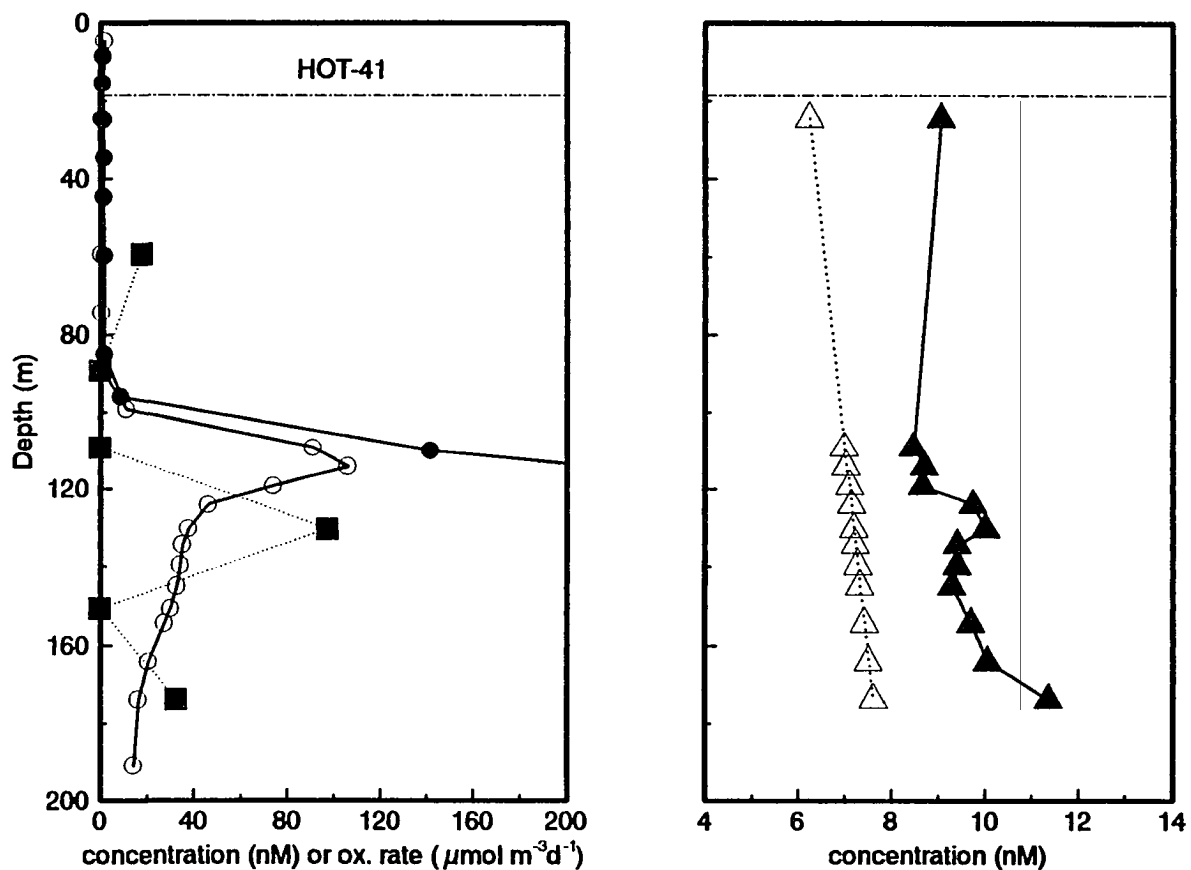


Fig. 4.5. Depth profiles (0-200 m) of selected parameters at Station ALOHA during HOT-41 (Oct. 1992). Left panel: solid and open circles represent $[\text{NO}_3^- + \text{NO}_2^-]$ and $[\text{NO}_2^-]$, respectively; solid squares represent ammonium oxidation rate as measured by ^{14}C assay. Right panel: solid triangles represent $[\text{N}_2\text{O}]$, open triangles represent saturation values of $[\text{N}_2\text{O}]$. Horizontal dashed lines in each panel show cruise mean depth of the mixed layer ($\Delta\sigma_\theta/\Delta z < 5 \text{ g m}^{-4}$).

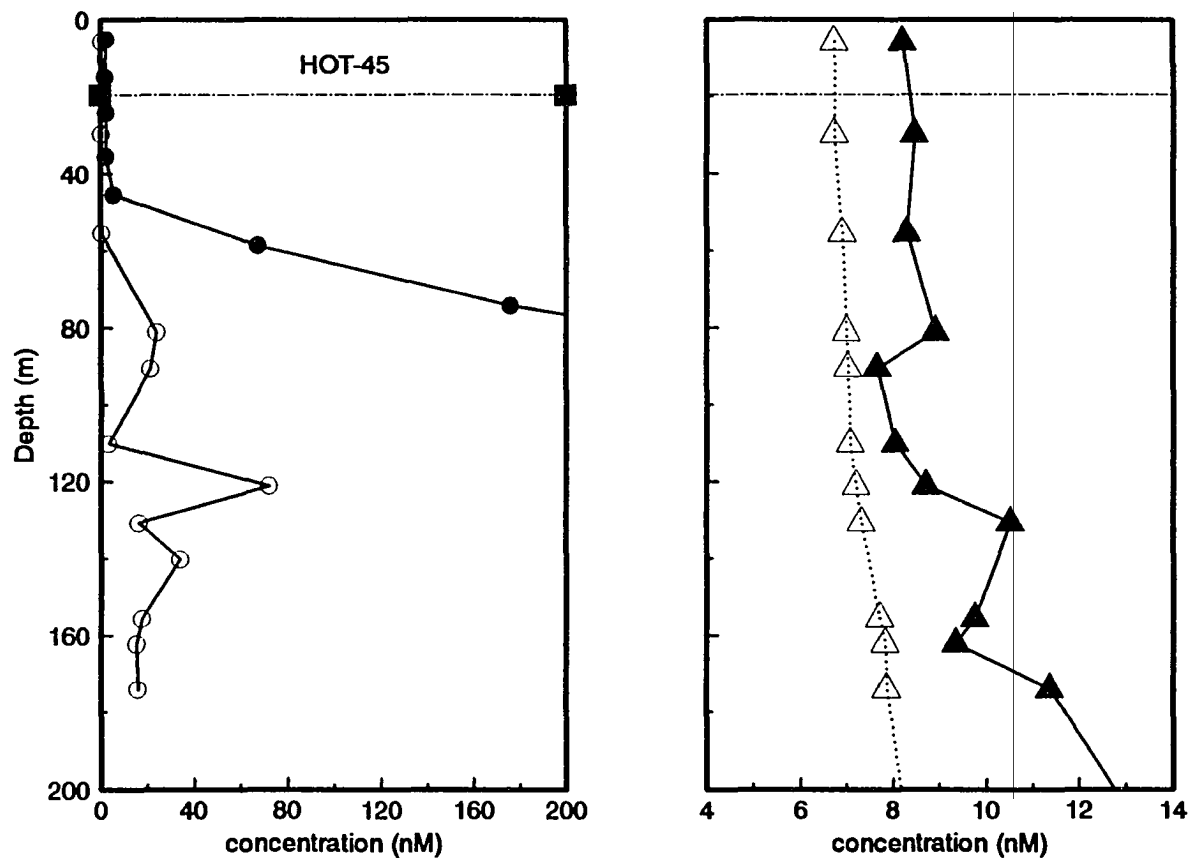


Fig. 4.6. Depth profiles (0-200 m) of selected parameters at Station ALOHA during HOT-45 (Feb. 1993). Left panel: solid and open circles represent $[\text{NO}_3^- + \text{NO}_2^-]$ and $[\text{NO}_2^-]$, respectively. Right panel: solid triangles represent $[\text{N}_2\text{O}]$, open triangles represent saturation values of $[\text{N}_2\text{O}]$. Horizontal dashed lines in each panel show cruise mean depth of the mixed layer ($\Delta\sigma_\theta/\Delta z < 5 \text{ g m}^{-4}$).

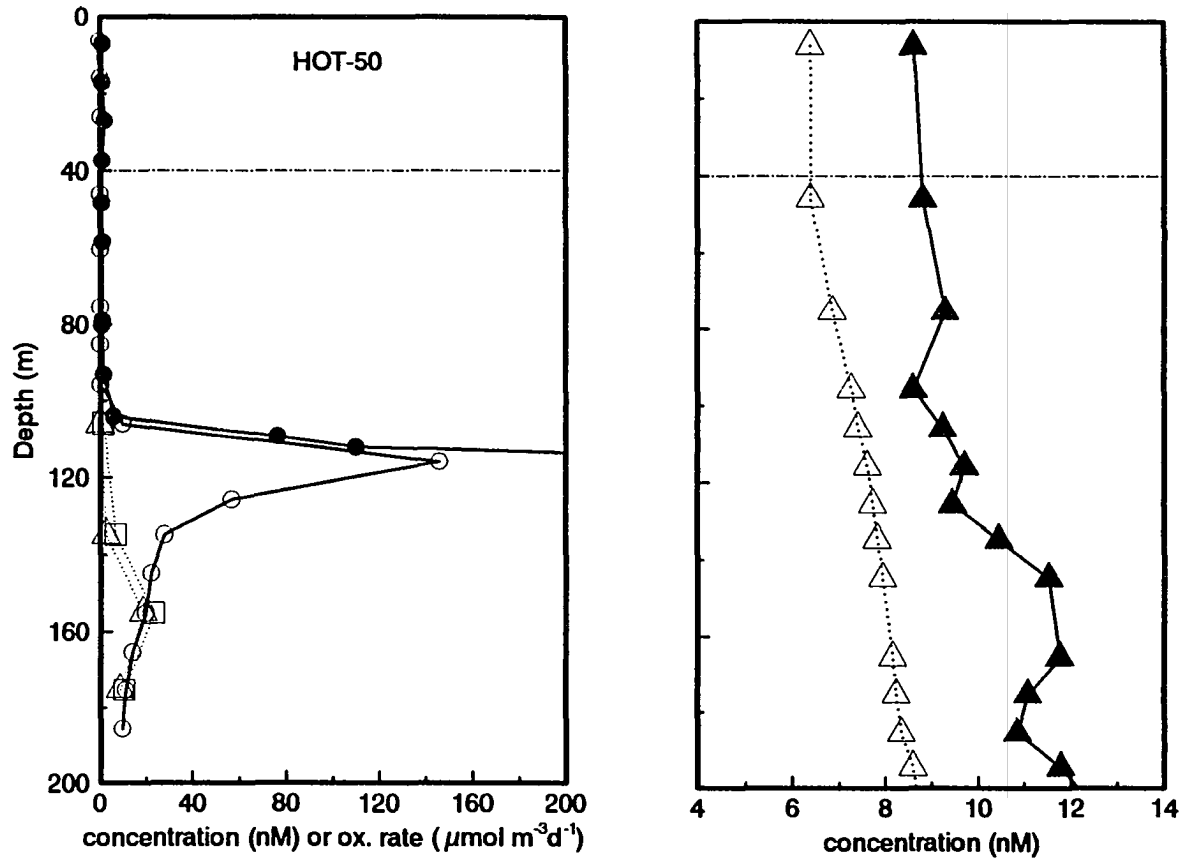


Fig. 4.7. Depth profiles (0-200 m) of selected parameters at Station ALOHA during HOT-50 (Oct. 1993). Left panel: solid and open circles represent $[\text{NO}_3^- + \text{NO}_2^-]$ and $[\text{NO}_2^-]$, respectively; open squares represent ammonium oxidation rate as measured by chemical assay; open triangles represent nitrite oxidation rate as measured by chemical assay. Right panel: solid triangles represent $[\text{N}_2\text{O}]$, open triangles represent saturation values of $[\text{N}_2\text{O}]$. Horizontal dashed lines in each panel show cruise mean depth of the mixed layer ($\Delta\sigma_\theta/\Delta z < 5 \text{ g m}^{-4}$).

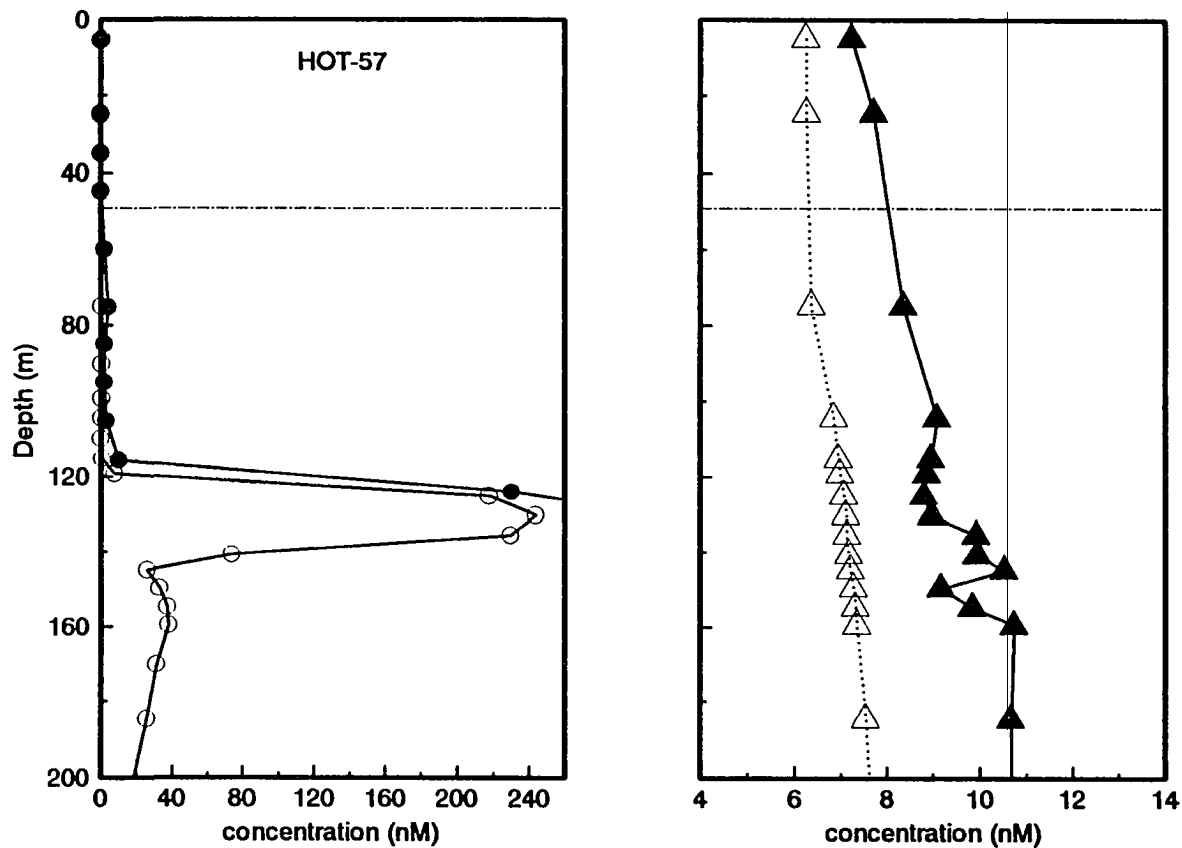


Fig. 4.8. Depth profiles (0-200 m) of selected parameters at Station ALOHA during HOT-57 (Sept. 1994). Left panel: solid and open circles represent $[\text{NO}_3^- + \text{NO}_2^-]$ and $[\text{NO}_2^-]$, respectively. Right panel: solid triangles represent $[\text{N}_2\text{O}]$, open triangles represent saturation values of $[\text{N}_2\text{O}]$. Horizontal dashed lines in each panel show cruise mean depth of the mixed layer ($\Delta\sigma_\theta/\Delta z < 5 \text{ g m}^{-4}$).

Nitrification and N₂O

Chemoautotrophic ammonium oxidation produces nitrous oxide as a by-product, and the relative yield of N₂O with respect to NO₂⁻ varies inversely with the dissolved oxygen concentration (Goreau et al., 1980). This relationship may at least partly explain the observed distributions of [N₂O] and [O₂] over the upper 1000 m of the water column at Station ALOHA (Fig 4.9). [N₂O] varies from about 8 nM (appx. 130% air saturation) at the surface to over 50 nM (appx. 400% air saturation) at 750 m within the oxygen minimum zone. The negative correlation of [N₂O] and [O₂] in the water column is a common feature of much of the deep ocean worldwide, and is most likely indicative of N₂O production via nitrification (Yoshinari, 1976; Elkins et al., 1978; Cohen and Gordon, 1978, 1979; Hahn, 1981; Liu and Kaplan, 1982; Oudot et al., 1990).

A paucity of data on N₂O distributions in the central subtropical North Pacific limits the potential for direct comparison of our data with those of other investigators. The 0-1000 m depth distribution of [N₂O] observed in our study is very similar to that measured by Elkins et al. (1978) at 20°N, 150°W, including the strong supersaturation in the oxygen minimum zone, and a moderate surface saturation of approximately 125%. Also, the 130% saturation we observe for surface N₂O is consistent with the approximately 130% saturation observed during a north-south transect across the Pacific by Singh et al. (1979) as they passed by 20° N at about 135° W. Weiss et al. (1992) also report surface supersaturations throughout several transects running both north and south of the Hawaiian Islands, but of lower magnitude (approximately 103% saturation).

The high degree of N₂O supersaturation within the O₂ minimum is probably not due to an enhanced rate of nitrification per se but rather to the larger relative yield of N₂O produced by nitrification under low oxygen tension (Goreau et al., 1980; Ward et al.,

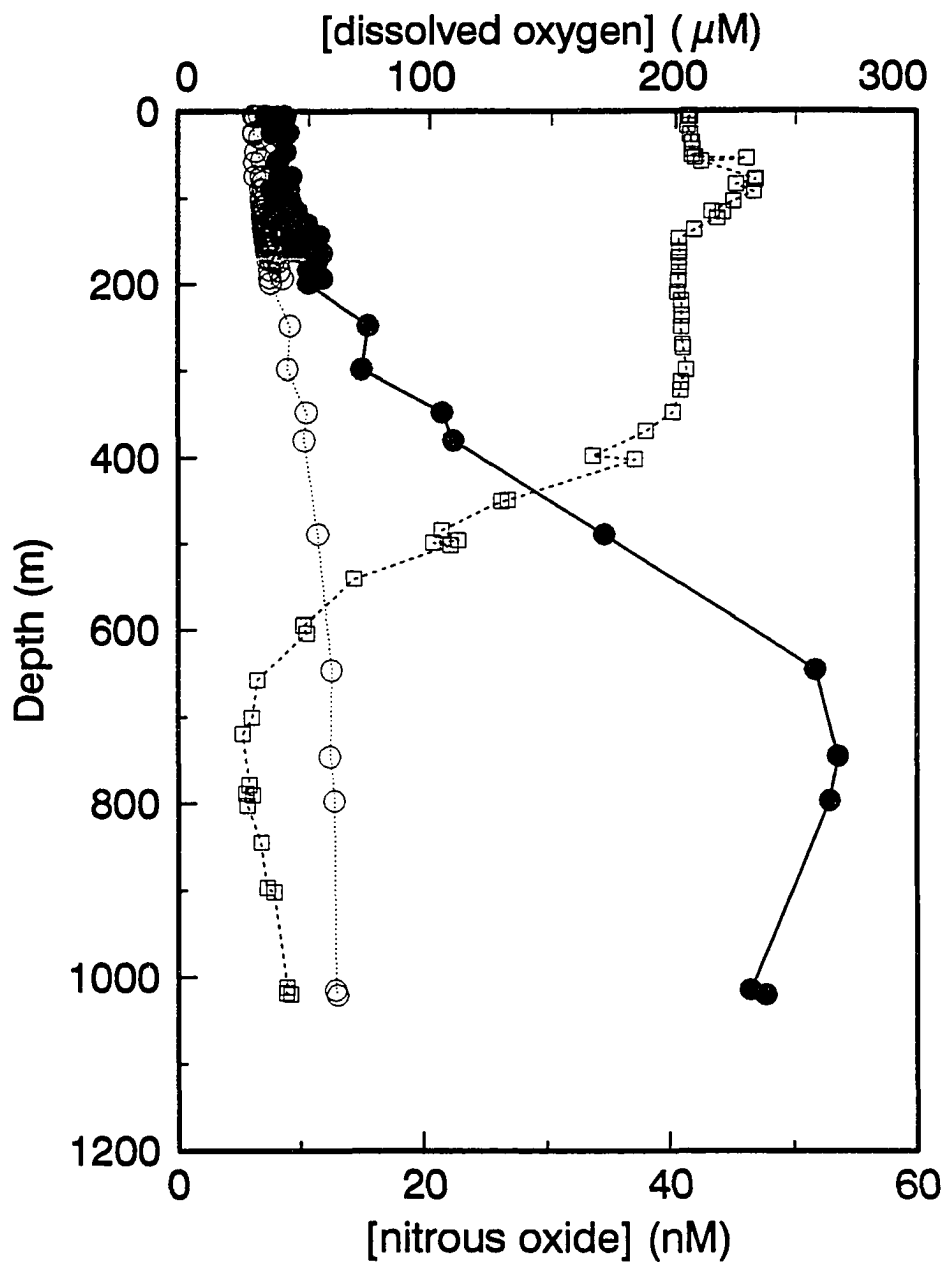


Fig. 4.9. Depth profiles (0-1000 m) of $[N_2O]$ and $[O_2]$ at Station ALOHA. Solid circles represent pooled $[N_2O]$ measurements from five cruises, open circles represent air saturation values for the same samples at in situ temperature. $[N_2O]$ data are from HOT-40 (Sept. 1992), HOT-41 (Oct. 1992), HOT-45 (Feb. 1993), HOT-50 (Oct. 1993) and HOT-57 (Sept. 1994). Solid triangles represent pooled $[O_2]$ measurements from two casts made during HOT-50, displayed for comparison.

1989a). Within the well-oxygenated euphotic zone, however, this yield is expected to be much smaller, except perhaps within microsites capable of maintaining low-oxygen interiors (Scranton and Brewer, 1977; Sieburth, 1983; Alldredge and Cohen, 1987; Tilbrook and Karl, 1994); nevertheless, we suspected that the high ammonium oxidation rates at the level of the LPNM might result in a local maximum of $[N_2O]$. Such a local $[N_2O]$ maximum in the vicinity of the primary nitrite maximum has been described previously from the oxygenated waters of the Gulf Stream (Yoshinari, 1976) and the eastern North Atlantic (Hahn, 1975; Hahn, 1981), and maximum potential production of N_2O via nitrification was determined to be in this layer in the western North Pacific by Yoshida et al. (1989). None of these observed N_2O maxima were at stations within oligotrophic subtropical gyre waters, and in none of these studies was sampling performed on a fine enough vertical scale to elucidate the precise position of the N_2O peak with respect to the UPNM and the LPNM.

We find a pronounced N_2O maximum below the UPNM in four of the five cruises where N_2O was measured (HOT-41, HOT-45, HOT-50 and HOT-57; Figs. 4.5-4.8), and perhaps some evidence of one in a fourth (HOT-40; Fig. 4.4). During both HOT-41 and HOT-50, this N_2O maximum was coincident with a strong maximum in ammonium oxidation rate (Figs. 4.5 and 4.7). Although these limited observations are insufficient for determining a clear cause-and-effect relationship, they do suggest that a local source of N_2O exists within a zone of elevated nitrification rates in the lower euphotic zone at Station ALOHA. A second local N_2O maximum is found associated with the UPNM in four of these five profiles (HOT-40, HOT-45, HOT-50 and HOT-57; Figs. 4.4 and 4.6-4.8), and perhaps in the HOT-41 profile (Fig. 4.5) as well. This shallower N_2O maximum is associated with undetectable nitrification rates (Figs. 4.4, 4.5 and 4.7) and therefore suggests N_2O generation through some other process (see below).

We can make a rough estimation of the importance of euphotic zone nitrification to N_2O production as follows. The depth of the euphotic zone, defined here as the phytoplankton compensation depth (Sverdrup, 1953), can be estimated as the depth at which inorganic carbon incorporation in the light is not significantly ($P < 0.05$) greater than in the dark, assuming that total community respiration is the same in the light as in the dark. This depth has been found to be 173 ± 7 m at Station ALOHA (Letelier et al., 1995); for convenience we will place it at 175 m. The flux of a chemical species can be estimated from a one-dimensional eddy-diffusive model, in which the flux is equal to the product of the concentration gradient and an eddy-diffusivity coefficient. From our five $[\text{N}_2\text{O}]$ profiles, we determine that the average vertical $[\text{N}_2\text{O}]$ gradient at 175 m is about $0.01 \mu\text{mol m}^{-4}$. Using an eddy diffusivity coefficient of $3.7 \times 10^{-5} \text{ m}^2 \text{ s}^{-1}$ (Lewis et al., 1986), we calculate a vertical flux of N_2O of $0.03 \mu\text{mol m}^{-2} \text{ d}^{-1}$. At the same time, we take our median ammonium oxidation rate of $21.8 \mu\text{mol m}^{-3} \text{ d}^{-1}$ over the 125-175 m depth range as a conservative estimate, and assume no ammonium oxidation in the 0-125 m range, because the median value there is below the detection limits for the assays. We then assume that N_2O is produced at a rate that is 0.15% of the ammonium oxidation rate as has been demonstrated for cultured ammonium oxidizers when grown at oxygen levels similar to those found in the euphotic zone at Station ALOHA (Goreau et al., 1980). We find in this way that N_2O in the euphotic zone is produced by nitrification at a rate of $1.6 \mu\text{mol m}^{-2} \text{ d}^{-1}$.

The above calculations reveal that the production of N_2O by nitrifying bacteria between 0-175 m may exceed the vertical flux into this layer from below by a factor of 50! We recognize that these are only order-of-magnitude calculations that depend heavily on the choice of eddy diffusivity coefficient and on the ratio of N_2O to NO_2^- produced during ammonium oxidation. However, these results do strongly suggest that much of the

dissolved N₂O that potentially could be released to the atmosphere at Station ALOHA is produced within the euphotic zone. Furthermore, there may be some ammonium oxidation occurring within the 0-125 m layer at a rate below the detection limits of our assays, which nevertheless would contribute to N₂O production in the euphotic zone.

It is of interest to determine if this production of N₂O by nitrifiers in the euphotic zone is sufficient to explain the observed N₂O supersaturation in the euphotic zone and the inferred sea-air flux of this important trace gas. We can estimate the sea-air flux based on an empirically-derived relationship between gas transfer and wind speed (Wanninkhof, 1992), using our measurements of surface ΔN_2O ($= [N_2O]_{\text{measured}} - [N_2O]_{\text{air saturation}}$), temperature and wind speed. This model takes into account the effects of wind speed variability and the solubility of the gas in seawater. Using our mean surface ΔN_2O of 2.02 nM, an approximate mean sea surface temperature of 25°C, and an approximate mean wind speed of 7.5 m s⁻¹, we arrive at a sea-air N₂O flux of 9.2 $\mu\text{mol m}^{-2} \text{d}^{-1}$. This flux estimate is consistent with previous estimates in the Pacific of 7.1 $\mu\text{mol m}^{-2} \text{d}^{-1}$ (Singh et al., 1979) and 10.6 $\mu\text{mol m}^{-2} \text{d}^{-1}$ (Pierotti and Rasmussen, 1980), among others.

Upon inspection, we find that the combined contribution of euphotic zone nitrification and the upward vertical flux of N₂O from deep waters can only account for <20% of the estimated sea-air N₂O flux. This finding suggests that there is another significant source for N₂O within the euphotic zone at Station ALOHA. A similar conclusion was reached by Rönner (1983) in his study of N₂O in the Baltic Sea. In that study, no diffusion of N₂O from below the euphotic zone was possible due to its negative concentration gradient, and nitrification was unmeasurable within the euphotic zone, yet still a surface saturation of 120-135% was observed across the entire Baltic Sea. There are several possible unmeasured processes which could be contributing to the production of N₂O in the euphotic zone, including: (1) autotrophic nitrification associated with

particles, (2) respiratory denitrification or non-respiratory dissimilatory nitrate reduction within particles or the guts of zooplankton, or (3) assimilatory nitrate (and/or nitrite) reduction by phytoplankton. It is worthwhile to consider each of these possibilities in turn.

Ammonium oxidizing bacteria have been demonstrated to be an active component of the microbial consortia associated with large, rapidly sinking marine particles (Karl et al., 1984). Such particles are inadequately sampled using bottle collections, therefore their associated nitrifying activities would not be measured in our study. At the same time, the exchange of gases from these particles with the water column as they sink can be significant, as has been demonstrated for methane (Karl and Tilbrook, 1994). Furthermore, ammonium oxidation within the low-oxygen microenvironments that can exist within large marine particles would produce a high yield of N_2O compared to NO_2^- (Goreau et al., 1980). In addition, suspended particles may also be capable of maintaining low-oxygen interiors, especially aggregates such as marine snow (Alldredge and Cohen, 1987; Sieburth, 1991), which are similarly difficult to sample quantitatively with bottle collections.

Under anaerobic conditions, many bacteria utilize nitrate as a terminal electron acceptor in the process of respiratory nitrate reduction. When gaseous end products (N_2O , N_2) result, this dissimilatory process is termed denitrification (Hattori, 1983). Although denitrification has historically been considered impossible in the oxygenated marine euphotic zone, the interiors of large particles and the intestinal tracts of zooplankton may be anoxic even when the bulk oxygen concentration of the surrounding water is high. This phenomenon has been observed in microprobe studies of marine particulates (Alldredge and Cohen, 1987) and is also suggested by the evident methanogenesis (an anaerobic process) observed within oxygenated marine water columns

(Tilbrook and Karl, 1994), in sediment trap collections of sinking particles (Marty, 1993; Karl and Tilbrook, 1994), and in freshly excreted zooplankton fecal pellets (Marty, 1993). Under such conditions, the production of N_2O via denitrification in the marine euphotic zone is certainly possible, although it remains to be demonstrated. Suggestive evidence has been presented by Wilson (1978), who measured elevated N_2 production in aerobic pelagic surface sediments, and proposed that denitrification was occurring within freshly deposited zooplankton fecal pellets. Furthermore, a sulfur bacterium isolated from wastewater, *Thiosphaera pantotropha*, has been found capable of aerobic denitrification (Robertson and Kuenen, 1984; Bell and Ferguson, 1991). Also possible is the production of N_2O through non-respiratory dissimilatory nitrate reduction. Bacteria capable of reducing NO_3^- to N_2O under aerobic and anaerobic conditions, without coupling the process to respiration, have been isolated and described (Smith and Zimmerman, 1981; Bleakley and Tiedje, 1982). Many of these are enteric, and thus it is interesting to speculate that similar bacteria might exist within the intestinal tracts of zooplankton. N_2O production may also be the result of close associations of nitrate-reducing bacteria with phytoplankton as suggested by Rönner (1983); a similar association between denitrifying bacteria and macroalgae has been demonstrated in a temperate estuary (Law et al., 1993).

Finally, there is the possibility that N_2O is produced during the assimilatory reduction of nitrate by phytoplankton as has been suggested by a number of authors (Hahn, 1975; Elkins et al., 1978; Pierotti and Rasmussen, 1980; Oudot et al., 1990). Although production of N_2O from NO_3^- has not been observed in experiments with cultures of the green alga *Chlorella* sp. (Yoshida and Alexander, 1970) or the dinoflagellate *Exuviaella* sp. (Goreau et al., 1980), circumstantial evidence for this pathway exists, based on the correlation between high $[N_2O]$ and regions or layers of high nitrate assimilation such as upwelling areas (Pierotti and Rasmussen, 1980) and the PNM

(Hahn, 1975). However, because upwelling can bring N_2O rich waters from deeper low-oxygen layers to the surface, and because nitrification is known to occur within the LPNM, neither of the above arguments provides a solid case for N_2O production through assimilatory nitrate reduction. On the other hand, more recent studies have demonstrated N_2O production from NO_2^- (but not from NO_3^-) by a number of cultures of green algae (Weathers, 1984) and cyanobacteria (Weathers and Niedzielski, 1986). While it is not known whether this pathway from nitrite to nitrous oxide is carried out by natural phytoplankton populations in the marine euphotic zone, this remains an intriguing possibility. The production of N_2O from NO_2^- by phytoplankton could explain the N_2O maximum associated with the UPNM (Figs. 4.5-4.8), especially in light of the fact that within the upper few meters of the nitracline $[NO_2^-]$ is often the dominant fraction of the total $[NO_3^- + NO_2^-]$.

Nitrification and new production

When the new production concept was developed by Dugdale and Goering (1967), accurate measurements of marine nitrification rates were not available. Nevertheless, these authors were keenly aware that nitrification could prove to be a bane to their model, stating "If nitrification rates are eventually shown to be sufficiently higher than has been assumed, the assumption that nitrate is a nonregenerated nutrient form in the euphotic zone would have to be modified." More recently, the new production concept has been extended to equate nitrate-based production with export production to determine the fraction of carbon that can be removed from the euphotic zone by the "biological pump" (Eppley and Peterson, 1979; Longhurst and Harrison, 1989). However, with improvements in techniques for the measurement of nitrification rates in the sea indicating

a significant role for this process (Olson, 1981a; Ward et al., 1982), the validity of the new production concept as it is commonly applied has come into question (Priscu and Downes, 1985; Ward et al., 1989b).

Consider now the situation at Station ALOHA. We take our median nitrite oxidation rate ($9.6 \mu\text{mol m}^{-3} \text{d}^{-1}$; Table 4.1) as a conservative estimate of nitrate production via nitrification in the 125-175 m layer. Note that this rate is similar to the maximum ammonium oxidation rate of $7.30 \mu\text{mol m}^{-3} \text{d}^{-1}$ measured by Olson (1981a), and is more than an order of magnitude lower than the maximum ammonium and nitrite oxidation rates measured in this study (Table 4.1). We also assume zero nitrite oxidation in the upper 125 m, based upon our single measurement which was below the detection limit of the chemical assay. From these conservative estimates we arrive at a *minimum* annual euphotic zone "regenerated nitrate" production of 175mmol m^{-2} . This rate is 2-4 times higher than the eddy-diffusive nitrate import at Station ALOHA estimated by Karl et al. (1992), using measured nitrate gradients and an eddy diffusivity of $3.7 \times 10^{-5} \text{m}^2 \text{s}^{-1}$ (Lewis et al., 1986). Considering that estimates of eddy diffusivity in the thermocline as low as $1.1 \times 10^{-5} \text{m}^2 \text{s}^{-1}$ have recently been reported (Ledwell et al., 1993), and that the true euphotic zone mean nitrite oxidation rate at Station ALOHA is likely to be higher than the minimum estimate used here, we suspect that nitrate production within the euphotic zone may be an order of magnitude larger than the vertical eddy-diffusive flux of nitrate from below. It therefore appears that at Station ALOHA, in the absence of episodic deep mixing events, most nitrate-based production is in fact regenerated, not new. Similar conclusions have been reached for the western Cook Strait, New Zealand (Priscu and Downes, 1985) and for the Southern California Bight (Ward et al., 1989b). If Station ALOHA is truly representative of oligotrophic oceanic gyre habitats in general,

then the measurement of nitrate assimilation rates to estimate new production is precluded over vast areas of the world's oceans.

Traditionally the oceanic euphotic zone has been modeled as a two-layer system with respect to nutrient dynamics and primary production (Dugdale, 1967), particle production (Coale and Bruland, 1987) and particle export (Small et al., 1987). The upper layer is characterized by high rates of primary production, a low f ratio (new production/total production), nutrient-limited growth, and little production or export of sinking particles. The lower layer is characterized by low rates of primary production, a high f ratio, light-limited growth, and much production and export of large sinking particles. The dividing line between the layers, while not precisely defined as a particular depth, is conceptually the depth at which photosynthetic primary production switches from being nutrient limited to being light limited. The nitrogen cycle in this traditional model (Fig. 4.10a) is considered to be a balance between two major fluxes: the eddy-diffusive input of nitrate from below and the sinking of organic nitrogen out of the euphotic zone in large particles (Eppley and Peterson, 1979; Platt et al., 1989). Other fluxes of nitrogen are considered insignificant, including nitrogen fixation and nitrification. Thus when averaged over annual timescales, measurements of the downward particulate nitrogen flux should equal those of nitrate assimilation within the euphotic zone; such a balance has been measured at a site in the central North Pacific (Knauer et al., 1990).

In light of our results on nitrification at Station ALOHA, however, it is apparent that the measurement of nitrate assimilation in the euphotic zone will yield large overestimates of new production and of the inferred upward vertical flux of nitrate from deep waters. Euphotic zone nitrification is probably at least part of the explanation for the disparity between the new production estimates based on nitrate assimilation ($0.81 \text{ mmol N m}^{-2} \text{ d}^{-1}$) and based on upward nitrate diffusion ($0.14 \text{ mmol N m}^{-2} \text{ d}^{-1}$) that were made in

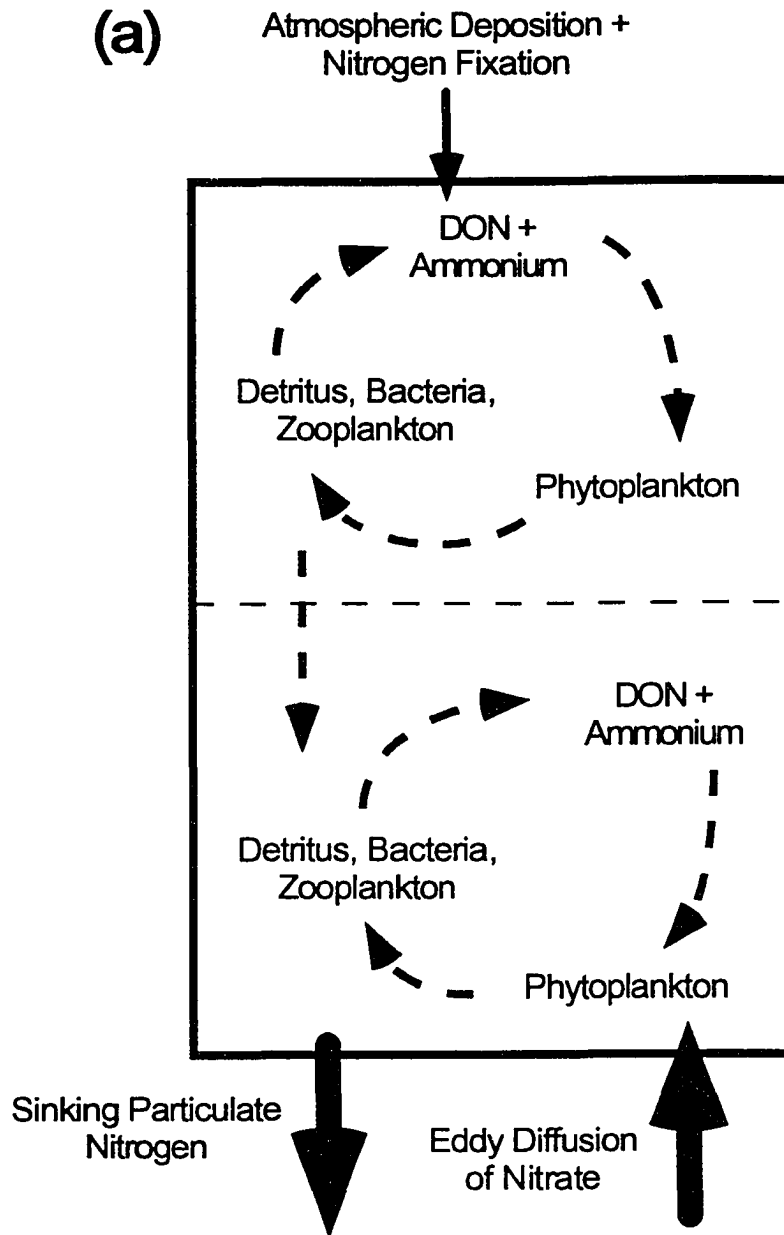


Fig. 4.10. Schematic diagrams of the nitrogen cycle in the oligotrophic oceanic euphotic zone. Large solid arrows indicate major nitrogen import and export fluxes, narrow solid arrows represent minor nitrogen import and export fluxes. Dashed arrows indicate recycling processes occurring within the euphotic zone. Horizontal dashed lines separate upper and lower layers of the euphotic zone based on differences in processes and are not meant to define a specific depth (see text). (a) "Traditional" model. (b) proposed model including "nitrifier loop".

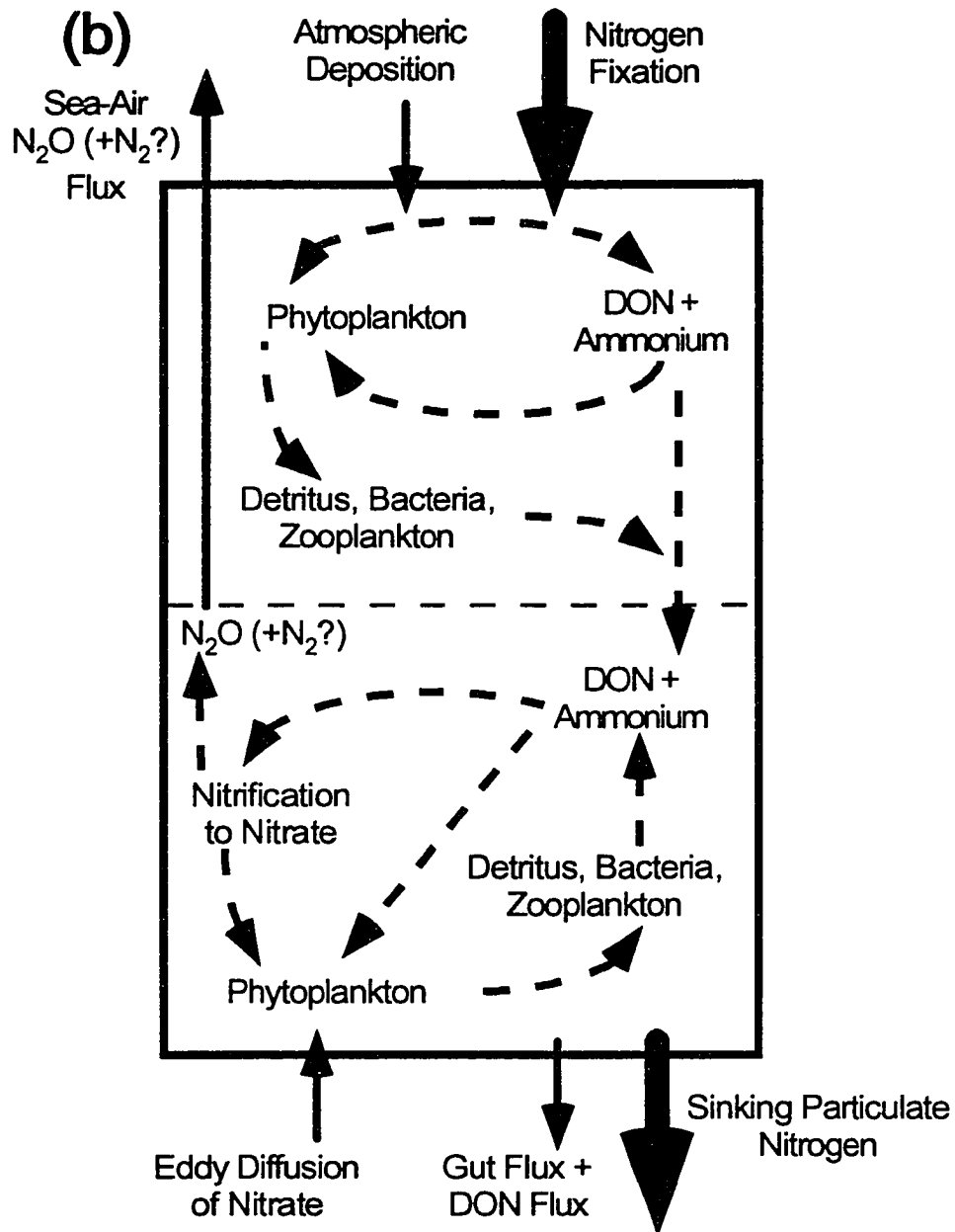


Fig. 4.10. (Cont.) Schematic diagrams of the nitrogen cycle in the oligotrophic oceanic euphotic zone.

the oligotrophic eastern Atlantic by Lewis et al. (1986). An implication here is that if the observed rate of nitrate assimilation in the euphotic zone is equal to the observed rate of nitrogen export via gravitational settling of particles (Knauer et al., 1990), then the diffusive nitrate flux is actually far too low to support the observed export of particulate nitrogen, hence another source term must be invoked to maintain the overall mass balance of nitrogen in the euphotic zone. Also, whatever the "extra" nitrogen source is, enough of the nitrogen introduced by it must pass through the "nitrifier loop" and become regenerated nitrate for measurements of nitrate assimilation to closely approximate measurements of the particulate nitrogen flux as they did in the Knauer et al. (1990) study. This does not rule out the shunting of some new nitrogen inputs back to the atmosphere as gaseous nitrogen compounds (as discussed above for N_2O) or as N_2 (if denitrification occurs in the euphotic zone).

Deep mixing events of an episodic nature are often invoked as a mechanism for introducing "extra" new nitrogen into the euphotic zone (Jenkins, 1988; Platt et al., 1989). Such events are clearly important at some oligotrophic sites such as the BATS station near Bermuda, where the depth of winter mixed layers may be 200 m or more (Michaels et al., 1994), but at Station ALOHA mixed layers rarely reach the nitracline and have never been observed to exceed 115 m depth (Karl et al., 1995; Letelier et al., 1995). Of course, with monthly sampling it is possible that infrequent events are missed, but even if the top of the nitracline is occasionally eroded to a depth within the 125-175 m layer, much of the nitrate mixed upward will be of a regenerated nature due to in situ nitrification. Another possible source of new nitrogen is via the entrainment of nitrate in buoyant algal mats (Villareal et al., 1993). However, if these mats obtain their nitrate at the top of the nitracline, they too are to a large extent redistributing regenerated nitrate in their upward migration, rather than introducing new nitrate to the euphotic zone. A third possible source of new

nitrogen is input of NH_4^+ and NO_3^- from the atmosphere via wet and dry deposition. Estimates of this flux for the North Atlantic (Michaels et al., 1993) and the North Pacific (Duce, 1986) indicate that it is small compared to the export flux of nitrogen, but it is not insignificant, particularly when episodic deposition events and the continuing increase in anthropogenic nitrogen sources to the atmosphere are considered (Owens et al., 1992).

Recent studies have indicated that the role of nitrogen fixation in contributing new nitrogen to the euphotic zone in oligotrophic waters has been underestimated (Martínez et al., 1983; Carpenter and Romans, 1991; Karl et al, 1992; Letelier, 1994; Karl et al., 1995). We believe that nitrogen fixation is an important source of new nitrogen at Station ALOHA, and propose a conceptual model of the euphotic zone nitrogen cycle that includes a larger role for this often neglected source and also includes the "nitrifier loop" described above (Fig. 4.10b). Our model, like the original, involves a two-layer euphotic zone, but the roles of these layers in the nitrogen cycle are quite different from those in the traditional model. The depth of the dividing line between layers is not rigorously defined in our model, but conceptually it separates the upper layer, in which there is sufficient light energy for nitrogen fixation and for photoinhibition of nitrification, from the lower layer, in which no nitrogen fixation occurs but nitrifiers are free from light inhibition. The main components of our model are: (1) a large source of new nitrogen via nitrogen fixation (plus atmospheric deposition) to the upper layer of the euphotic zone, (2) a reduction in the importance of the vertical diffusive nitrate flux to the lower euphotic zone, (3) a downward flux of fixed nitrogen via the gravitational settling of large particles (this does not differ from the traditional model, except that we recognize that these particles may be formed in the upper as well as the lower euphotic zone), combined with a potential export flux via the diel migration and excretion of zooplankton ("gut flux"; Longhurst and Harrison, 1988) and a minor diffusional export flux of dissolved organic nitrogen (DON),

(4) potential sea-air fluxes of gaseous nitrogen species, and (5) a nitrifier loop which regenerates nitrate from ammonium.

Nitrogen fixation in the upper euphotic zone is ultimately the source of this NH_4^+ that fuels the nitrifier loop, but the ammonium may be produced and transported downward by more than one process. One possibility is the downward mixing/diffusion of ammonium directly produced through remineralization by bacteria and microzooplankton of DON excreted by phytoplankton, including that excreted by the nitrogen-fixing cyanobacteria themselves (Bronk et al., 1994; Capone et al., 1994; Glibert and Bronk, 1994). Alternatively, organic matter produced in the upper euphotic zone may settle downward as small particles which are then decomposed and remineralized by bacteria and zooplankton in the lower euphotic zone, releasing ammonium.

The major prediction of this model is that most new production actually occurs in the upper layer and is based on ammonium generated directly or indirectly through nitrogen fixation, while most nitrate-based production, but little new production, occurs in the lower layer. In a sense, we have replaced new nitrate and recycled ammonium with recycled nitrate and new ammonium. The major difficulty with our formulation is that there is no process analogous to nitrogen fixation that can meet the phosphorus requirements of the phytoplankton in the upper layer of the euphotic zone. High nitrogen fixation rates tend to drive the pelagic ecosystem toward phosphorus limitation (Karl et al., 1995). The availability of phosphorus for net ecosystem productivity depends not only on the external supply rate to the euphotic zone, but also on the internal supply through biochemical cycling (Smith, 1984). Therefore, a decoupling of the recycling rates of organic phosphorus and nitrogen compounds could to some extent compensate for an excess of external nitrogen inputs with respect to external phosphorus inputs (Smith et al., 1986). In addition, novel mechanisms of phosphorus delivery, including an upward flux

of buoyant phosphorus-rich particles and an active transport of phosphorus by buoyant organisms, have been hypothesized (Karl et al., 1992; Letelier, 1994). Finally, some part of the nitrogen fixed in the water column at Station ALOHA is released in gaseous form back into the atmosphere as N_2O , and possibly also as N_2 (see above), which indicates that the apparent phosphorus demand of the ecosystem may be greater than the true demand if these fluxes are not taken into account.

Our proposed nitrogen cycle model is only conceptual, but it is consistent with the high nitrogen fixation rates (Carpenter and Romans, 1991; Karl et al., 1992; Letelier, 1994), high nitrification rates (Ward et al., 1989b; this study), and low thermocline eddy-diffusivity (Lewis et al., 1986; Ledwell et al., 1993) that characterize the open ocean. Dugdale and Goering (1967) recognized that their conceptual model of new production would have to be altered if either nitrogen fixation or nitrification were later found to be significant in the euphotic zone; both processes have now been found to be so. The conceptual problems to be expected when equating nitrate-based production with new or export production that we have discussed here are further compounded by the difficulties encountered in attempting to reconcile the effects of the different space and time scales of integration used in estimating new and export production (Platt et al., 1989). In addition, methodological difficulties, such as the substantial losses of ^{15}N labeled tracers to the DON pool observed during bottle incubations (Bronk et al., 1994), cast doubt upon the validity of ^{15}N -based nitrate assimilation measurements in general. The traditional two-layer model has served us well for nearly three decades, but it is now time to rework it into a model that is consistent with modern measurements of nitrogen cycle processes, at least in those subtropical gyre areas for which Station ALOHA is representative.

CONCLUSIONS

Measurements of bacterial nitrification rates at Station ALOHA indicate nitrification as an important source of regenerated nitrate within the euphotic zone, requiring modification of the traditional new production concept. We propose a new conceptual model of the euphotic zone nitrogen cycle, consistent with these findings, that indicates an important role for nitrogen fixation. When comparing nitrification rates to nitrite distributions, we find that there may be a contribution of nitrification to the LPNM but not to the UPNM. Nitrification also appears to be an important source of nitrous oxide within the euphotic zone, contributing to the sea-air flux of this trace gas, but another significant euphotic zone source of unknown nature is indicated. Circumstantial evidence suggests that N_2O may be produced during nitrite assimilation by phytoplankton. However, should the unknown source prove to be related to denitrification, the possibility of a significant N_2 flux to the atmosphere would have to be considered for the oxygenated surface waters of the oceanic gyres.

REFERENCES

- Allredge, A.L. and Y. Cohen. 1987. Can microscale chemical patches persist in the sea? Microelectrode study of marine snow, fecal pellets. *Science* **235**:689-691.
- Bell, L.C. and S.J. Ferguson. 1991. Nitric and nitrous oxide reductases are active under aerobic conditions in cells of *Thiosphaera pantotropha*. *Biochem. J.* **273**:423-427.
- Belser, L.W. 1984. Bicarbonate uptake by nitrifiers: effects of growth rate, pH, substrate concentration, and metabolic inhibitors. *Appl. Environ. Microbiol.* **48**:1100-1104.
- Billen, G. 1976. Evaluation of nitrifying activity in sediments by dark C-14 bicarbonate incorporation. *Water Res.* **10**:51-57.
- Bingham, F. and R. Lukas. 1995. Seasonal cycles of temperature, salinity and dissolved oxygen observed in the Hawaii Ocean Time-series. *Deep-Sea Res.*, submitted.
- Bleakley, B.H. and J.M. Tiedje. 1982. Nitrous oxide production by organisms other than nitrifiers or denitrifiers. *Appl. Environ. Microbiol.* **44**:1342-1348.
- Boden, T.A., R.J. Sepanski and F.W. Stoss (eds). 1991. Trends '91: A Compendium of Data on Global Change. Publication No. ORNL/CDIAC-46, Carbon Dioxide Information Analysis Center, Environmental Sciences Division, Oak Ridge National Laboratory, Oak Ridge, Tennessee, pp. 352-363.
- Brandhorst, W. 1959. Nitrification and denitrification in the eastern tropical North Pacific. *J. Cons. Perm. Int. Explor. Mer.* **25**:2-20.
- Bronk, D.A., P.M. Glibert and B.B. Ward. 1994. Nitrogen uptake, dissolved organic nitrogen release, and new production. *Science* **265**:1843-1846.
- Butler, J.H. and J.W. Elkins. 1991. An automated technique for the measurement of dissolved N₂O in natural waters. *Mar. Chem.* **34**:47-61.
- Capone, D.G. 1991. Aspects of the marine nitrogen cycle with relevance to the dynamics of nitrous and nitric oxide. In: Microbial Production and Consumption of Greenhouse Gases: Methane, Nitrogen Oxides, and Halomethanes, J.E. Rogers and W.B. Whitman (eds), American Society for Microbiology, Washington, D.C., pp. 255-275.
- Capone, D.G., M.D. Ferrier and E.J. Carpenter. 1994. Amino acid cycling in colonies of the planktonic marine cyanobacterium *Trichodesmium thiebautii*. *Appl. Environ. Microbiol.* **60**:3989-3995.

- Carlucci, A.F. and J.D.H. Strickland. 1968. The isolation, purification and some kinetic studies of marine nitrifying bacteria. *J. Exp. Mar. Biol. Ecol.* **2**: 156-166.
- Carpenter, E.J. and K. Romans. 1991. Major role of the cyanobacterium *Trichodesmium* in nutrient cycling in the North Atlantic Ocean. *Science* **254**:1356-1358.
- Carpenter, J.H. 1965. The accuracy of the Winkler method for dissolved oxygen analysis. *Limnol. Oceanogr.* **10**:135-140.
- Coale, K.H. and K.W. Bruland. 1987. Oceanic stratified euphotic zone as elucidated by ^{234}Th : ^{238}U disequilibria. *Limnol. Oceanogr.* **32**:189-200.
- Cohen, Y. and L.I. Gordon. 1978. Nitrous oxide in the oxygen minimum of the eastern tropical North Pacific: evidence for its consumption during denitrification and possible mechanisms for its production. *Deep-Sea Res.* **25**:509-524.
- Cohen, Y. and L.I. Gordon. 1979. Nitrous oxide production in the ocean. *J. Geophys. Res.* **84**:347-353.
- Cox, R.D. 1980. Determination of nitrate and nitrite at the parts per billion level by chemiluminescence. *Anal. Chem.* **52**:332-335.
- Dore, J.E. and D.M. Karl. 1995. Nitrite distributions and dynamics at Station ALOHA. *Deep-Sea Res.*, submitted.
- Duce, R.A. 1986. The impact of atmospheric nitrogen, phosphorus, and iron species on marine biological productivity. In: The Role of Air-Sea Exchange in Geochemical Cycling, P. Baut-Menard (ed), NATO ASI Series, Vol. 362, D. Riedel Publishing Co., Dordrecht, The Netherlands, pp. 497-529.
- Dugdale, R.C. 1967. Nutrient limitation in the sea: Dynamics, identification and significance. *Limnol. Oceanogr.* **12**:685-695.
- Dugdale, R.C. and J.J. Goering. 1967. Uptake of new and regenerated forms of nitrogen in primary productivity. *Limnol. Oceanogr.* **12**:196-206.
- Elkins, J.W. 1980. Determination of dissolved nitrous oxide in aquatic systems by gas chromatography using electron-capture detection and multiple phase equilibration. *Anal. Chem.* **52**:263-267.
- Elkins, J.W., S.C. Wofsy, M.B. McElroy, C.E. Kolb and W.A. Kaplan. 1978. Aquatic sources and sinks for nitrous oxide. *Nature* **275**:602-606.

- Eppley, R.W. and B.J. Peterson. 1979. Particulate organic matter flux and planktonic new production in the deep ocean. *Nature* **282**:677-680.
- Feliatra, F. and M. Bianchi. 1993. Rates of nitrification and carbon uptake in the Rhône River plume (northwestern Mediterranean Sea). *Microb. Ecol.* **26**:21-28.
- Garside, C. 1982. A chemiluminescent technique for the determination of nanomolar concentrations of nitrate and nitrite in seawater. *Mar. Chem.* **11**:159-167.
- Glibert, P.M. and D.A. Bronk. 1994. Release of dissolved organic nitrogen by marine diazotrophic cyanobacteria, *Trichodesmium* spp. *Appl. Environ. Microbiol.* **60**:3996-4000.
- Glover, H.E. 1985. The relationship between inorganic nitrogen oxidation and organic carbon production in batch and chemostat cultures of marine nitrifying bacteria. *Arch. Microbiol.* **74**:295-300.
- Goreau, T.J., W.A. Kaplan, S.C. Wofsy, M.B. McElroy, F.W. Valois and S.W. Watson. 1980. Production of NO_2^- and N_2O by nitrifying bacteria at reduced concentrations of oxygen. *Appl. Environ. Microbiol.* **40**:526-532.
- Hahn, J. 1975. N_2O measurements in the northeast Atlantic Ocean. "*Meteor*" *Forschungsergeb. Reihe A* **16**:1-14.
- Hahn, J. 1981. Nitrous oxide in the oceans. In: Denitrification, Nitrification, and Atmospheric Nitrous Oxide, C.C. Delwiche (ed), Wiley & Sons, New York, pp. 191-240.
- Hattori, A. 1983. Denitrification and dissimilatory nitrate reduction. In: Nitrogen in the Marine Environment, E.J. Carpenter and D.G. Capone (eds), Academic Press, New York, pp. 191-232.
- Herbland, A. and B. Voituriez. 1979. Hydrological structure analysis for estimating the primary production in the tropical Atlantic Ocean. *J. Mar. Res.* **37**:87-101.
- Houghton, J.T., G.J. Jenkins and J.J. Ephraums (eds). 1990. Climate Change: The IPCC Scientific Assessment, Intergovernmental Panel on Climate Change, Cambridge University Press, Cambridge, 365 pp.
- Hynes, R.K. and R. Knowles. 1981. Effect of acetylene on autotrophic and heterotrophic nitrification. *Can. J. Microbiol.* **28**:334-340.

Jenkins, W.J. 1988. Nitrate flux into the euphotic zone near Bermuda. *Nature* **331**:521-523.

Jones, R.D. and R.Y. Morita. 1984. Effect of several nitrification inhibitors on carbon monoxide and methane oxidation by ammonium oxidizers. *Can. J. Microbiol.* **30**:1276-1279.

Kaplan, W.A. 1983. Nitrification. In: Nitrogen in the Marine Environment, E.J. Carpenter and D.G. Capone (eds), Academic Press, New York, pp. 139-190.

Karl, D.M., G.A. Knauer, J.H. Martin and B.B. Ward. 1984. Bacterial chemolithotrophy in the ocean is associated with sinking particles. *Nature* **309**:54-56.

Karl, D.M., R. Letelier, D.V. Hebel, D.F. Bird and C.D. Winn. 1992. *Trichodesmium* blooms and new nitrogen in the North Pacific gyre. In: Marine Pelagic Cyanobacteria: Trichodesmium and other Diazotrophs, E.J. Carpenter, D.G. Capone and J.G. Reuter (eds), NATO ASI Series, Vol. 362, Kluwer Academic Publishers, Dordrecht, The Netherlands, pp. 219-238.

Karl, D.M., R. Letelier, D. Hebel, L. Tupas, J. Dore, J. Christian and C. Winn. 1995. Ecosystem changes in the North Pacific subtropical gyre attributed to the 1991-92 El Niño. *Nature* **373**:230-234.

Karl, D.M. and R. Lukas. 1995. The Hawaii Ocean Time-series (HOT) program: Background, rationale and field implementation. *Deep-Sea Res.*, submitted.

Karl, D.M. and B.D. Tilbrook. 1994. Production and transport of methane in oceanic particulate organic matter. *Nature* **368**:732-734.

Kiefer, D.A., R.J. Olson and O. Holm-Hansen. 1976. Another look at the nitrite and chlorophyll maxima in the central North Pacific. *Deep-Sea Res.* **23**:1199-1208.

Knauer, G.A., D.G. Redalje, W.G. Harrison and D.M. Karl. 1990. New production at the VERTEX time-series site. *Deep-Sea Res.* **37**:1121-1134.

Law, C.S., A.P. Rees and N.J.P. Owens. 1993. Nitrous oxide production by estuarine epiphyton. *Limnol. Oceanogr.* **38**:435-441.

Laws, E.A. and D.C.L. Wong. 1978. Studies of carbon and nitrogen metabolism by three marine phytoplankton species in nitrate-limited continuous culture. *J. Phycol.* **14**:406-416.

- Ledwell, J.R., A.J. Watson and C.S. Law. 1993. Evidence for slow mixing across the pycnocline from an open-ocean tracer-release experiment. *Nature* **364**:701-703.
- Letelier, R.M. 1994. Studies on the ecology of *Trichodesmium* spp. (Cyanophyceae) in the central North Pacific Gyre. Ph.D. Dissertation, University of Hawaii, Honolulu, Hawaii, 218 pp.
- Letelier, R.M., J.E. Dore, C.D. Winn and D.M. Karl. 1995. Temporal variability in photosynthetic carbon assimilation efficiencies at Station ALOHA. *Deep-Sea Res.*, submitted.
- Lewis, M.R., W.G. Harrison, N.S. Oakey, D. Hebert and T. Platt. 1986. Vertical nitrate fluxes in the oligotrophic ocean. *Science* **234**:870-873.
- Liu, K. and I.R. Kaplan. 1982. Nitrous oxide in the sea off southern California. In: The Environment of the Deep Sea, W.G. Ernst and J.G. Morin (eds), Prentice-Hall, Englewood Cliffs, New Jersey, pp. 73-92.
- Longhurst, A.R. and W.G. Harrison. 1988. Vertical nitrogen flux from the oceanic photic zone by diel migrant zooplankton and nekton. *Deep-Sea Res.* **35**:881-889.
- Longhurst, A.R. and W.G. Harrison. 1989. The biological pump: profiles of plankton production and consumption in the upper ocean. *Prog. Oceanogr.* **22**:47-123.
- Martínez, L., M.W. Silver, J.M. King and A.L. Alldredge. 1983. Nitrogen fixation by floating diatom mats: a source of new nitrogen to oligotrophic ocean waters. *Science* **221**:152-154.
- Marty, D.G. 1993. Methanogenic bacteria in seawater. *Limnol. Oceanogr.* **38**:452-456.
- Michaels, A.F., A.H. Knap, R.L. Dow, K. Gundersen, R.J. Johnson, J. Sorensen, A. Close, G.A. Knauer, S.E. Lohrenz, V.A. Asper, M. Tuel and R. Bidigare. 1994. Seasonal patterns of ocean biogeochemistry at the U.S. JGOFS Bermuda Atlantic Time-series Study site. *Deep-Sea Res.* **41**:1013-1038.
- Michaels, A.F., D.A. Siegel, R.J. Johnson, A.H. Knap and J.N. Galloway. 1993. Episodic inputs of atmospheric nitrogen to the Sargasso Sea: contributions to new production and phytoplankton blooms. *Global Biogeochem. Cycles* **7**:339-351.
- Olson, R.J. 1981a. ¹⁵N tracer studies of the primary nitrite maximum. *J. Mar. Res.* **39**:203-226.

- Olson, R.J. 1981b. Differential photoinhibition of marine nitrifying bacteria: a possible mechanism for the formation of the primary nitrite maximum. *J. Mar. Res.* **39**:227-238.
- Oudot, C., C. Andrie and Y. Montel. 1990. Nitrous oxide production in the tropical Atlantic Ocean. *Deep-Sea Res.* **37**:183-202.
- Owens, N.J.P., J.N. Galloway and R.A. Duce. 1992. Episodic atmospheric nitrogen deposition to oligotrophic oceans. *Nature* **357**:397-399.
- Pierotti, D. and R.A. Rasmussen. 1980. Nitrous oxide measurements in the eastern tropical Pacific Ocean. *Tellus* **32**:56-72.
- Platt, T., W.G. Harrison, M.R. Lewis, W.K.W. Li, S. Sathyendranath, R.E. Smith and A.F. Vezina. 1989. Biological production of the oceans: the case for a consensus. *Mar. Ecol. Prog. Ser.* **52**:77-88.
- Poth, M. and D.D. Focht. 1985. ¹⁵N kinetic analysis of N₂O production by *Nitrosomonas europaea*: an examination of nitrifier denitrification. *Appl. Environ. Microbiol.* **49**:1134-1141.
- Priscu, J.C. and M.T. Downes. 1985. Nitrogen uptake, ammonium oxidation and nitrous oxide (N₂O) levels in the coastal waters of western Cook Strait, New Zealand. *Estuarine Coastal Shelf Sci.* **20**:529-542.
- Rakestraw, N. W. 1936. The occurrence and significance of nitrite in the sea. *Biol. Bull. (Woods Hole)* **71**:133-167.
- Ritchie, G.A.F. and D.J.D. Nicholas. 1972. Identification of the sources of nitrous oxide produced by oxidative and reductive processes in *Nitrosomonas europaea*. *Biochem. J.* **126**:1181-1191.
- Robertson, L.A. and J.G. Kuenen. 1984. Aerobic denitrification: a controversy revived. *Arch. Microbiol.* **139**:351-354.
- Rönner, U. 1983. Distribution, production and consumption of nitrous oxide in the Baltic Sea. *Geochim. et Cosmochim. Acta* **47**:2179-2188.
- Scranton, M.I. and P.G. Brewer. 1977. Occurrence of methane in near-surface waters of the western subtropical North Atlantic. *Deep-Sea Res.* **234**:127-138.
- Sieburth, J.McN. 1983. Microbiological and organic-chemical processes in the surface and mixed layers. In: Air-Sea Exchange of Gases and Particles, P.S. Liss and W.G.N. Slinn (eds), D. Reidel Publishing Co., Dordrecht, Netherlands, pp. 112-172.

- Sieburth, J.McN. 1991. Methane and Hydrogen Sulfide in the Pycnocline: a Result of Tight Coupling of Photosynthetic and "Benthic" Processes in Stratified Waters. In: Microbial Production and Consumption of Greenhouse Gases: Methane, Nitrogen Oxides, and Halomethanes, J.E. Rogers and W.B. Whitman (eds), American Society for Microbiology, Washington, D.C., pp. 147-174.
- Singh, H.B., L.J. Salas and H. Shigeishi. 1979. The distribution of nitrous oxide (N₂O) in the global atmosphere and the Pacific Ocean. *Tellus* **31**:313-320.
- Small, L.F., G.A. Knauer and M.D. Tuel. 1987. The role of sinking fecal pellets in stratified euphotic zones. *Deep-Sea Res.* **34**:1705-1712.
- Smith, M.S. and K. Zimmerman. 1981. Nitrous oxide production by nondenitrifying soil nitrate reducers. *Soil Sci. Soc. Am. J.* **45**:865-871.
- Smith, S.V. 1984. Phosphorus versus nitrogen limitation in the marine environment. *Limnol. Oceanogr.* **29**:1149-1160.
- Smith, S.V., W.J. Kimmerer and T.W. Walsh. 1986. Vertical flux and biogeochemical turnover regulate nutrient limitation of net organic production in the North Pacific Gyre. *Limnol. Oceanogr.* **31**:161-167.
- Somville, M. 1978. A method for the measurement of nitrification rates in water. *Water Res.* **12**:843-848.
- Sverdrup, H.U. 1953. On conditions for the vernal blooming of phytoplankton. *J. Cons. Perm. Int. Explor. Mer.* **18**:287-295.
- Tilbrook, B.D. and D.M. Karl. 1994. Methane sources, distributions and sinks from California coastal waters to the oligotrophic North Pacific gyre. *Mar. Chem.*, in press.
- Vaccaro, R.F. and J.H. Ryther. 1960. Marine phytoplankton and the distribution of nitrite in the sea. *J. Cons. Perm. Int. Explor. Mer.* **25**:260-271.
- Villareal, T.A., M.A. Aitabet and K. Culver-Rymsza. 1993. Nitrogen transport by vertically migrating diatom mats in the North Pacific Ocean. *Nature* **363**:709-712.
- Walter, H.M., D.R. Keeney and I.R. Fillerey. 1979. Inhibition of nitrification by acetylene. *Soil Sci. Soc. Am. J.* **43**:195-196.
- Wanninkhof, R. 1992. Relationship between wind speed and gas exchange over the ocean. *J. Geophys. Res.* **97**:7373-7382.

- Ward, B.B. 1982. Oceanic distribution of ammonium-oxidizing bacteria determined by immunofluorescent assay. *J. Mar. Res.* **40**:1155-1172.
- Ward, B.B. 1986. Nitrification in marine environments. In: Nitrification. J.I. Prosser (ed), IRL Press, Oxford, pp. 157-184.
- Ward, B.B., H.E. Glover and F. Lipschultz. 1989a. Chemoautotrophic activity and nitrification in the oxygen minimum zone off Peru. *Deep-Sea Res.* **36**:1031-1051.
- Ward, B.B., K.A. Kilpatrick, E.H. Renger and R.W. Eppley. 1989b. Biological nitrogen cycling in the nitracline. *Limnol. Oceanogr.* **34**:493-513.
- Ward, B.B., R.J. Olson and M.J. Perry. 1982. Microbial nitrification rates in the primary nitrite maximum off southern California. *Deep-Sea Res.* **29**:247-255.
- Weathers, P.J. 1984. N₂O evolution by green algae. *Appl. Environ. Microbiol.* **48**:1251-1253.
- Weathers, P.J. and J.J. Niedzielski. 1986. Nitrous oxide production by cyanobacteria. *Arch. Microbiol.* **146**:204-206.
- Weiss, R.F. and B.A. Price. 1980. Nitrous oxide solubility in water and seawater. *Mar. Chem.* **8**:347-359.
- Weiss, R.F., F.A. Van Woy and P.K. Salameh. 1992. Surface Water and Atmospheric Carbon Dioxide and Nitrous Oxide Observations by Shipboard Automated Gas Chromatography: Results From Expeditions Between 1977 and 1990. Publication No. ORNL/CDIAC-59, Carbon Dioxide Information Analysis Center, Environmental Sciences Division, Oak Ridge National Laboratory, Oak Ridge, Tennessee, 134 pp.
- Wilson, T.R.S. 1978. Evidence for denitrification in aerobic pelagic sediments. *Nature* **274**:354-356.
- Winn, C.D., F.T. Mackenzie, C.J. Carrillo, C.L. Sabine and D.M. Karl. 1994. Air-sea carbon dioxide exchange in the North Pacific subtropical gyre: implications for the global carbon budget. *Global Biogeochem. Cycles* **8**:157-163.
- Yoshida, N., H. Morimoto, M. Hirano, I. Koike, S. Matsuo, E. Wada, T. Saino and A. Hattori. 1989. Nitrification rates and ¹⁵N abundances of N₂O and NO₃⁻ in the western North Pacific. *Nature* **342**:895-897.

Yoshida, T. and M. Alexander. 1970. Nitrous oxide formation by *Nitrosomonas europaea* and heterotrophic microorganisms. *Soil Sci. Soc. Am. Proc.* **34**:880-882.

Yoshinari, T. 1976. Nitrous oxide in the sea. *Mar. Chem.* **4**:189-202.

CHAPTER 5

COMBINED OXIDATION/REDUCTION MODEL OF THE PRIMARY NITRITE MAXIMUM AT STATION ALOHA

ABSTRACT

The maintenance of the marine primary nitrite maximum (PNM) has been variously attributed to oxidative and reductive nitrogen cycle processes. Models based on phytoplankton nitrite excretion during nitrate assimilation or on the differential photoinhibition of ammonium oxidation and nitrite oxidation alone have been reasonably successful in predicting an accumulation of nitrite near the 1% light level in stratified oceanic waters. Recent evidence, however, suggests that both oxidative and reductive pathways contribute to the PNM, and that these competing processes may exhibit vertical separation with only minimal overlap. We have developed a combined oxidation/reduction PNM model for stratified oligotrophic oceanic waters that successfully predicts this vertical separation of processes and reproduces the asymmetric shape of the PNM based on measured chemical and bio-optical parameters.

INTRODUCTION

Nitrite (NO_2^-) is a redox intermediate between ammonium (NH_4^+) and nitrate (NO_3^-) in seawater, and as such it is a useful indicator of sites of marine nitrogen cycle oxidation/reduction activity. Over much of the world's oceans, an accumulation of nitrite appears in the lower reaches of the euphotic zone, known as the primary nitrite maximum

(PNM). Both oxidative and reductive processes have been suggested as the source of nitrite within the PNM, including the excretion of NO_2^- during assimilatory NO_3^- reduction by phytoplankton (Vaccaro and Ryther, 1960; Kiefer et al., 1976) and bacteria (Wada and Hattori, 1971), the buildup of nitrite due to the differential photoinhibition of ammonium and nitrite oxidizing bacteria (Olson, 1981b), or a combination of these processes (Wada and Hattori, 1991; Dore and Karl, 1995). All of these processes are governed by the activities of the responsible microorganisms, which in turn depend on their biomass, light, and substrate availability.

Previous attempts to model the development of the PNM have met with some success. A box model of the PNM was used to demonstrate the potential for nitrite accumulation via phytoplankton excretion during nitrate assimilation (Kiefer et al., 1976), but the depth distribution of $[\text{NO}_2^-]$ was not addressed. A PNM model involving the photoinhibition of nitrification was later developed which did predict $[\text{NO}_2^-]$ profiles, based on light levels, ammonium distributions and kinetic parameters of nitrification reactions taken from laboratory and field experiments (Olson, 1981b). This model was successful in predicting the accumulation of nitrite in approximately the correct depth stratum, but did not recreate the asymmetric character of the PNM (Zafiriou et al., 1992; Dore and Karl, 1995), especially when applied to oligotrophic central North Pacific waters. In the same year, a model combining phytoplankton growth, seasonal mixing and stratification, and biologically mediated nitrogen transformations was described, which included nitrite production by phytoplankton nitrate reduction but did not include nitrification (Kiefer and Kremer, 1981). While the use of this model was restricted to temperate oceans with deep winter mixed layers, it is of note that it predicted a summer nitrite profile with an abrupt upper peak and a depth-decaying tail into deeper waters.

We have developed a PNM model which combines the processes of phytoplankton nitrate reduction to nitrite, bacterial ammonium oxidation to nitrite, and bacterial oxidation of nitrite to nitrate. We apply this model to data from the Hawaii Ocean Time-series project collected at the oligotrophic North Pacific deep water Station ALOHA from 1991-94, compare the predicted $[\text{NO}_2^-]$ profiles to those measured, and comment on the strengths and weaknesses of the model.

MATERIALS AND METHODS

Station location and sampling

All data used to design and test the model were collected at the central North Pacific deep water station ALOHA (A Long-term Oligotrophic Habitat Assessment; Fig. 1.3). Station ALOHA, located at $22^{\circ}45' \text{ N}$, 158° W and visited at approximately monthly intervals by Hawaii Ocean Time-series (HOT) project scientists, was chosen to be representative of the North Pacific subtropical gyre ecosystem (Karl and Lukas, 1995). Discrete 12 l water samples are collected in PVC bottles with a CTD-rosette system at up to 24 depths during each cast. Samples for nutrient measurements are drawn from the rosette into 125 ml acid-washed high-density polyethylene (HDPE) bottles and immediately frozen for later analysis at our land-based laboratory. Samples for chlorophyll-a determinations are drawn into clean 4 l or 10 l HDPE bottles and pressure-filtered for later analysis by high-performance liquid chromatography (HPLC), as described in Letelier et al. (1993). Samples for adenosine-5'-triphosphate (ATP) are drawn into clean 4 l HDPE bottles, filtered and extracted at sea, and later analyzed by firefly luminescence (Karl and Holm-Hansen, 1978), as described in Letelier et al. (1995).

Continuous CTD data are processed as described in Bingham and Lukas (1995). These physical data are used to calculate the potential density at each bottle trip and the average depth-density relationship over a 72 hour period on station during each cruise. The average depth associated with a particular sampled isopycnal is used instead of the actual depth at the time of sampling. Using this density-averaging technique for samples collected from within the pycnocline, much of the short-term physical variability caused by internal waves and tidal motions can be filtered out, allowing an accurate assessment of the relative positions of features sampled on different casts at different times during each cruise.

Optical measurements

The incident flux of photosynthetically available radiation (PAR; 400-700 nm) is measured on deck continuously with a Licor cosine collector. Underwater PAR is measured using a hand-lowered profiling natural fluorometer (PNF; Biospherical). Underwater PAR measurements are used to calculate an average extinction coefficient within the euphotic zone assuming uniform exponential decay below 10 m depth. The percent transmission through the sea surface is calculated by extrapolating the PAR data from below 10 m to the surface and dividing by the PAR flux measured simultaneously with the on-deck cosine collector. Because much of the 600-700 nm (red) light energy is lost in the upper 10 m of the water column (Kirk, 1994), the above calculation predicts less PAR transmission than if only the air-sea interface is considered; nevertheless this approach results in a reasonably accurate simulation of the underwater PAR distribution below 10 m.

Nutrient analyses

Nitrite was measured using chemiluminescence as described in Dore and Karl (1995), as was nitrate+nitrite, except where $[\text{NO}_3^- + \text{NO}_2^-]$ exceeded $1 \mu\text{M}$. These chemiluminescent methods offer precision and accuracy in the 1-2 nM range (Dore and Karl, 1995). In the case of $[\text{NO}_3^- + \text{NO}_2^-] > 1 \mu\text{M}$, autoanalytic measurements (Dore et al., 1995) were used. Because $[\text{NO}_3^- + \text{NO}_2^-]$ samples were often collected on different casts than the $[\text{NO}_2^-]$ samples, calculating $[\text{NO}_3^-]$ by difference for individual samples was not possible, therefore in the model we substitute $[\text{NO}_3^- + \text{NO}_2^-]$ for $[\text{NO}_3^-]$. This substitution has little effect other than to slightly change the relative positions of the PNM and nitracline, but never by more than a few meters. Ammonium concentrations were measured on two occasions by manual colorimetry (Strickland and Parsons, 1972), but the low ambient concentrations (typically $[\text{NH}_4^+] < 0.2 \mu\text{M}$) make it nearly impossible to determine the $[\text{NH}_4^+]$ profile accurately. In testing the PNM model, therefore, it is necessary for us to make certain assumptions about the $[\text{NH}_4^+]$ distributions.

HOT-50 in situ incubations

During HOT-50 (Oct. 1993) we performed an incubation experiment in order to determine where in the water column net transformations of nitrite and nitrate were occurring and at what rates, so that we could use the results in fine-tuning the model parameters. On an early morning rosette cast we collected 21 water column samples, beginning at 200 m and sampling every 10 m to the surface. From each of these a single 250 ml acid-washed clear polycarbonate incubation bottle was filled and tightly capped under subdued light. Replicate samples were immediately frozen in 125 ml HDPE bottles

for time-zero nitrite and nitrate analyses. Before dawn the incubation bottles were connected to the HOT free-floating sediment trap array (Karl et al., 1995) as it was being deployed, using plastic tie-wraps. Each bottle was attached such that it would remain at the depth from which it was collected. The deployment lasted approximately 72 hours. Although the long duration of the incubation could possibly result in artifacts (Venrick et al., 1977), we needed to capture at least one full diel cycle to determine net daily rates and the 3-day sediment trap array deployment was a convenient vehicle for doing this. After recovery, the incubation bottles were immediately frozen and returned along with the time-zero samples to our shore-based laboratory for chemiluminescent nitrite and nitrate determinations. In this experiment, both $[\text{NO}_2^-]$ and $[\text{NO}_3^- + \text{NO}_2^-]$ were determined on each sample, with $[\text{NO}_3^-]$ calculated by difference.

Model code

The PNM model has been written in the MATLAB™ programming language, and can be run on any personal computer using Microsoft Windows™ and MATLAB™ for Windows. A 486-based machine with a math co-processor is highly desirable, but not essential, for running the model. Output is to a color monitor, but output data can easily be saved to ASCII files using simple MATLAB™ commands. Appendix A contains a complete printout of all routines used in the model, as well as instructions on how to configure data input files. Statements in the model code beginning with % are comments only.

Model equations

In our PNM model, the depth profile of nitrite is determined for a time $t+\Delta t$ by taking the profile at time t and adding the contributions of nitrite from each modeled process at each depth during the time Δt . Symbolically, this is represented by the equation:

$$(1) \quad [NO_2^-]_{t+\Delta t} = [NO_2^-]_t + \Delta t \cdot (R_{4-2} + R_{3-2} - R_{2-3} - R_{2-4})$$

In the above equation, $[NO_2^-]_t$ is a 201×1 array, representing the nitrite concentration at time t at 1 m intervals from 0 m to 200 m. Similarly, $[NO_2^-]_{t+\Delta t}$ is an array representing nitrite concentration at time $t+\Delta t$. The time step Δt used in the model is one day. The R terms represent the depth-dependent daily rates of ammonium oxidation to nitrite (R_{4-2}), nitrate reduction to nitrite (R_{3-2}), nitrite oxidation to nitrate (R_{2-3}), and nitrite assimilation (R_{2-4}).

We model the oxidation of ammonium at each depth based on kinetic parameters of ammonium oxidizing bacteria and the ambient $[NH_4^+]$ as per Olson (1981b):

$$(2) \quad R_{4-2} = \frac{A_4 \cdot [NH_4^+] \cdot R_{4-2}^m}{(K_{4-2} + [NH_4^+])}$$

In equation (2), A_4 represents the depth-dependent relative activity of ammonium oxidation that is allowed by light, R_{4-2}^m is the maximum rate of ammonium oxidation under optimal conditions, and K_{4-2} is the half-saturation constant for ammonium oxidation. We also model the oxidation of nitrite to nitrate according to Olson (1981b):

$$(3) \quad R_{2-3} = \frac{A_2 \cdot [NO_2^-] \cdot R_{2-3}^m}{(K_{2-3} + [NO_2^-])}$$

In equation (3), A_2 represents the depth-dependent relative activity of nitrite oxidation that is allowed by light, R_{2-3}^m is the maximum rate of nitrite oxidation under optimal conditions, and K_{2-3} is the half-saturation constant for nitrite oxidation.

In equations (2) and (3) above, the terms A_4 and A_2 must be calculated at each depth from the light field and the dose-response characteristics of nitrifiers with respect to light inhibition (Olson, 1981b):

$$(4) \quad A_4 = 1 - \frac{(I_z - T_4)}{(I_z - T_4) + D_4}$$

$$(5) \quad A_2 = 1 - \frac{(I_z - T_2)}{(I_z - T_2) + D_2}$$

In equations (4) and (5), I_z is a vector containing the daily-averaged PAR as a function of depth z , the D_4 and D_2 terms are the half-saturation doses of PAR for light inhibition of ammonium and nitrite oxidation, respectively, and the T_4 and T_2 terms are threshold doses of PAR for photoinhibition of the two processes. The PAR vector I_z is calculated based on the average flux of PAR over a 24 hr day:

$$(6) \quad I_z = I_m \cdot f_t \cdot e^{(-k \cdot z)}$$

In equation (6) above, I_m is the daily-averaged PAR at the sea surface, f_t is the fraction of PAR that passes through the sea surface (actually the upper few m; see methods), k is the diffuse attenuation (extinction) coefficient for PAR, and z is the depth.

For the reduction of nitrate to nitrite, we assume a linear dependence of nitrite production on light, phytoplankton biomass, and nitrate concentration:

$$(7) \quad R_{3-2} = K_{3-2} \cdot B \cdot [NO_3^-] \cdot I_z$$

In equation (7), I_z is the ambient average PAR array, B is a phytoplankton biomass array and K_{3-2} is a rate constant for nitrate reduction to nitrite. This equation models the *net* production of nitrite during nitrate assimilation, thus incorporates nitrite assimilation already. For this reason, we neglect the nitrite assimilation term in equation (1):

$$(8) \quad R_{2-4} \approx 0$$

A complete list of the variables and constants used in the model, including the units used and the values of the constants, is located in Appendix B. Note that not all of the constants dealing with nitrification are exactly as presented by Olson (1981b). We have replaced the maximum rates of ammonium and nitrite oxidation ($R_{4-2}^m = R_{2-3}^m = 5 \text{ nmol l}^{-1} \text{ d}^{-1}$) with higher rates which we feel are more representative of the in situ rates at Station ALOHA ($R_{4-2}^m = R_{2-3}^m = 30 \text{ nmol l}^{-1} \text{ d}^{-1}$; see Chapt. 4). Also, we have used substrate half-saturation concentrations for ammonium and nitrite oxidation that produce more accurate model results, while not being unreasonable given the measured substrate concentrations at Station ALOHA ($K_{4-2} = 200 \text{ nM}$ and $K_{2-3} = 27 \text{ nM}$, instead of $K_{4-2} = K_{2-3} = 70 \text{ nM}$). The nitrate reduction constant, K_{3-2} , was chosen so that the modeled rate

of nitrite production at the highest nitrite concentration during HOT-50 would approximately match the rate observed in our in situ incubation experiment. We also had to convert our PAR units ($\mu\text{E m}^{-2} \text{ s}^{-1}$; $1\text{E} = 1 \text{ mol quanta}$) to units of W m^{-2} for use with the Olson equations, assuming $1 \text{ W m}^{-2} = 4.6 \mu\text{E m}^{-2} \text{ s}^{-1}$ for sunlight in the 400-700 nm range (Kirk, 1994).

Model assumptions

In order to keep the model simple, some assumptions were necessary. First, we have left physical mixing and diffusion processes out of the model. The PNM exists in a highly stratified layer at Station ALOHA, where eddy-diffusive mixing is slow compared to the biological nitrogen transformation rates, so if we do not attempt to extrapolate our results too far ahead in time, neglecting mixing and diffusion should not be problematic. Second, we assume that the nitrate, phytoplankton biomass, phytoplankton species composition, and ammonium distributions are constant during the time span of the model simulation. While none of these parameters is expected to be truly constant in the real ocean, this assumption reduces the complexity required of the model and it allows us to focus on the effects of light intensity on the processes involved. The assumption of constant species composition is made because our value of K_{3-2} is an average value for the entire phytoplankton population, not any particular species. Third, due to our lack of reliable ammonium measurements, we use the same "best guess" ammonium profile for all cruises modeled. This is not a requirement of the model, and in fact the model is designed to use actual ammonium data if available. The contribution of nitrification to the PNM is strongly influenced by the ammonium profile (Olson, 1981b), hence we will discuss this shortcoming in some detail later.

Our fourth assumption is that no nitrite is produced by phytoplankton nitrate reduction if the nitrate concentration is <20 nM. At these low nitrate levels the assumption that nitrate is constant cannot hold, and the high light levels would cause the model to produce more nitrite than there is available nitrate. In the real ocean, *net* nitrite production presumably only occurs beyond a threshold nitrate concentration. We have found that by neglecting the production of nitrite by phytoplankton at these low nitrate levels, accurate nitrite profiles can be generated.

A fifth assumption is that the net excretion of nitrite by phytoplankton is directly proportional to both nitrate concentration and light intensity. Studies with pure cultures of phytoplankton have revealed that nitrite excretion follows enzyme kinetics when expressed as a function of either light intensity or nitrate concentration (Serra et al., 1978; Olson et al., 1980; Collos, 1982). However, the concentrations of nitrate in the upper 200 m at Station ALOHA are generally <5 μ M, thus not high enough to saturate the nitrite excretion process, except perhaps near the base of this layer (Serra et al., 1978; Olson et al., 1980; Collos, 1982). Similarly, light levels below the nitracline at Station ALOHA are never high enough to be saturating. In surface waters above the mixed layer light does reach saturation levels, but because our model neglects phytoplankton nitrate reduction in this zone, it is not necessary for this to be taken into account.

Sixth, we assume that both ammonium oxidizers and nitrite oxidizers are distributed uniformly throughout the upper 200 m. This assumption was also made by Olson (1981b), and is supported by data on nitrifier distributions that show no consistent patterns with depth (Ward and Carlucci, 1985). Because in its formulation the model estimates overall nitrification rates rather than cell-specific or biomass-specific rates, the actual biomass or numbers of nitrifiers need not be known as long as the maximum

nitrification rates are chosen to be representative of the actual maximum overall rates for the ecosystem being modeled.

Our seventh assumption is that phytoplankton are entirely responsible for the production of nitrite via nitrate reduction. While it is possible that bacteria may also contribute to this process (Wada and Hattori, 1972), there is little direct evidence that this is a significant pathway, while there is ample evidence for the production of nitrite by phytoplankton. Because we need to convert measured biomass parameters (ATP or chlorophyll-a) into phytoplankton biomass, we use conversion factors that have been derived from data collected at Station ALOHA. Since our focus is on the layer beneath the nitracline, we use a factor of 15 g phytoplankton C per g chlorophyll-a as determined for phytoplankton within the chlorophyll maximum (Christian and Karl, 1994), recognizing that this will lead to underestimates of phytoplankton biomass in surface waters. Similarly, we use a biomass C: ATP ratio of 375 g g^{-1} , and assume that 35% of this C is phytoplankton biomass (Christian and Karl, 1994). In the model, one can choose to use phytoplankton biomass estimates based on either ATP or chlorophyll-a; the same constants are used in both cases, but the simulated PNM will be slightly different in shape depending upon which parameter phytoplankton biomass is estimated from.

Our eighth and final assumption is that the activities of phytoplankton and nitrifying bacteria can be adequately modeled using the average daily light flux rather than a day/night cycle. While phytoplankton nitrite excretion may continue in the dark (Laws and Wong, 1978) and the recovery from inhibition of nitrifying bacteria is possible during the night (Vanzella et al., 1990), we find that accurate simulation of the PNM is achieved without adding the extra complexity of a diel light cycle to the model.

RESULTS AND DISCUSSION

Measurements of model input parameters

Model input parameters include depth distributions of photosynthetically available radiation (PAR), nitrate, ammonium, and phytoplankton biomass (estimated from ATP or chlorophyll-a). We will discuss these in turn and display some examples; complete listings of these distributions are tabulated in Appendix C.

Daily integrated PAR varied from 34.5 to 57.0 E m⁻² over the five cruises for which the PNM model was tested (Table 5.1). The measured value for each cruise was used as model input. The diffuse PAR attenuation coefficient varied both between cruises and with depth, but mean values between 10 and 175 m were in the range from 0.036 to 0.048 m⁻¹ for all five cruises. Since the model requires an attenuation coefficient that can be applied over a period of at least several days, rather than an instantaneous value, we chose to apply an approximate mean value of 0.040 m⁻¹ to all the simulations. Similarly, the derived percent transmission of PAR through the sea surface ranged from 58% to 95%, but because the variability over a few days or less was large we chose to use an approximate mean value of 75% in all simulations. Note that due to our method of calculation, transmission through the "sea surface" here includes transmission through the air-sea interface and the upper few meters of the water column. Model PAR distributions calculated for the highest (HOT-36) and lowest (HOT-50) daily light fluxes are presented in Fig. 5.1.

Nitrate concentrations were <20 nM from the surface to a depth of 90-100 m (nitracline depth), then increased abruptly, reaching values of approximately 2-5 μM at

Table 5.1. Surface PAR[†] fluxes used in PNM model

Cruise	Month	Surface PAR Flux (E m ⁻² d ⁻¹)	Mean PAR Flux [‡] (μE m ⁻² s ⁻¹)
HOT-31	Oct. 1991	40.4	468
HOT-36	Apr. 1992	57.0	660
HOT-40	Sept. 1992	50.6	586
HOT-41	Oct. 1992	46.4	537
HOT-50	Oct. 1993	34.5	399

[†] PAR = photosynthetically available radiation (400-700 nm).

[‡] Calculated from the daily flux by dividing by the number of seconds in one day.

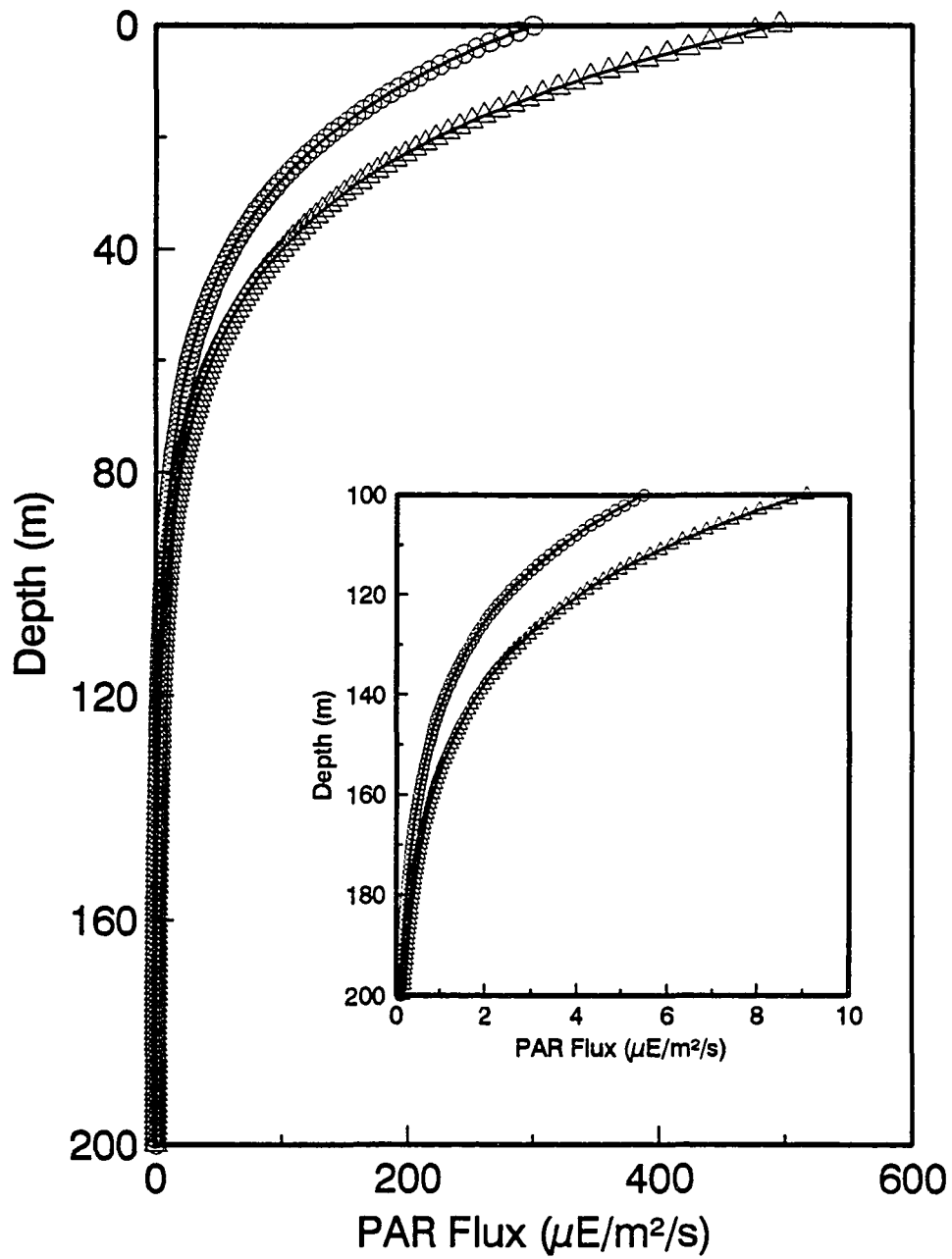


Fig. 5.1. Distributions of PAR used in model simulations for HOT-36 (triangles) and HOT-50 (circles). Inset shows expanded view of 100-200 m depth range (note change in scale).

200 m. This rise of nitrate with depth was generally monotonic, as shown in HOT-50, but on one occasion (HOT-31) a distinct inversion was present near 160 m (Fig. 5.2).

Ammonium was measured on two cruises, HOT-50 (Oct. 1993) and HOT-51 (Jan. 1994), and was found to be both low (<300 nM) and variable. About half of the measured concentrations were below the nominal 100 nM detection limit for the assay (Dore et al., 1995), and duplicate sample analyses differed by as much as 100 nM. We therefore take the approximate mean value of $[\text{NH}_4^+] = 100$ nM and apply it to the entire upper 200 m of the water column for all model simulations.

Our phytoplankton biomass estimates range from about $1\text{-}7 \mu\text{g C l}^{-1}$ above the nitracline and from about $0\text{-}5 \mu\text{g C l}^{-1}$ below the nitracline. Above the nitracline, estimates based on ATP are higher than those based on chl-a, mainly because we applied a C:chl-a conversion factor that is suitable for the lower euphotic zone but underestimates algal biomass above the nitracline. The extremely low nitrate concentrations above the nitracline prevent this underestimation from causing aberrant behavior in the model. Below the nitracline the two independent estimates of phytoplankton biomass give similar distributions, as shown for HOT-50 (Fig. 5.3). Estimates based on chl-a, however, are generally somewhat higher than those from ATP in the 100-150 m layer and lower in the 150-200 m layer.

Determination of model constants

Our HOT-50 in situ incubation revealed that most assimilation of nitrate occurs within a layer that begins at and extends to about 50 m beneath the nitracline (Fig. 5.4). Between 150 and 180 m, production and consumption of nitrate are more or less in balance, and below 180 m nitrate production exceeds its consumption. Nitrite, on the

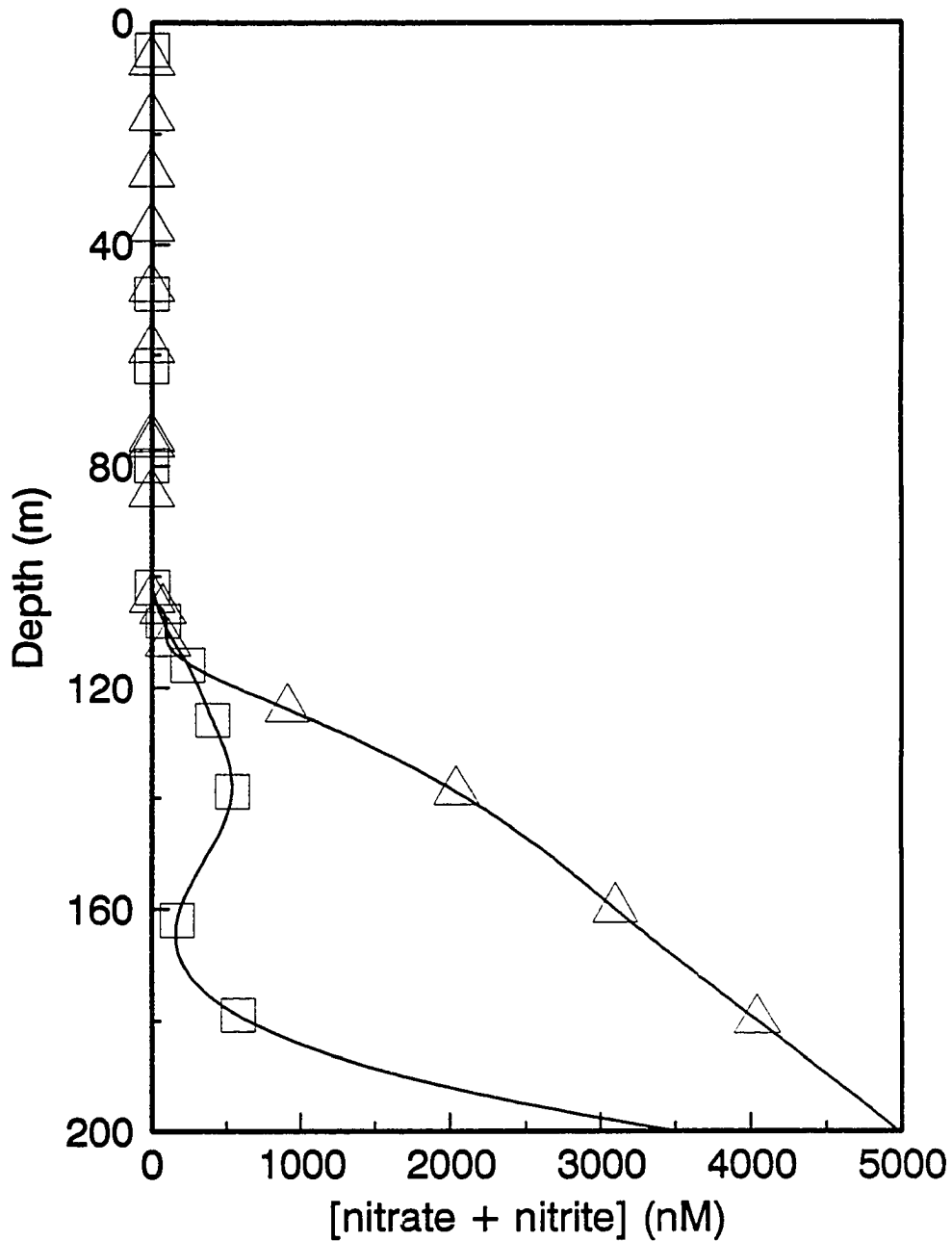


Fig. 5.2. Distributions of nitrate used in model simulations for HOT-31 (squares) and HOT-50 (triangles). Markers indicate actual data points, solid lines are cubic spline interpolations. Extrapolation to 0 m was made by assuming constant nitrate concentration from the uppermost data point to the surface. Extrapolation to 200 m was made assuming a linear increase to deeper data points (not shown).

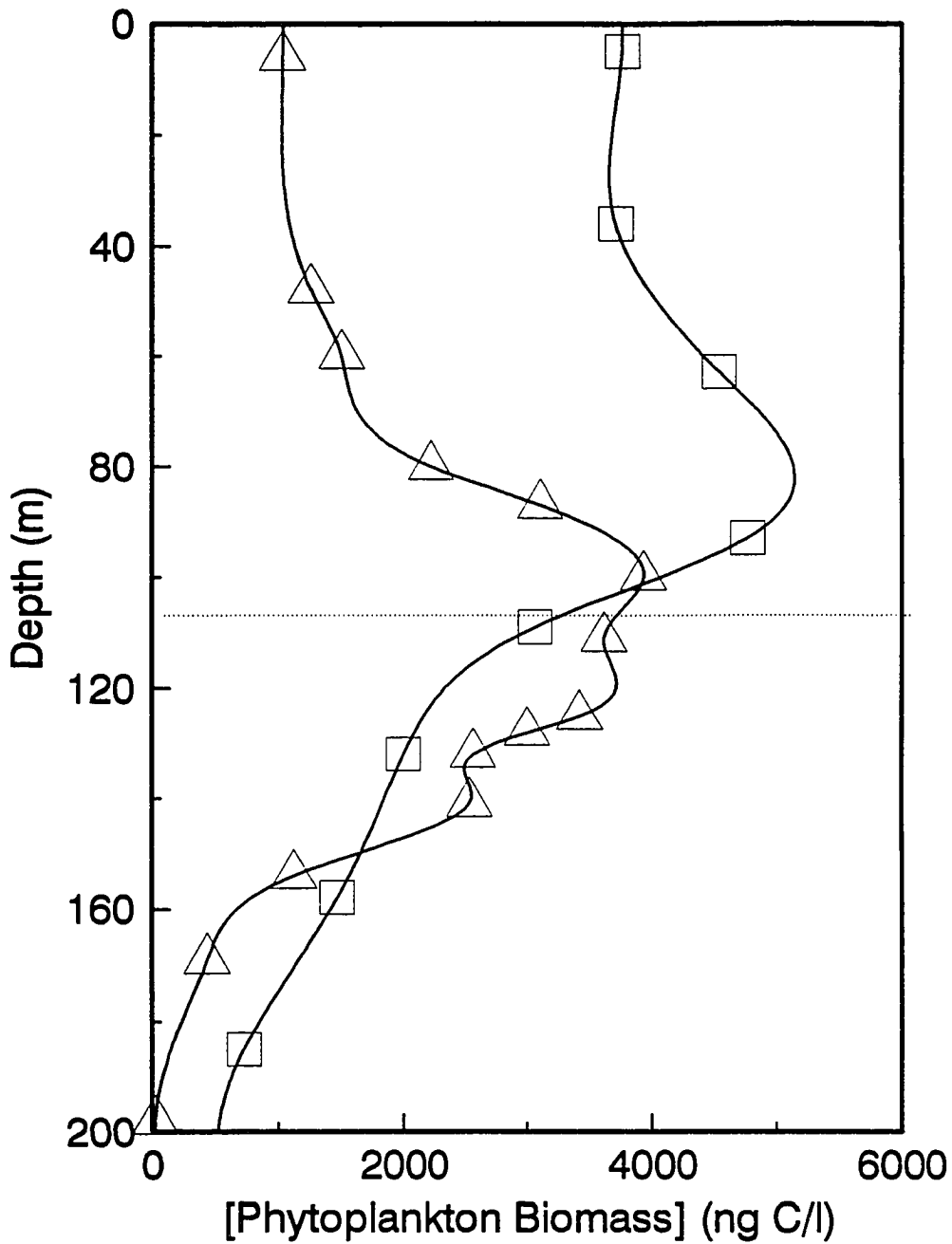


Fig. 5.3. Distributions of biomass carbon estimated from ATP (squares) and chlorophyll-a (triangles) used in model simulations for HOT-50. Solid lines indicate cubic spline interpolations used in model calculations. Dotted line indicates approximate depth of the nitracline.

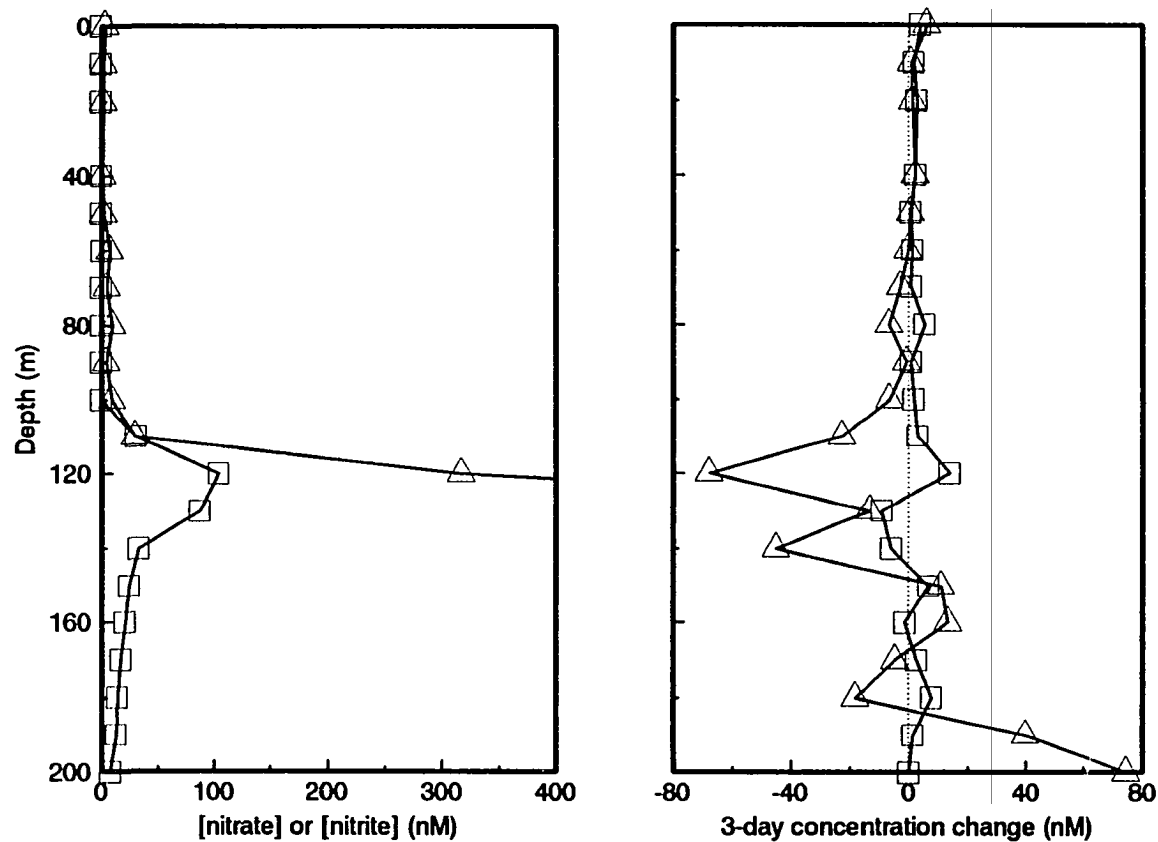


Fig. 5.4. Results of HOT-50 in situ incubation. Left panel: initial concentrations of nitrite (squares) and nitrate (triangles). $[\text{NO}_3^-]$ is offscale below 120 m. Right panel: net changes in nitrite (squares) and nitrate (triangles) during 3-day incubation. Dotted line indicates no net change in concentration. The 30 m incubation bottle was lost during recovery of the array.

other hand, shows a maximum in net production of nearly $5 \text{ nmol l}^{-1} \text{ d}^{-1}$ around 120 m, coincident with the maximum rate of nitrate disappearance, and a layer of more modest net production from 150 m downward. These observations are consistent with the hypothesized vertical separation of oxidative and reductive nitrite-forming processes (Dore and Karl, 1995). The large upper primary nitrite maximum (UPNM) at 120 m (Fig. 5.4) is probably maintained by the excretion of nitrite during reduction of nitrate by phytoplankton, while nitrification contributes to the net production in the 150-200 m layer.

We used the results of this incubation experiment to determine a rough value of the nitrate reduction constant ($K_{3,2}$) in our model. This was accomplished by running the HOT-50 simulation with different values of $K_{3,2}$ until (1) the simulation produced a nitrite distribution closely matching the measured distribution and (2) the rate of production of nitrite at 120 m depth was in the $4\text{-}6 \text{ nmol l}^{-1} \text{ d}^{-1}$ range, consistent with that observed during the incubation. The final value used was $K_{3,2} = 9.0 \times 10^{-7} \text{ (nmol NO}_2^- \text{ produced l}^{-1} \text{ d}^{-1}) \text{ (ng l}^{-1} \text{ phytoplankton C)}^{-1} \text{ (nM NO}_3^-)^{-1} \text{ (}\mu\text{E m}^{-2} \text{ s}^{-1})^{-1}$. Applied to a control volume of 1 m^2 area and 1 m vertical thickness over 1 d this translates into $K_{3,2} = 126 \text{ (mol NO}_2^- \text{ (mol C)}^{-1} \text{ (mol NO}_3^-)^{-1} \text{ (E)}^{-1}$.

Model PNM simulations

The model simulations for all five cruises successfully recreate the general features of the PNM (Figs. 5.5-5.9). In all cases, a large upper primary nitrite maximum (UPNM; Dore and Karl, 1995) is produced, mostly as a result of phytoplankton nitrate reduction, about 15-30 m below the nitracline. Beneath this peak nitrite concentrations decline with depth to about 20-25 nM at 200 m. In this lower zone from about 150-200 m, nitrification is the main source of nitrite. In some of the model simulations, a lower

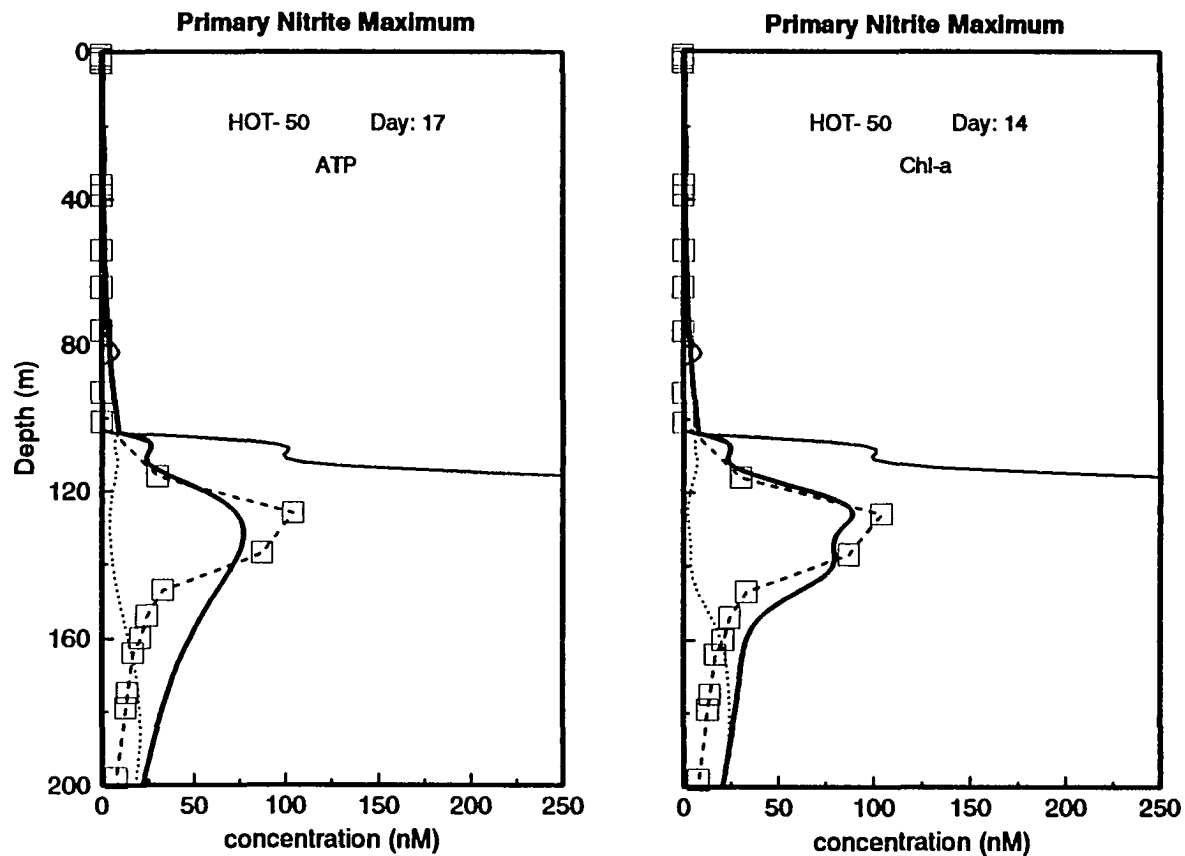


Fig. 5.5. Model output for HOT-50 (Oct. 1993). Interpolated nitrate data indicated by narrow solid line. Measured nitrite data indicated by squares and dashed line. Wide solid line is the model nitrite output. Dotted line is the net contribution to the modeled nitrite made by nitrifying bacteria. Left panel: ATP used to estimate phytoplankton biomass. Right panel: chlorophyll-a used to estimate phytoplankton biomass. Number of timesteps (days) used in simulation is listed in the upper right of each plot.

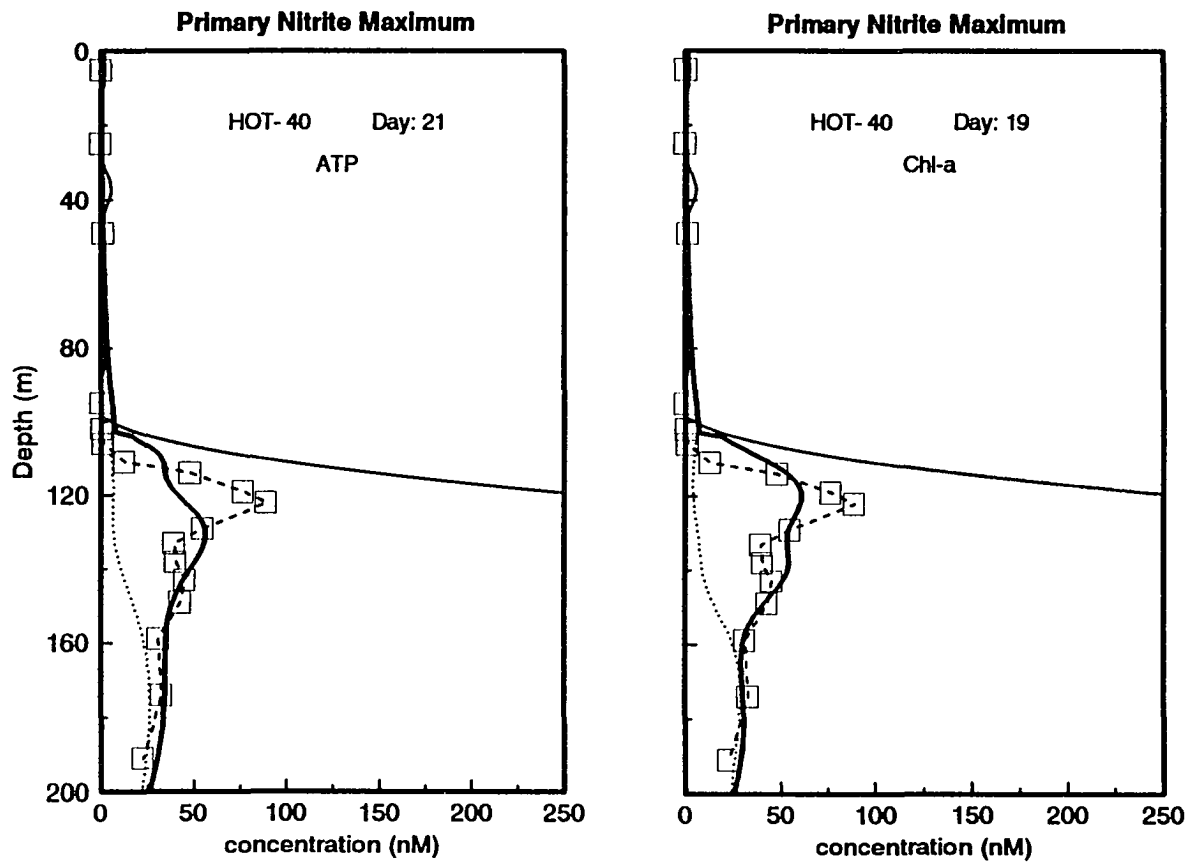


Fig. 5.6. Model output as in Fig. 5.5 except for HOT-40 (Sept. 1992).

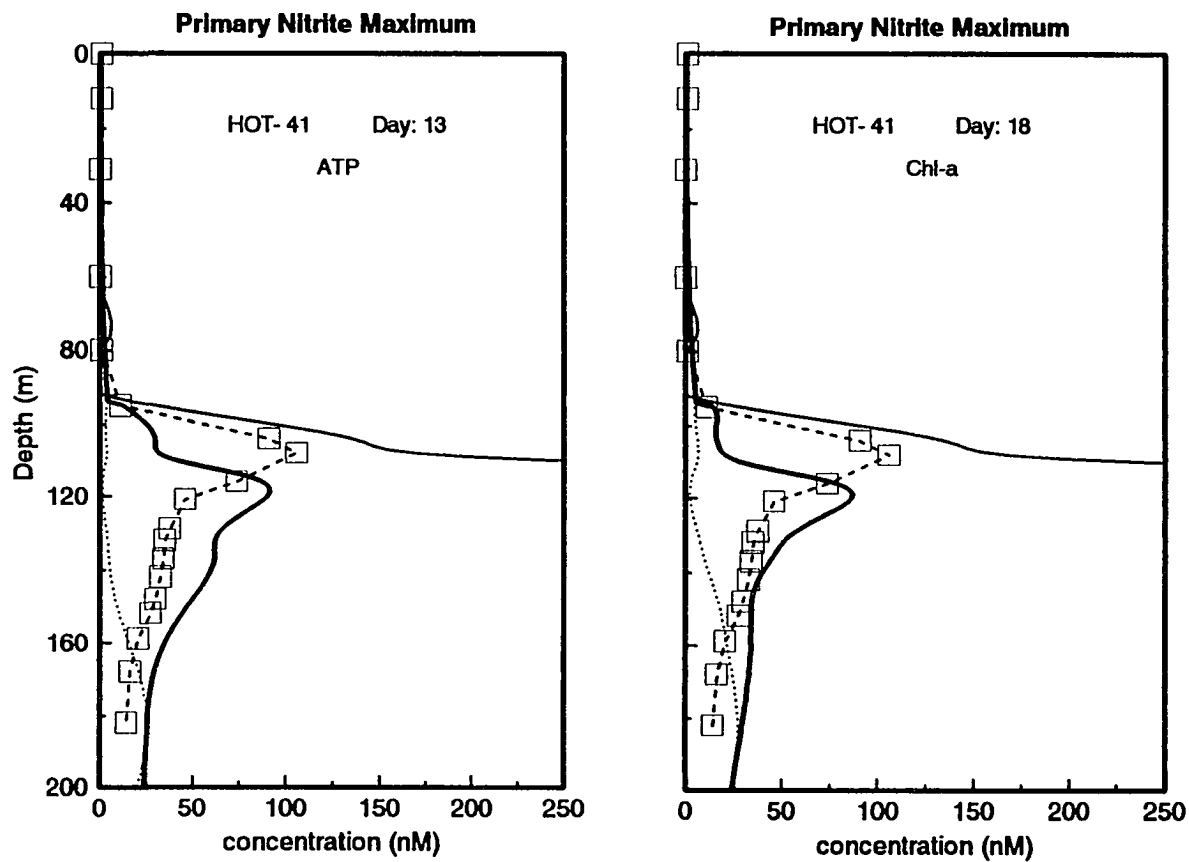


Fig. 5.7. Model output as in Fig. 5.5 except for HOT-41 (Oct. 1992).

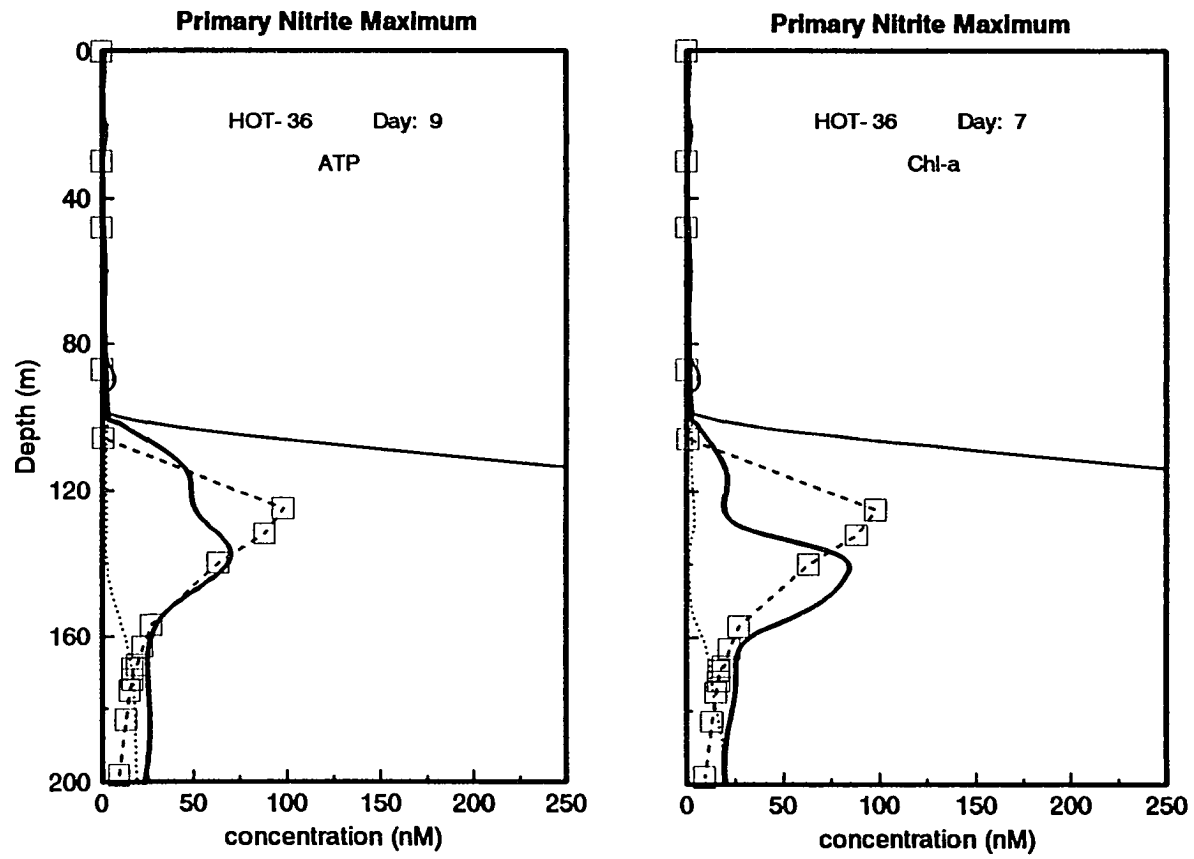


Fig. 5.8. Model output as in Fig. 5.5 except for HOT-36 (Apr. 1992).

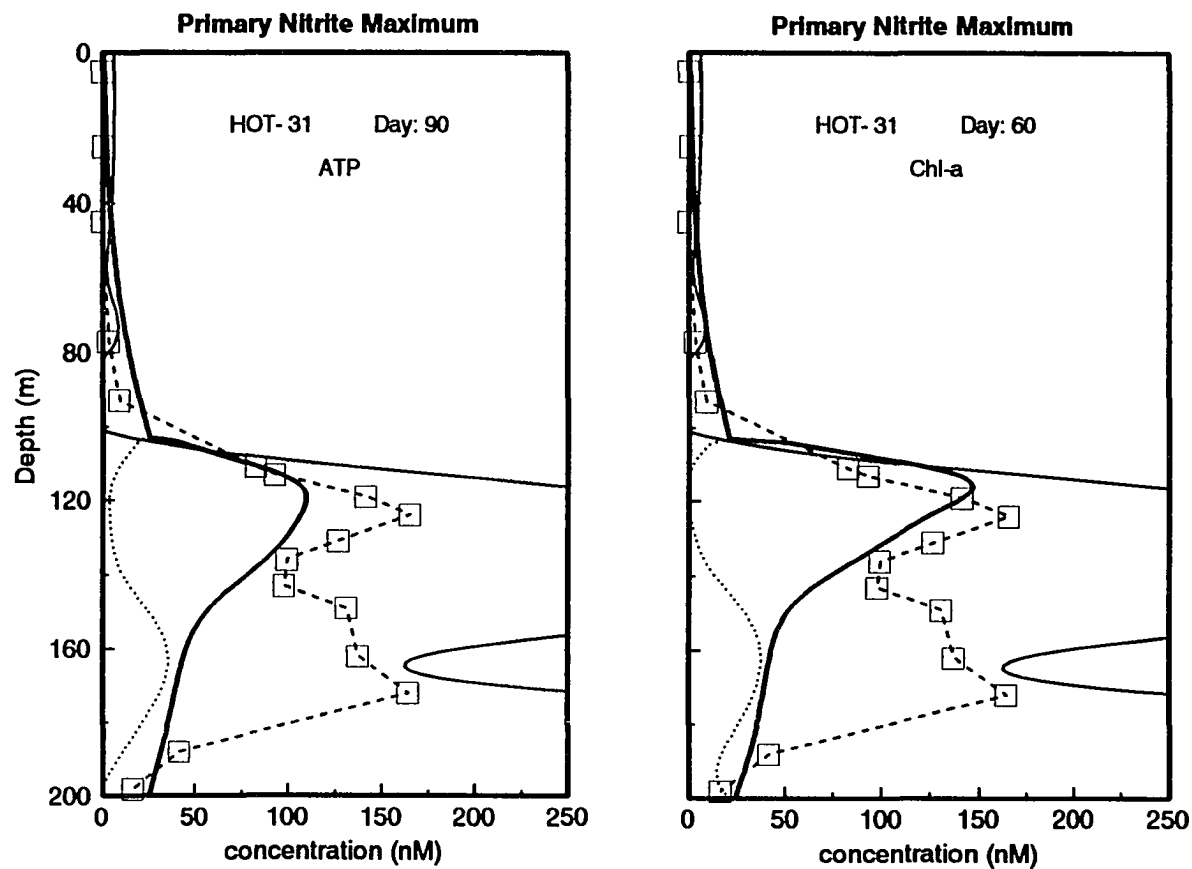


Fig. 5.9. Model output as in Fig. 5.5 except for HOT-31 (Oct. 1991).

primary nitrite maximum (LPNM; Dore and Karl, 1995) develops below 160 m. In general, the simulations using chlorophyll-a for biomass estimates more accurately reproduced the measured nitrite distributions than those in which ATP was used, but the predicted distributions were sufficiently similar to warrant the use of either biomass estimator. The precise depths of the simulated peaks are sometimes offset with respect to the measured features, as in HOT-36 (Fig. 5.8). This may be caused by short-term vertical motions of isopycnals between the casts from which input parameters were sampled which were not adequately filtered by our density-averaging technique.

The number of days required to simulate the PNM is a rough estimate of the turnover time for PNM nitrite. Excluding HOT-31, these turnover times ranged from 7-21 days, in between the rapid 2.6 day turnover estimated by Dore and Karl (1995) and the slower turnover of 25 days estimated by Olson (1981a). HOT-31 (Fig. 5.9) appears to be an unusual case in two respects. First, the estimated turnover time for the UPNM of >60 days is unreasonably large. Second, a large LPNM is evident which is not simulated by the model. It is possible that the large LPNM resulted from a rather sudden large input of ammonium to this layer, causing a transient excess of ammonium oxidation over nitrite oxidation, as suggested previously (Dore and Karl, 1995). Such changes in the ammonium distribution can strongly affect the response of ammonium oxidizers (see sensitivity analysis below). Another possibility is suggested by the nitrate inversion at 160 m: it is possible that the HOT-31 LPNM is really a displaced UPNM, and that the peak above is of remote origin associated with an intrusive water mass. The CTD records confirm that a low-salinity tongue intruded into this layer during the course of the cruise. Such a situation would also explain why our model was unable to recreate the HOT-31 UPNM in a reasonable number of days, because the conditions under which it formed were not accurately simulated. Also, because nitrite excretion by phytoplankton is

enhanced when nitrate starvation is followed by a sudden nitrate pulse (Laws and Wong, 1978; Martinez, 1991), it is possible that an intrusion of high-nitrate water could trigger a transient nitrite excretion rate in excess of that predicted using our model $K_{3,2}$ value.

Sensitivity analysis

We performed a simple sensitivity analysis of the model by beginning with the actual data from one cruise (HOT-50), and then modifying each of the major parameters in turn, observing the behavior of the model. Chlorophyll-a was used as a biomass estimator for this analysis. The parameters tested were $[\text{NO}_3^-]$, $[\text{NH}_4^+]$, [chl-a], and the PAR attenuation coefficient k .

We found, as expected, that the development of the UPNM is controlled by light, phytoplankton biomass and nitrate, but is little affected by the ammonium profile. The UPNM always develops a few m below the nitracline, but the speed with which it develops is dependent on the relative positions of the nitracline and the chlorophyll-a maximum, and on light availability. Raising k or lowering the ambient $[\text{NO}_3^-]$ or [chl-a] does not substantially alter the shape of the modeled PNM, but slows the development of the UPNM. Lowering k or raising $[\text{NO}_3^-]$ or [chl-a] does the opposite, speeding UPNM development. In this regard, the model is more sensitive to changes in k than it is to changes in nitrate or phytoplankton biomass. For example, lowering k from 0.040 m^{-1} to 0.034 m^{-1} has the same net effect as doubling the available [chl-a], which is to halve the time required for UPNM development without appreciably altering the shape of the nitrite profile.

Changes to the $[\text{NH}_4^+]$ profile result in observable differences in the LPNM, but have little effect on the UPNM, due to the inhibition of nitrification by light. When the

[NH₄⁺] profile is altered to include a 300 nM peak at 160 m, a robust LPNM develops quickly (Fig. 5.10), suggesting that transient episodes of enhanced regenerative activity may result in rapid increases in the size of the LPNM.

Strengths and weaknesses of the model

The PNM model described here simulates the measured nitrite distributions at Station ALOHA quite well under stable stratified conditions. With transient changes in input parameters, caused by physical disturbances or other non-steady state perturbations, nitrite distributions are not adequately reproduced. Among these perturbations could be changes in the ammonium profile or horizontal intrusions of water masses. However, this weakness of the model can also be a strength, in that one can determine in retrospect whether transient effects have been at play in the recent past. For example, the water mass intrusion observed during HOT-31 prevented accurate simulation of the PNM, indicating unusual circumstances. When we examine the HOT data base more closely, we find that this intrusion was the most significant to have occurred within the 100-200 m layer over the course of fifty cruises.

Our model has been successful in recreating the observed vertical separation of oxidative and reductive nitrite-producing processes hypothesized previously (Dore and Karl, 1995). It shows quite clearly that without precise and closely-spaced sampling, one could easily come to the conclusion that either nitrate reduction or ammonium oxidation was the dominant source of nitrite in the PNM, depending on the exact position within the PNM sampled. This observation may well reconcile the debate as to the oxidative or reductive source for PNM nitrite.

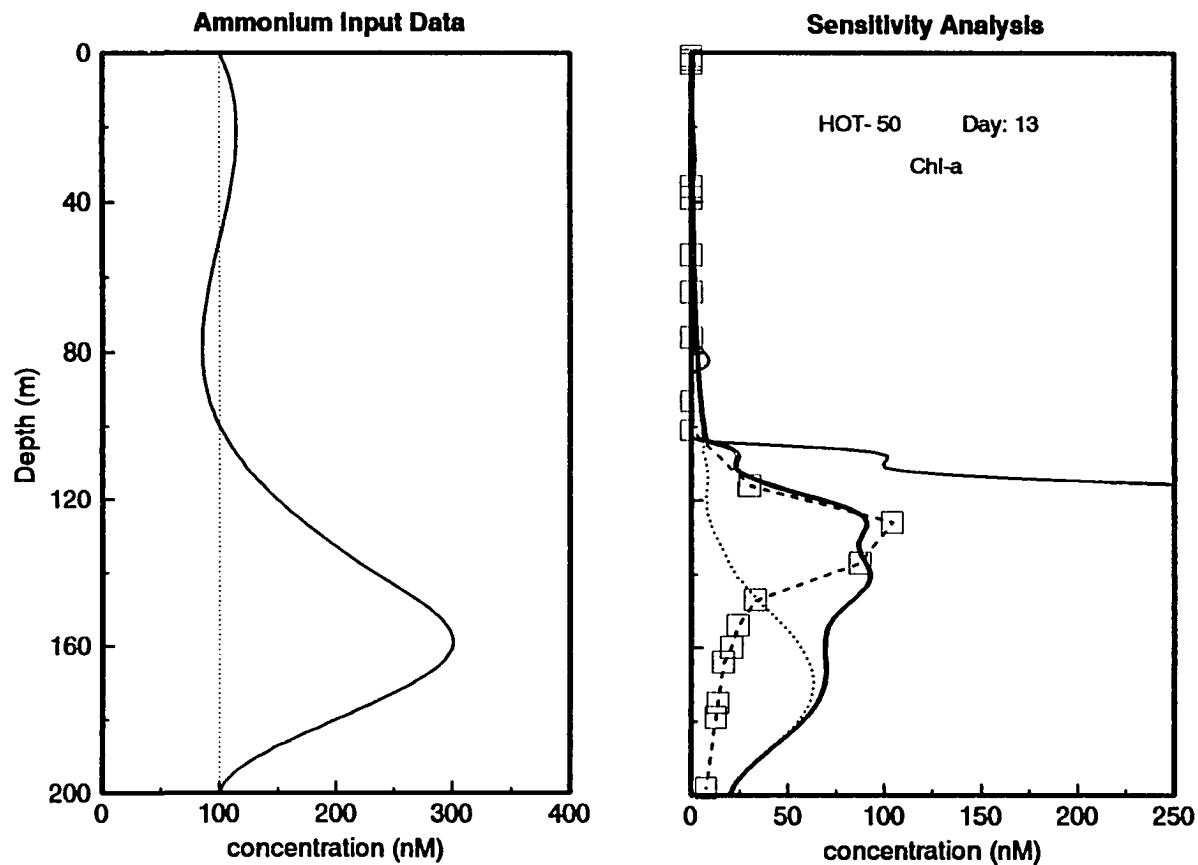


Fig. 5.10. Demonstration of model sensitivity to changes in $[\text{NH}_4^+]$ profile. All input parameters as for HOT-50 using chlorophyll-a as a biomass parameter, except $[\text{NH}_4^+]$. Left panel shows $[\text{NH}_4^+]$ used in all other simulations (dotted line) and interpolated $[\text{NH}_4^+]$ used in this sensitivity analysis (solid line). Right panel shows interpolated nitrate data (narrow solid line), measured nitrite data (squares and dashed line), model nitrite output (wide solid line), and the net contribution to the modeled nitrite made by nitrifying bacteria (dotted line). Compare right panel to Fig. 5.5, right panel.

It is well established that both nitrate reduction by phytoplankton and differential nitrification contribute to nitrite production in the sea. Previous PNM models either focused on nitrate reduction and ignored nitrification (Kiefer et al., 1976; Kiefer and Kremer, 1981) or focused on nitrification and ignored nitrate reduction (Olson, 1981b). The main advantage of our model over previous PNM models is that it takes both processes into account.

With minor modifications, this model can also be used to predict nitrite concentrations in other marine systems. For simulations of the PNM at Station ALOHA, we have been successful in assuming that neither light nor nitrate reach saturating levels for the process of nitrite excretion by phytoplankton. Under conditions of high phytoplankton biomass and high nitrate at the sea surface, as are found in Southern Ocean waters, this assumption does not hold. However, in preliminary tests we have found that by adding a half-saturation constant for light under these conditions we can generate depth-decaying nitrite profiles without a subsurface PNM, similar to those seen during the Antarctic spring bloom (Dore and Karl, 1993). Of course, some modification of model constants is necessary. Future efforts with the model should involve reworking the code so that the proper assumptions are made and the proper constants used depending upon the water type to be studied.

CONCLUSIONS

We have developed a computer model of the primary nitrite maximum (PNM) that accurately simulates nitrite distributions in the upper 200 m at Station ALOHA under stable stratified conditions. The model combines the processes of nitrite excretion by phytoplankton and oxidation of ammonium and nitrite by chemoautotrophic bacteria, and

considers the effects of light and substrate distributions on these processes. Input parameters are all based on measurements made at Station ALOHA, and model constants are estimated from rate experiments performed there. The model successfully predicts the observed vertical separation of oxidative and reductive processes contributing to nitrite production within the PNM, and recreates the asymmetric distribution of nitrite within the PNM.

REFERENCES

- Bingham, F. and R. Lukas. 1995. Seasonal cycles of temperature, salinity and dissolved oxygen observed in the Hawaii Ocean Time-series. *Deep-Sea Res.*, submitted.
- Christian, J.R. and D.M. Karl. 1994. Microbial community structure at the U.S.-Joint Global Ocean Flux Study Station ALOHA: Inverse methods for estimating biomass indicator ratios. *J. Geophys. Res.* **99**:14269-14276.
- Collos, Y. 1982. Transient situations in nitrate assimilation by marine diatoms. 2. Changes in nitrate and nitrite following a nitrate perturbation. *Limnol. Oceanogr.* **27**:528-535.
- Dore, J.E., T. Houlihan, D.V. Hebel, G. Tien, L. Tupas and D.M. Karl. 1995. Freezing as a method of sample preservation for the analysis of dissolved inorganic nutrients in seawater. *Mar. Chem.*, submitted.
- Dore, J.E. and D.M. Karl. 1993. RACER: Distribution of nitrite in the Gerlache Strait. *Antarctic J. U.S.* **27**:164-166.
- Dore, J.E. and D.M. Karl. 1995. Nitrite distributions and dynamics at Station ALOHA. *Deep-Sea Res.*, submitted.
- Karl, D.M., J.R. Christian, J.E. Dore, D.V. Hebel, R. M. Letelier, L.M. Tupas and C.D. Winn. 1995. Seasonal and interannual variability in primary production and particle flux at Station ALOHA. *Deep-Sea Res.*, submitted.
- Karl, D.M. and O. Holm-Hansen. 1978. Methodology and measurements of adenylate energy charge ratios in environmental samples. *Mar. Biol.* **48**:185-197.
- Karl, D.M. and R. Lukas. 1995. The Hawaii Ocean Time-series (HOT) program: Background, rationale and field implementation. *Deep-Sea Res.*, submitted.
- Kiefer, D.A. and J.N. Kremer. 1981. Origins of vertical patterns of phytoplankton and nutrients in the temperate, open ocean: a stratigraphic hypothesis. *Deep-Sea Res.* **28**:1087-1105.
- Kiefer, D.A., R.J. Olson and O. Holm-Hansen. 1976. Another look at the nitrite and chlorophyll maxima in the central North Pacific. *Deep-Sea Res.* **23**:1199-1208.
- Kirk, J.T.O. 1994. Light & Photosynthesis in Aquatic Ecosystems (2nd. ed.), Cambridge University Press, Cambridge, 509 pp.

- Laws, E.A. and D.C.L. Wong. 1978. Studies of carbon and nitrogen metabolism by three marine phytoplankton species in nitrate-limited continuous culture. *J. Phycol.* **14**:406-416.
- Letelier, R.M., R.R. Bidigare, D.V. Hebel, C.D. Winn and D.M. Karl. 1993. Temporal variability of phytoplankton community structure at the U.S.-JGOFS time-series Station ALOHA (22°45'N, 158°00'W) based on pigment analyses. *Limnol. Oceanogr.* **38**:1420-1437.
- Letelier, R.M., J.E. Dore, C.D. Winn and D.M. Karl. 1995. Temporal variability in photosynthetic carbon assimilation efficiencies at Station ALOHA. *Deep-Sea Res.*, submitted.
- Martinez, R. 1991. Transient nitrate uptake and assimilation in *Skeletonema costatum* cultures subject to nitrate starvation under low irradiance. *J. Plankton Res.* **13**:499-512.
- Olson, R.J. 1981a. ¹⁵N tracer studies of the primary nitrite maximum. *J. Mar. Res.* **39**:203-226.
- Olson, R.J. 1981b. Differential photoinhibition of marine nitrifying bacteria: a possible mechanism for the formation of the primary nitrite maximum. *J. Mar. Res.* **39**:227-238.
- Olson, R.J., J.B. Soo-Hoo and D.A. Kiefer. 1980. Steady-state growth of the marine diatom *Thalassiosira pseudonana*: uncoupled kinetics of nitrate uptake and nitrite production. *Plant Physiol.* **66**:383-389.
- Serra, J.L., M.J. Llama and E. Cadenas. 1978. Nitrate utilization by the diatom *Skeletonema costatum*. I. Kinetics of nitrate uptake. *Plant Physiol.* **62**: 987-990.
- Strickland, J.D.H., and Parsons, T.R., 1972. A Practical Handbook of Seawater Analysis. Bull. Fish. Res. Board Can., 167 (2nd edn.), 310 pp.
- Vanzella, A., M.A. Guerrero and R.D. Jones, 1990. Recovery of nitrification in marine bacteria following exposure to carbon monoxide or light. *Mar. Ecol. Prog. Ser.* **60**:91-95.
- Venrick, E.L., J.R. Beers and J.F. Heinbokel. 1977. Possible consequences of containing microplankton for physiological rate measurements. *J. Exp. Mar. Biol. Ecol.* **26**:55-76.
- Wada, E. and A. Hattori. 1972. Nitrite distribution and nitrate reduction in deep sea waters. *Deep-Sea Res.* **19**:123-132.

Ward, B.B. 1982. Oceanic distribution of ammonium-oxidizing bacteria determined by immunofluorescent assay. *J. Mar. Res.* **40**:1155-1172.

Ward, B.B. 1986. Nitrification in marine environments. In: Nitrification, J.I. Prosser (ed), IRL Press, Oxford, pp. 157-184.

Ward, B.B. and A.F. Carlucci. 1985. Marine ammonia- and nitrite-oxidizing bacteria: serological diversity determined by immunofluorescence in culture and in the environment. *Appl. Environ. Microbiol.* **50**:194-201.

CHAPTER 6

CONCLUSIONS AND DIRECTIONS FOR FUTURE RESEARCH

SUMMARY

The goal of this study, as discussed in Chapter 1, has been to illuminate the role of in situ chemoautotrophic bacterial nitrification within the euphotic zone at Station ALOHA with respect to the production of nitrite, nitrous oxide and nitrate. The results have revealed nitrification as an important nitrogen cycle process in the euphotic zone with respect to the in situ generation of all three of these nitrogen compounds.

Crucial to any study of dissolved nutrients in natural waters is the accuracy of the nutrient concentration measurements. Often water samples can not be analyzed at sea, therefore storage procedures must be used that do not alter the time-zero concentrations of analytes. In Chapter 2, I have shown that the slow freezing of seawater samples in polyethylene bottles is an adequate method of storing samples for later nutrient analyses, without the sacrifice of analytical accuracy.

The origin of the primary nitrite maximum (PNM) near the base of the euphotic zone in oxic oceanic waters has been a subject of debate for decades. In Chapter 3, I have described the temporal variability of this feature on timescales ranging from hours to years. I have observed that the asymmetrical shape of the PNM includes two peaks, which I dubbed the upper and lower primary nitrite maxima (UPNM and LPNM). Based on the observed positions of these features with respect to the nitracline and the light field, I have presented an hypothesis that the UPNM is maintained by phytoplankton nitrate reduction, and that the contribution of nitrification to the nitrite profile is restricted mainly to the

LPNM layer below. In this chapter I have also compared the temporal patterns of integrated euphotic zone nitrite with those observed in the sinking flux of particulate nitrogen, rejecting the hypothesis that the former can be used to predict the latter. Finally, I have presented evidence for substantial temporal variability in the deep nitrite pool and have suggested possible causes for this variability.

In Chapter 4 I have reported the results of nitrification rate measurements made during five cruises to Station ALOHA, along with measured water column distributions of nitrite, nitrate and nitrous oxide. I reached several important conclusions in this chapter. First, I found unmeasurably low nitrification rates in the UPNM and above, but variable and often substantial rates within the LPNM, indicating a vertical separation of nitrite-forming processes in the euphotic zone and supporting the hypothesis made in Chapter 3 regarding the formation of the two peaks of the PNM. Second, I found that the production of nitrous oxide via nitrification in the euphotic zone greatly exceeds its vertical eddy-diffusive flux from below the euphotic zone. At the same time, I found that the nitrification-based nitrous oxide source within the euphotic zone is insufficient to fuel the sea-air flux of this trace gas, indicating another source yet to be determined. Finally, I showed that the in situ production of nitrate via nitrification in the euphotic zone exceeds the eddy-diffusive input of nitrate from the deep water reservoir. This implies that nitrate-based primary production and new production cannot be equated, therefore calling for revision of the traditional new production concept. Including important roles for both nitrification and nitrogen fixation in the marine nitrogen cycle are two of the suggestions I have made for revision of the standard two-layer model of the euphotic zone.

Lastly, in Chapter 5 I have developed a computer model of the primary nitrite maximum that is consistent with the results of Chapters 3 and 4. This model has both oxidative and reductive nitrite sources included, and successfully recreates the observed

profiles of nitrite at Station ALOHA using measured input parameters. This model explains how the asymmetric shape of the PNM can be formed as a result of the light-dependent vertical separation of nitrification and phytoplankton nitrate reduction in the euphotic zone.

FUTURE RESEARCH DIRECTIONS

The global nitrogen cycle is a key structural filament in the web of life on Earth. Knowledge of the processes that govern the distributions and flows of nitrogen, in all of its various chemical guises, is essential for understanding the functioning of the biosphere as a whole. As we move forward into the twenty-first century, we must keep in mind that human activities have significantly disturbed, and continue to alter, the natural nitrogen cycle (Kinzig and Socolow, 1994). In order to comprehend and possibly predict the effects of these anthropogenic changes, we must strive to improve our understanding of the natural cycle of nitrogen in the global environment. The subtropical oceanic gyres represent a large fraction of the Earth's surface, hence the study of nitrogen cycling in these regions is clearly an endeavor of some importance.

The results of this study suggest that some aspects of our current conceptual models of the oceanic nitrogen cycle are in need of revision. Two items are particularly interesting in this regard. The first has to do with the source(s) of nitrous oxide in the oceanic environment. It is popular to assume that the N_2O flux to the atmosphere from the sea is driven by the eddy-diffusive flux of this gas from deep water. My results from Station ALOHA, on the contrary, suggest that this sea-air flux is driven by in situ production of N_2O within the euphotic zone, and that the responsible biochemical pathways remain largely unknown. I believe that this is an important area for future

research. The potential role of denitrification in the euphotic zone is of particular significance, because it could support a large export flux of nitrogen gas that is entirely ignored in most oceanic nitrogen-cycle models.

The other major change in our view of marine nitrogen cycling that is implied by this study has to do with the traditional concept of new production. The equation of nitrate-based production with new production is a dogma that many biological oceanographers are not going to give up easily. However, this study is only one of many to confront the traditional view of new production with unsupportive evidence. Ironically, the authors of the new production concept were the first to suggest that the model might fail if nitrification and/or nitrogen fixation were found to be important processes within the euphotic zone (Dugdale and Goering, 1967).

I believe there are a growing number of oceanographers who, in the face of recent data, are leaning toward a remodeling of the new production concept. In this regard I shall quote three recent and highly regarded publications: (1) "We prefer to express our results in terms of NEZP [net euphotic zone production] because the concept of 'new' production of organic matter or O_2 becomes ambiguous whenever organic matter is formed with varying C:N or O_2 :N ratios, or whenever significant nitrification occurs in the euphotic zone." (Keeling and Shertz, 1992); (2) "The measurement of DON [dissolved organic nitrogen] release rates and the recognition that traditional uptake rates have been underestimated are the latest in a series of important findings that require that the assumptions of the new production paradigm be reevaluated." (Bronk et al., 1994); (3) "If, as we present here, N_2 fixation contributes significantly to the oligotrophic Pacific Ocean nutrient budget then our conventional views of new (nitrate-based) and regenerated (ammonium-based) primary production may be in need of revision." (Karl et al., 1995).

The growing evidence that oceanic nitrogen fixation has been underestimated leads me to a final suggestion for future research, which is to study the mechanisms of phosphorus delivery to the euphotic zone and the cycling of phosphorus within the euphotic zone. The processes governing the pools and fluxes of the bioelements are inexorably linked; we must seek a reconciliation of the apparent lack of balance between the nitrogen and phosphorus supply rates to the euphotic zone.

REFERENCES

- Bronk, D.A., P.M. Glibert and B.B. Ward. 1994. Nitrogen uptake, dissolved organic nitrogen release, and new production. *Science* **265**:1843-1846.
- Dugdale, R.C. and J.J. Goering. 1967. Uptake of new and regenerated forms of nitrogen in primary productivity. *Limnol. Oceanogr.* **12**:196-206.
- Karl, D.M., R. Letelier, D. Hebel, L. Tupas, J. Dore, J. Christian and C. Winn. 1995. Ecosystem changes in the North Pacific subtropical gyre attributed to the 1991-92 El Niño. *Nature* **373**:230-234.
- Keeling, R.F. and S.R. Shertz. 1992. Seasonal and interannual variations in atmospheric oxygen and implications for the global carbon cycle. *Nature* **358**:723-727.
- Kinzig, A.P. and R.H. Socolow. 1994. Human impacts on the nitrogen cycle. *Phys. Today* **47**:24-31.

APPENDIX A

MATLAB™ ROUTINES

The PNM model consists of a main control routine (`pnm.m`) and three subroutines (`pnminput.m`, `pnmconst.m`, and `pnmcalc.m`). Comments marked by a % are included within each routine to explain its function and execution. Seven data files are called upon during each simulation of which five are specific for the particular cruise to be modeled. All consist of one or two columns of data in ascii format, and each must have the `.txt` extension. The data files are:

const.txt: this file consists of a single column of nine numbers representing the following constants (in order): `r42m`, `k42`, `d2,d4`, `t2`, `t4`, `k23`, `r23m`, `k32`.

h#lit.txt (where # is the HOT cruise number, e.g. `h50lit.txt`): this file contains the cruise-specific optical parameters in a single column of three numbers representing the following constants (in order): `kz`, `iint`, `pt`.

h#nh4.txt, **h#no3.txt**, **h#no2.txt**, **h#atp.txt**, **h#chl.txt**: these files contain the ammonium, nitrate, nitrite, ATP and chlorophyll-a data for the given cruise. Each consists of two columns. The first column contains the density-averaged depths in meters (for samples in the upper 200 m), the second contains the analyte concentration at each depth in nM (for ammonium, nitrate and nitrite) or in ng l⁻¹ (for ATP and chl-a). The cubic spline interpolation works best if there are values at both 0 and 200 m, so it is suggested that the user provide these values based on whatever extrapolation seems fit.

The following pages contain the complete code, including comments, for each of the four routines written for the PNM model:

%pnm.m: J.Dore

%this is the main control routine for the PNM model simulation.

%the routine calls upon subroutines pnminput.m, pnmconst.m and pnmcalc.m

%begin program

disp('')

disp('Welcome to PNM Simulator (1994) by J. Dore...')

again = 'Y';

%begin main control loop

while again~='n'&again~='N'

 again = input('Run simulation? (y or n):','s');

 if again~='n'&again~='N'

 pnminput

 pnmconst

 pnmcalc

 end

end

%end main control loop

disp('')

disp('Y' all come back real soon!!!')

disp('')

%end program

%pnminput.m : J. Dore

%this routine takes unevenly spaced data vectors for the PNM model and
%creates interpolated
%0-200 m vectors of each (except nitrite, which is retained as actual data).

%input vectors are h#no2.txt, h#no3.txt, h#nh4.txt, and either h#atp.txt or h#chl.txt,
%where # = cruise number.

%Important! input vectors should contain "dummy" values at 0 and 200 m or
%interpolation may
%not proceed correctly.

%the routine also takes in the light data file h#lit.txt

%ask for cruise number and choice of biomass parameters

```
hotnum = input('Enter cruise number:');  
biomtype = input('Do you want to include (1)ATP or (2)Chl-a in the model?', 's');
```

%obtain parameters from data files for biomass, nitrate, nitrite and ammonium

```
if (biomtype == '1')
```

```
    biomfile = ['h',int2str(hotnum),'atp'];  
    biomload = ['load ',biomfile,'.txt'];  
    eval(biomload);  
    biomdat = eval(biomfile);  
    disp(' ')  
    disp('Using ATP as biomass vector')
```

```
else
```

```
    biomfile = ['h',int2str(hotnum),'chl'];  
    biomload = ['load ',biomfile,'.txt'];  
    eval(biomload);  
    biomdat = eval(biomfile);  
    disp(' ')  
    disp('Using Chl-a as biomass vector')
```

end

```
no3file = ['h',int2str(hotnum),'no3'];  
no3load = ['load ',no3file,'.txt'];  
eval(no3load);  
no3dat = eval(no3file);
```

```
no2file = ['h',int2str(hotnum),'no2'];  
no2load = ['load ',no2file,'.txt'];  
eval(no2load);  
no2dat = eval(no2file);
```

```
nh4file = ['h',int2str(hotnum),'nh4'];  
nh4load = ['load ',nh4file,'.txt'];  
eval(nh4load);  
nh4dat = eval(nh4file);
```

%obtain optical parameters

```
litfile = ['h',int2str(hotnum),'lit'];  
litload = ['load ',litfile,'.txt'];  
eval(litload);  
litdat = eval(litfile);
```

%create uninterpolated data vectors, convert chla or ATP to phytoplankton carbon

```
zno3 = no3dat(:,1);  
no3 = no3dat(:,2);
```

```
zbiom = biomdat(:,1);  
biom = biomdat(:,2);
```

```
if (biomtype ~= '1')
```

```
    biom = biom .* 15;
```

```

else
biom = biom .* 131.25;

end

zno2d = no2dat(:,1);
no2d = no2dat(:,2);

znh4 = nh4dat(:,1);
nh4 = nh4dat(:,2);

kz = litdat(1);
iint = litdat(2);
pt = litdat(3);

zno2 = 0:200;
zno2 = zno2';

%interpolate nitrate, biomass and ammonium vectors using cubic spline routine

no3int = spline(zno3,no3,zno2);
biomint = spline(zbiom,biom,zno2);
nh4int = spline(znh4,nh4,zno2);

%replace any negative values produced by interpolation routine with minimum values

for count1 = 1:201

    if no3int(count1) <= 0
        no3int(count1) = 0.1;
    end

    if biomint(count1) <= 0
        biomint(count1) = 1;
    end

    if nh4int(count1) <= 0
        nh4int(count1) = 0.001;
    end

end

```

%pnmconst.m: J.Dore

%this routine inputs constants for use in PNM model.

%these nine constants are found in the file const.txt

%three vector constants iz, a4 and a2, are calculated from the above.

%obtain constants

load const.txt;

r42m = const(1);

k42 = const(2);

d2 = const(3);

d4 = const(4);

t2 = const(5);

t4 = const(6);

k23 = const(7);

r23m = const(8);

k32 = const(9);

%convert daily integrated light to daily average light and calculate light profile

ia = iint*11.574;

iaz = pt*ia*exp(-kz*zno2);

%convert to W m⁻² for nitrification equations

iqz = iaz/4.6;

%calculate inhibition factors for nitrification

for count2 = 1:201

a2(count2) = 1-((iqz(count2)-t2)/(d2+(iqz(count2)-t2)));

a4(count2) = 1-((iqz(count2)-t4)/(d4+(iqz(count2)-t4)));

end

%pnmcalc.m: J.Dore

**%this routine takes all the parameters and calculates the nitrite distribution one time
%step at a time,
%until the indicated number of timesteps is reached.**

**%as it steps, it plots the total no2 and the no2 from nitrification,
%along with the actual no2 data and the no3 data.**

%ask for number of timesteps (days)

daynum = input('Enter the number of days for the simulation:');

%initialize output vectors

**no2 = zeros(201,1);
no2nit = zeros(201,1);
zno2 = -zno2;
zno2d = -zno2d;**

**%prepare graph window axes and titles, and plot interpolated nitrate and
%original nitrite data**

clg;

**axis([0 250 -200 0]);
plot(no2d,zno2d,'-c5',no3int,zno2,'-g');
text(0.4,0.8,'HOT-', 'sc');
text(0.5,0.8,int2str(hotnum), 'sc');
text(0.6,0.8,'Day: ', 'sc');
text(0.72,0.8,'0', 'sc');
title('Primary Nitrite Maximum');
xlabel('Concentration (nM)');
ylabel('Depth (m)');**

%provide a 10 second delay before simulation begins

delay1 = 0;

```

time1 = clock;

while delay1<10
    delay1 = etime(clock,time1);
end

%begin simulation; calculate output vectors for each time step

for count3 = 1:daynum

    for count4 = 1:201

        r42(count4) = a4(count4)*nh4int(count4)*r42m/(k42 + nh4int(count4));

        %exclude nitrate reduction term if nitrate is less than 20 nM

        if no3int(count4) > 20
            r32(count4) = k32*biomint(count4)*(no3int(count4))*iaz(count4);
        else
            r32(count4) = 0;
        end

        no2(count4) = no2(count4) + r32(count4) + r42(count4);

        no2nit(count4) = no2nit(count4) + r42(count4);

        r23(count4) = a2(count4)*no2(count4)*r23m/(k23 + no2(count4));

        no2(count4) = no2(count4) - r23(count4);

        no2nit(count4) = no2nit(count4) - r23(count4);

    end

    %plot output vectors

```

```

plot(no2d,zno2d,'-c5',no3int,zno2,'-g',no2,zno2,'-r',no2nit,zno2,'-b');

%add cruise number and days elapsed to plot

text(0.4,0.8,'HOT-', 'sc');
text(0.5,0.8,int2str(hotnum), 'sc');
text(0.6,0.8,'Day: ', 'sc');
text(0.72,0.8,int2str(count3), 'sc');

%add 1/2 second delay between time steps

delay2 = 0;
time2 = clock;

while delay2<0.5
    delay2 = etime(clock,time2);
end

end

%end simulation calculations

%replot axes and labels

text(0.4,0.8,'HOT-', 'sc');
text(0.5,0.8,int2str(hotnum), 'sc');
text(0.6,0.8,'Day: ', 'sc');
text(0.72,0.8,int2str(count3), 'sc');
title('Primary Nitrite Maximum');
xlabel('Concentration (nM)');
ylabel('Depth (m)');

```

APPENDIX B

MODEL CONSTANTS AND VARIABLES

Name	Description	Value (if const.)
a2	nitrite oxidizer relative activity (0-200 m)	
a4	ammonium oxidizer relative activity (0-200 m)	
again	user reply (Y/N) whether to run model	
biom	phytoplankton biomass data in ng C l ⁻¹	
biomdat	array of depth and biomass data	
biomfile	name of file containing biomass data	
biomint	interpolated biomass (0-200 m) in ng C l ⁻¹	
biomload	command to open chl-a or ATP file	
biomtype	user choice of (1)ATP or (2)chl-a	
const	array of model constants	
count1	counter used in negative value correction loop	
count2	counter used in inhibition calculation loop	
count3	timestep counter for output loop	
count4	depth counter for output loop	
d2	half-saturating light dose for nitrite oxidizers	0.036 W m ⁻²
d4	half-saturating light dose for ammonium oxidizers	0.074 W m ⁻²
daynum	user-input number of days to run model	
delay1	counter used in delaying start of model by 10 sec.	
delay2	counter used in time-stepping output by 0.5 sec.	
h#chl	loaded chl-a file where # = HOT cruise number	
h#lit	loaded light file where # = HOT cruise number	
h#nh4	loaded ammonium file where # = HOT cruise number	
h#no2	loaded nitrite file where # = HOT cruise number	
h#no3	loaded nitrate file where # = HOT cruise number	
hotnum	user-input HOT cruise number	
ia	avg. surface light flux in $\mu\text{E m}^{-2} \text{s}^{-1}$	
iaz	avg. light flux in $\mu\text{E m}^{-2} \text{s}^{-1}$ (0-200 m)	
iint	avg. daily integrated surface light in E m^{-2}	
iqz	avg. light flux in W m^{-2} (0-200 m)	
k23	half-saturating substrate conc. for nitrite oxidation	27 nM
k32	constant for nitrate reduction to nitrite	9×10^{-7} (see text)

k42	half-saturating substrate conc. for ammonium oxidation	200 nM
kz	diffuse PAR attenuation coefficient in m^{-1}	
litdat	array of light data	
litfile	name of file containing light data	
litload	command to open light data file	
nh4	ammonium concentration data in nM	
nh4dat	array of depth and ammonium conc. data	
nh4file	name of file containing ammonium data	
nh4int	interpolated ammonium conc. (0-200 m) in nM	
nh4load	command to open ammonium data file	
no2	model output nitrite conc. (0-200 m) in nM	
no2d	measured nitrite concentration data in nM	
no2dat	array of depth and measured nitrite conc. data	
no2file	name of file containing measured nitrite data	
no2load	command to open measured nitrite data file	
no2nit	model output nitrite from nitrification (0-200 m) in nM	
no3	nitrate concentration data in nM	
no3dat	array of depth and nitrate conc. data	
no3file	name of file containing nitrate data	
no3int	interpolated nitrate conc. (0-200 m) in nM	
no3load	command to open nitrate data file	
pt	fraction of light passing through sea surface	
r23	rate of nitrite oxidation (0-200 m) in $nmol\ l^{-1}\ d^{-1}$	
r23m	maximum rate of nitrite oxidation	30 $nmol\ l^{-1}\ d^{-1}$
r32	rate of nitrate reduction to nitrite (0-200 m) in $nmol\ l^{-1}\ d^{-1}$	
r42	rate of ammonium oxidation (0-200 m) in $nmol\ l^{-1}\ d^{-1}$	
r42m	maximum rate of ammonium oxidation	30 $nmol\ l^{-1}\ d^{-1}$
t2	threshold light for inhibition of nitrite oxidation	0.0095 $W\ m^{-2}$
t4	threshold light for inhibition of ammonium oxidation	0.0364 $W\ m^{-2}$
time1	timer used in 10 sec. delay	
time2	timer used in 0.5 sec. delay	
zbiom	depths associated with biomass data	
znh4	depths associated with ammonium data	
zno2	depths (0-200 m) for plotting all calculated parameters	
zno2d	depths associated with measured nitrite data	
zno3	depths associated with nitrate data	

INPUT DATA FOR FIVE MODELED CRUISES

HOT-31 Model Input

kz 0.040 (m⁻¹)
 iint 40.4 (E m⁻²)
 pt 0.75

avg. z (m)	[NO ₃ ⁻] (nM)	avg. z (m)	[NH ₄ ⁺] (nM)	avg. z (m)	[NO ₂ ⁻] (nM)	avg. z (m)	[chl-a] (ng l ⁻¹)	avg. z (m)	[ATP] (ng l ⁻¹)
0	6.3	0	100	5	0.1	0	64	0	23.53
5	6.3	50	100	25	0.9	7	64	5	23.53
49	3.4	100	100	45	0.0	27	62	33	30.48
62	3.2	125	100	77	3.5	47	54	52	30.81
80	3.2	140	100	93	9.2	60	113	78	20.99
102	7.3	160	100	111	83.0	76	163	104	13.86
108	80.2	180	100	113	93.2	90	248	132	9.62
116	242.5	200	100	119	141.7	103	321	152	8.93
126	408.1			124	165.7	108	281	180	7.73
139	539.2			131	127.0	117	197	200	6.21
162	172.4			136	99.5	138	103		
179	580.0			143	98.1	146	83		
200	3512.0			149	131.2	163	55		
				162	137.5	194	44		
				172	164.7	200	7		
				188	41.5				
				198	16.5				

HOT-36 Model Input

kz 0.040 (m⁻¹)
 iint 57.0 (E m⁻²)
 pt 0.75

avg. z (m)	[NO ₃ ⁻] (nM)	avg. z (m)	[NH ₄ ⁺] (nM)	avg. z (m)	[NO ₂ ⁻] (nM)	avg. z (m)	[chl-a] (ng l ⁻¹)	avg. z (m)	[ATP] (ng l ⁻¹)
0	1.7	0	100	0	0	0	74	0	25.566
6	1.7	50	100	30	0	31	73	16	25.566
18	1.5	100	100	48	0	50	78	23	15.043
21	2.3	125	100	87	0.1	90	91	55	53.414
28	1	140	100	106	0.8	121	124	83	27.741
40	0.6	160	100	125	98.1	130	141	103	28.685
54	1.8	180	100	132	88.2	136	271	130	27.342
73	0.9	200	100	140	63.3	140	282	156	7.937
84	2			157	27	144	260	176	5.998
92	5			163	22.3	156	187	200	5.233
99	2.1			168	19.3	159	136		
117	304.2			169	16.8	173	95		
130	705.6			172	16.7	186	32		
146	2260			175	15.3	200	21		
169	2610			183	13.3				
181	3210			198	9.4				
193	4030								
200	4357								

HOT-40 Model Input

kz 0.040 (m⁻¹)
 iint 50.6 (E m⁻²)
 pt 0.75

avg. z (m)	[NO ₃ ⁻] (nM)	avg. z (m)	[NH ₄ ⁺] (nM)	avg. z (m)	[NO ₂ ⁻] (nM)	avg. z (m)	[chl-a] (ng l ⁻¹)	avg. z (m)	[ATP] (ng l ⁻¹)
0	1.8	0	100	5	0.4	0	69	0	18.634
7	1.8	50	100	25	0	5	69	5	18.634
31	1.7	100	100	49	1.5	25	75	25	30.936
37	5.6	125	100	95	0.1	45	110	37	27.322
44	1.2	140	100	102	0.7	60	135	101	22.232
60	1.3	160	100	106	1.3	77	207	105	23.243
79	1.2	180	100	111	12.9	92	235	107	25.488
87	1.1	200	100	114	48.2	102	273	113	18.195
99	1.4			119	76.9	112	297	122	15.066
110	86.2			122	89.3	129	152	124	15.668
122	311.2			129	55.1	142	155	152	8.803
130	509.1			133	39.6	158	42	175	6.676
138	656.4			138	40.4	185	31	200	6.275
158	880			143	45.3	200	20		
196	1720			149	43				
200	1810			159	31.1				
				174	32.9				
				191	22.7				

HOT-41 Model Input

kz 0.040 (m⁻¹)
iint 46.4 (E m⁻²)
pt 0.75

avg. z (m)	[NO ₃ ⁻] (nM)	avg. z (m)	[NH ₄ ⁺] (nM)	avg. z (m)	[NO ₂ ⁻] (nM)	avg. z (m)	[chl-a] (ng l ⁻¹)	avg. z (m)	[ATP] (ng l ⁻¹)
0	1.1	0	100	0	1.2	0	72	0	28.676
15	1.1	50	100	12	1.2	5	72	5	28.676
33	1	100	100	31	0.3	10	69	12	20.52
39	1.3	125	100	60	0.3	30	69	30	27.968
41	1.6	140	100	80	1.1	66	150	59	20.952
43	1.3	160	100	95	11.1	78	195	78	22.933
65	1.6	180	100	104	91	80	218	105	20.057
79	1.6	200	100	108	105.9	85	287	144	17.496
93	8.7			116	73.9	90	292	166	5.898
105	141.7			121	46.1	95	154	200	5.15
110	243.6			129	37.7	114	102		
115	656.6			132	35.1	143	51		
133	960			137	34.2	162	37		
136	1100			142	32.8	184	8		
147	1540			148	30	200	5		
172	2440			152	27.4				
200	3459			159	20.6				
				168	16.3				
				182	14.2				

HOT-50 Model Input

kz 0.040 (m⁻¹)
 iint 34.5 (E m⁻²)
 pt 0.75

avg. z (m)	[NO ₃ ⁻] (nM)	avg. z (m)	[NH ₄ ⁺] (nM)	avg. z (m)	[NO ₂ ⁻] (nM)	avg. z (m)	[chl-a] (ng l ⁻¹)	avg. z (m)	[ATP] (ng l ⁻¹)
0	1.2	0	100	1	0	0	69	0	28.626
7	1.2	50	100	2	0	6	69	5	28.626
17	0.8	100	100	3	0	48	84	36	28.234
27	2	125	100	36	0.1	60	100	63	34.57
37	1	140	100	39	0	80	148	93	36.272
48	0.8	160	100	54	0.1	87	207	109	23.345
59	0.9	180	100	64	0	100	262	132	15.219
75	1	200	100	76	0	111	241	158	11.164
76	0.8			93	0	125	228	185	5.555
85	1.6			101	0	128	200	200	4
104	5.6			116	30.2	132	171		
106	76.3			126	104.2	141	169		
112	110			137	87.3	154	75		
124	910			147	33.1	169	29		
139	2040			154	24.3	198	2		
160	3100			160	20.9	200	2		
180	4040			164	16.9				
200	4980			175	13.9				
				179	12.9				
				198	7.8				